Institute of Photogrammetry
and GeoInformation
University of Hannover, Germany

Intermap Technologies
Corporation
Calgary, Canada

Diploma Thesis

Automated Road Extraction from Radar and Optical Imagery

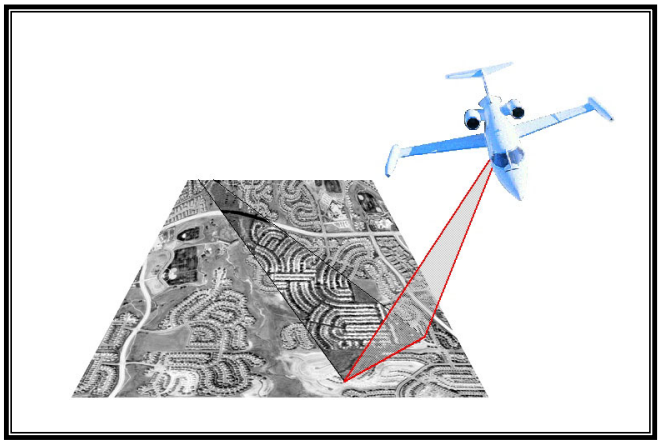

Stefan Hoheisel

May 2003

I hereby confirm to have created the present diploma thesis by myself and only with help of the stated resources.

Calgary, May 5th, 2003

“Roads are the veins and arteries of the body politic, for through them flow the agricultural productions and the commercial supplies which are the lifeblood of the state... But roads belong to that unappreciated class of blessings, of which the value and importance are not fully felt because of the very greatness of their advantages, which are so manifold and indispensable, as to have rendered their extent almost universal and their origin forgotten.”

W. M. Gillespie, 1849

Acknowledgements

The writing of my diploma thesis in Canada has been a wonderful time for me. Not only was this an opportunity to broaden my international experience, but it has also given me the chance to meet interesting people and face new challenges. I would like to express my appreciation for the support I have received during the time of my studies in Calgary and thank the following people:

- To Prof. Dr.-Ing. Christian Heipke, Head of the Institute for Photogrammetry and GeoInformation at the University of Hannover, Germany, for establishing the link with Intermap Technologies Corp. and making this invaluable experience possible within such a short time of notice.

- To Dr. Bryan Mercer, Chief Scientist at Intermap Technologies Corp. Calgary, Canada, for supplying me with the necessary research environment and supporting my investigations.

- To Dipl.-Ing. Markus Gerke and Dipl.-Ing. Matthias Butenuth of the Institute for Photogrammetry and GeoInformation at the University of Hannover, Germany, for your quick and valuable technical support and helpful comments to make this work so much more successful.

- To Natalie Glass and Jeremy Allan of Intermap Technologies Corp. Calgary, Canada, for helping me to cope with many problems along the way.

- To all Intermap staff at the Calgary office for making this work possible. I will always think of the time we spent together as colleagues. And I will never forget the good times we had on those special Friday afternoons.

On a more personal note, I would like to express my appreciation to my family and friends who have supported me not only during this thesis, but throughout my studies, especially:

- To my parents for their emotional and financial support. This experience would not have been possible without you. To my sisters and brothers-in-law, for cheering me up and showing me that there are things beside a thesis that are also important. And to Annalena, for believing in me.

- To Jorge and Amy, for being my family during my stay in Canada. Your support has been extraordinary and I always enjoyed the weekends in Edmonton to relax from the work at the office.

Table of Contents

1. Introduction

1.1. Motivation

Roads and road networks have always been considered as highly important for any country's economic progress, as they represent the means for the conventional transport of goods and individuals. In highly industrialized countries, they serve as the primary solution for the tasks and demands that arise from a growing population and economy.

The infrastructural importance of roads can be seen by the rapid development of new roads and the rising costs that are connected to this development. In the USA, the capital expenditures for highways have increased by approximately 246 % between 1978 and 1998 [FHWA, 1998].

In order to handle and efficiently manage this growing amount of roads, commercial and non-commercial institutions often use *Geographic Information Systems* (GIS), which can serve as powerful tools to cope with the numerous tasks connected to any kind of road management. In order to do so, a GIS usually handles the given information as *vector data*; in the case of roads, the required information mostly consists of linear features. To acquire the vector data, the information contained in imagery of any source – generally raster images – can be digitized manually. This work process may take up a great amount of working time and cost, because a trained operator has to interpret the image, identify the desired vector data, digitize it and finally import it into the GIS. Because of the rapid changes that occur in road networks, the manual creating and updating of geographic data can become overwhelming.

An alternative approach to the creation and management of linear vectors within Geographic Information Systems is offered by the means of automated object extraction. The manual process of digitizing is transferred to a processing system, partly replacing manpower by computational power. This automated approach meets the requests for near-to-date road data, because it is less time-consuming and eventually more cost-effective.

The means of remote sensing in connection with digital photogrammetry and automated image analysis are especially well suited for providing the requested information and interpret it automatically. Imagery from aerial photography or radar sensors can be used as a reliable source, because they provide – if applied on an area where their respective advantages come into effect – fast and accurate access to the demanded raster images. Areas of wide extension, holding the general surface information, can be covered quickly.

The whole process chain from image interpretation to the import of vectors can become more time-efficient by applying automated object extraction. Basis for an

automated extraction process is the definition and adaptation of suitable extraction algorithms to the given imagery sources.

1.2. Goal and contents

The goal of this thesis is to show and compare possibilities of automated road extraction from different imagery sources. The advantages and disadvantages of two selected extraction algorithms are explained and evaluated in detail by applying them to digital aerial photographs on one hand, and imagery stemming from airborne synthetic aperture radar on the other.
The main topic of the present work is the control of road extraction algorithms by adapting their alterable *parameters* to the given imagery sources, which are black and white orthophotos and radar imagery. Of special importance is the investigation of possible adaptations to regions that bear different general appearances.
The thesis also provides detailed insight into these two extraction algorithms in order to be able to optimize their application to both data sources. Furthermore, a combination of optical and radar imagery with the objective of achieving enhanced extraction results is researched. Extensive investigations and convincing examples will show the potential of automated road extraction, taking into account the arising opportunities as well as present limitations.

Chapter 2 focuses on the basic principles of radar systems and gives an overview of airborne and spaceborne radar systems. Properties of radar images and their major differences with optical imagery are explained. Additionally, an overview of applications for radar data is provided.

In **chapter 3**, an explanation of road models in aerial and radar imagery, which are a prerequisite to the extraction itself, is given. This is followed by different approaches towards road extraction from both image sources. In conclusion, two algorithms are chosen for further investigation and reasons for the choices are given.

A detailed description and investigation of both algorithms is presented in **chapter 4**. Both general approaches are explained in detail. Concluding, the particular adaptations for use with respective imagery sources are shown.

Chapter 5 focuses on the practical analysis of automated extraction applied on SAR imagery. The test approaches are presented, and the achieved results are shown and evaluated for both extraction algorithms.

In **chapter 6**, similar tests as in chapter 5 are carried out on optical imagery. After a presentation of test approaches, the results are shown and evaluated for both extraction algorithms. Additionally, comparisons between both imagery sources and extraction algorithms are presented.

Chapter 7 concludes this work by summarizing the achieved results and offering an outlook regarding further investigations.

2. Radar systems

In order to be able to extract certain features from a radar image, one has to understand the basic steps that are necessary to obtain the basis for the extraction, which is the image itself. These steps include the acquisition of the radar data and its processing, which finally leads to the resulting grey scale image. The extraction software has to be adapted by taking into account the image's properties in order to derive the desired information.
In the first part, this chapter focuses on the basic principles of radar systems, explaining the geometric and radiometric properties of radar data. This is followed by a description of space- and airborne systems that are currently in operation. The third part offers a closer look at radar image properties, while the main differences between radar and optical imagery are explained in subchapter four. The chapter is completed with an overview of radar applications, focusing on radar systems' advantages and disadvantages and explaining 3D imaging possibilities.

2.1. Basic principles of radar systems

The RADAR (**Ra**dio **D**etection **a**nd **R**anging) principle is based on the reflective properties of microwaves, ranging approximately in between 1 mm and 1 m wavelengths. A distinction has to be made between *passive* and *active radar systems*. While passive systems merely collect the microwaves emitted by an object with a sensor, active systems generate radar signals themselves that are then sent to and reflected by the object and again collected by the sensor. In this thesis, only active systems are examined.

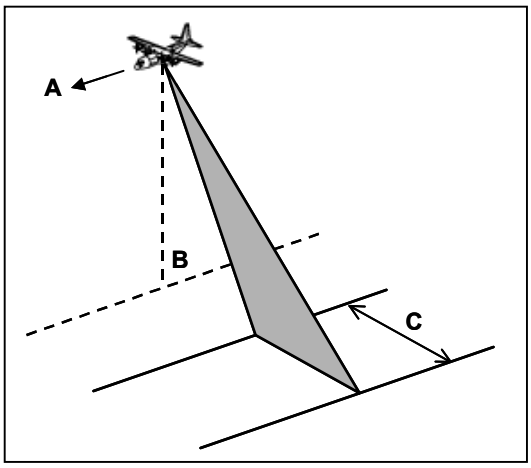

Figure 1: Radar viewing geometry

Figure 1 shows a typical side-looking radar system configuration (SLAR). The aircraft or satellite bearing the radar system is moving forward in flight while radar pulses are sent out at a right angle to the flight direction (A) with the system's nadir (B) beneath the platform, illuminating a swath (C) on the earth's surface. When a radar pulse reaches an object, it is either reflected, absorbed or passes through the object, depending on the object's reflective properties and the wavelength of the radar pulse (cf. [CCRS, 2001]). A closer look at these properties follows in chapter 2.3.
The distance of an object – and therefore its position in the image space – is determined by measuring the time delay between the transmission of a radar pulse and the reception of its signal, backscattered by the object. This leads to *geometric distortions* in the resulting image, because the distance to objects is not measured as the true horizontal distance along the ground, but in *slant range*. The closer the objects are located to the radar, the more compressed they appear in a raw image. However, the ground range distance can easily be calculated from slant range distance and platform altitude, using trigonometry.

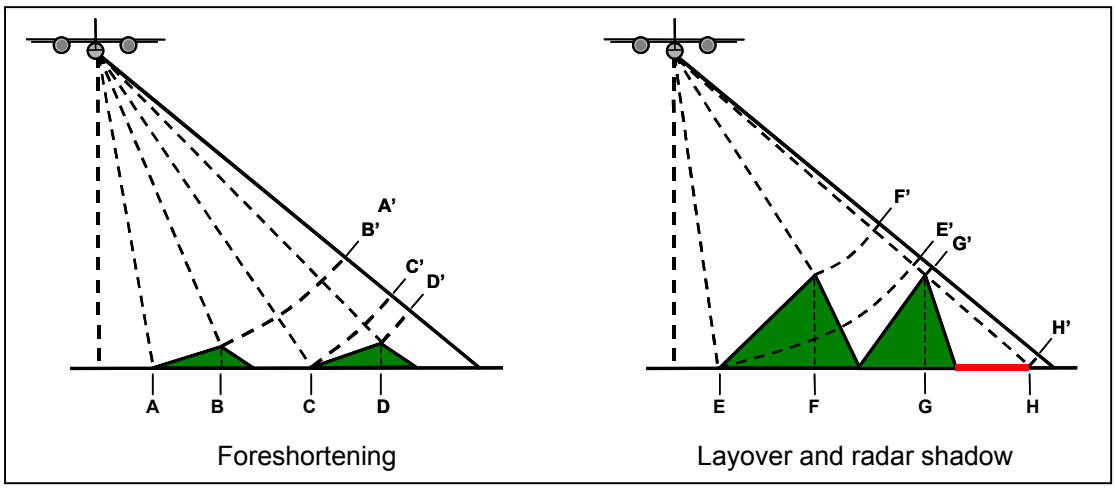

Figure 2: Foreshortening, layover and radar shadow caused by viewing geometry

The viewing geometry also leads to three further effects explained in Figure 2. In ground range distance, the objects A to H have a consequent order. However, in slant range distance, some changes are visible:
The distance between C and D is shortened in slant range projection. This effect is called *foreshortening*. Maximal foreshortening can be seen in objects A and B, where the two points come together as one (A' and B') in the projection.
If a radar pulse reaches the top of a structure before it reaches its bottom, the position in the projection is reversed (E' and F'). This effect is known as *layover*. Layover and foreshortening are most severe for small incidence angles, in near range and in mountainous terrain.
The third possible effect in radar images is *radar shadowing*, represented by points G and H. The radar pulse cannot illuminate any object between those two points, due to the high elevation of G. As a consequence, no information is obtained about this part

of the terrain in the projection. Radar shadow effects increase from near to far range as the radar beam points more obliquely at the surface.

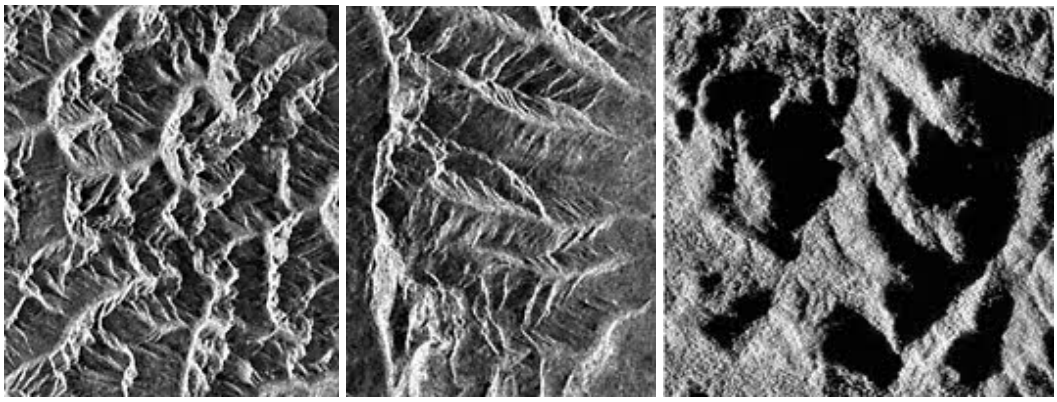

Figure 3: Foreshortening, layover and radar shadow effects in radar images

The appearance of the explained effects in the resulting images is shown in Figure 3. The images show, from left to right, the foreshortening, layover and radar shadow effects in mountainous areas. A detailed description of image distortion effects can be taken from [Leberl, 1990].

A radar system's spatial resolution depends on the specific properties of the applied microwave radiation as well as geometrical effects: the *range resolution* is defined by the length of the radar pulse. Two objects will be resolved if their distance in range is greater than half the pulse length. The *ground range resolution* depends on the incidence angle, i.e. it will decrease with increasing range. The *azimuth* or *along-track resolution* depends upon the beam width and the slant range distance. Because the beam width is inversely proportional to the antenna length, longer antennas produce narrower beams and therefore a finer resolution.

Thus, to achieve a higher overall resolution, two parameters can be changed: Firstly, the radar pulse length can be shortened. This can only be done within certain engineering restrictions. Secondly, the antenna length can be increased. This, also, can only be done to a certain extent, because of size limitations of the airborne or spaceborne platform.

A solution to these limitations can be found by exploiting the forward motion of the platform, employing a so-called *Synthetic Aperture Radar* (SAR). Special recording and processing techniques simulate a longer antenna than the actual one carried aboard. The scheme is depicted in Figure 4.

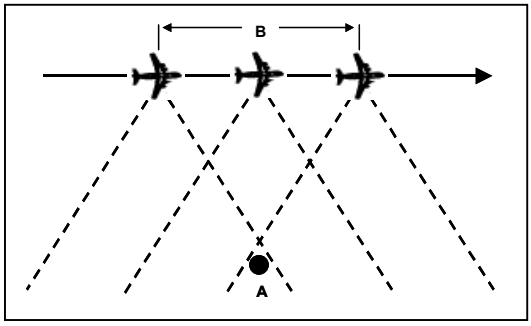

Figure 4: Synthetic Aperture Radar (SAR)

As a target A enters the radar beam, the backscattered pulses begin being recorded. The platform continues moving forward while the echoes returning from the target are recorded during the entire time that the target is within the radar beam. The points where the target enters and leaves the radar beam define the length of the synthesized antenna (B). With increasing distance from the radar, the objects remain longer in the beam, thus compensating the coarser azimuth resolution, leading to a uniform, fine azimuth resolution along the entire swath. SAR is employed by most air- and spaceborne radar systems.
The amount of published literature and documentation on SAR and radar technology in general is increasing constantly. An overview is given by [Long, 2001]. A general explanation can be taken from [CCRS, 2001].

2.2. Airborne and spaceborne radar systems

Radar systems currently in operation can generally be divided into *airborne* and *spaceborne systems*, depending on whether the platform carrying the radar is an aircraft or a satellite. The main differences between both systems arise from the different viewing geometry and swath coverage, caused by the difference in flight or respectively orbit altitude, and their operational flexibility.
To achieve coverage of a significantly large area illuminated by the radar beam, the incidence angle has to be increased the more, the lower the observation altitude is. Larger incidence angles cause, however, higher image distortions, as discussed in chapter 2.1, which is the main problem with airborne systems.
To cover a swath of about 50 to 70 km width, the incidence angle of an airborne system would have to be 60 to 70 degrees, while the spaceborne system's angle would range in between 5 to 15 degrees, causing a much more uniform illumination of the surface and avoiding imaging variations across the swath.
Acquiring imagery from more than one look direction can reduce these effects. Airborne systems are especially well-suited for multi-look operations, their main advantage being a high operational flexibility as they can collect data virtually anywhere and at anytime, and are only limited by flight conditions. In contrast, the

viewing geometry and data acquisition schedule of a spaceborne system is above all fixed to its orbit and therefore very inflexible. However, it can acquire more imagery in less time over a larger area with consistent viewing geometry.
Furthermore, an aircraft's position and variation of motion has to be recorded and calculated precisely in order to correct the radar data acquired. Satellite systems have generally very stable orbits, but corrections of the data have to take into account the earth's rotation and curvature.
Imaging radars were first used during World War II for the detection and positioning of aircraft and ships. In 1950, advances in SLAR and the development of SAR were achieved. The first civilian remote sensing satellite to carry a spaceborne SAR sensor was *SEASAT*, launched in 1978. It was mostly designed for ocean and sea ice observations, but also collected imagery over land areas, having a swath width of approximately 100 km and a spatial resolution of 25m (cf. [Seeber, 1993]).
Missions that followed were the *ERS-1*, launched in 1991 by the European Space Agency (ESA), with a 100 km swath width and 30 m spatial resolution, the *JERS-1*, launched in 1992 by the National Space Development Agency of Japan (NASDA), and *RADARSAT*, launched by the Canadian Space Agency (CSA) in 1995. RADARSAT carries a steerable radar beam, allowing a variation of swaths in between 35 to 500 km width, resulting in resolutions from 10 to 100 m.
An experimental approach on airborne radar, testing new SAR technologies and signal processing, had been conducted by the Microwaves and Radar Institute, a department of the German Aerospace Research Establishment (DLR) in 1995. Their experimental radar system *E-SAR* carried out several experiments using various radar bands.
Experimental research in North America with airborne radar was - among others - carried out by the Canada Centre for Remote Sensing, where the *Convair-580 C/X SAR* system was developed and operated. This system has been in use by Environment Canada since 1996 to detect oil spills and undertake other environmental research.
Two of the first SAR systems used commercially were the *Sea Ice and Terrain Assessment* (STAR) systems 1 and 2, operated by Intera Technologies Ltd., now Intermap Technologies Corp. Primarily designed for monitoring sea ice, the systems were also used to acquire digital terrain data. Both systems operate in the X-band (wavelength of 3.2 cm).
The third generation of this system – STAR-3*i* – offers grey scale images with a spatial resolution of up to 1.25 m and the generation of digital elevation models (DEMs) of 0.5 m resolution, taking advantage of the radar signals' interferometric properties by using two radar antennas. Documentation on DEMs derived from interferometric SAR data (IFSAR) is given by [Mercer et al., 1998]. The operation in P-band mode (wavelengths of 30 to 100 cm) is currently under investigation (cf. [Hofmann et al., 1999]).

2.3. Radar image properties

The appearance of objects in a radar image is dependent on the portion of transmitted energy that is backscattered from the surface. The more energy an object returns, the brighter it appears in the resulting image. The amount of energy returned depends on several parameters defined by the radar system itself (energetic properties, e.g. the type of radar band used) as well as the surface properties. The most important parameters that control the energy – target interaction are:

a) Roughness of the target surface
b) Radar viewing and surface geometry relationship
c) Moisture content and electrical properties of the target

The dominant factor and therefore most responsible for the appearance of a radar image is the target's surface roughness. A surface is considered smooth if the variations in height are much smaller than the applied wavelength.

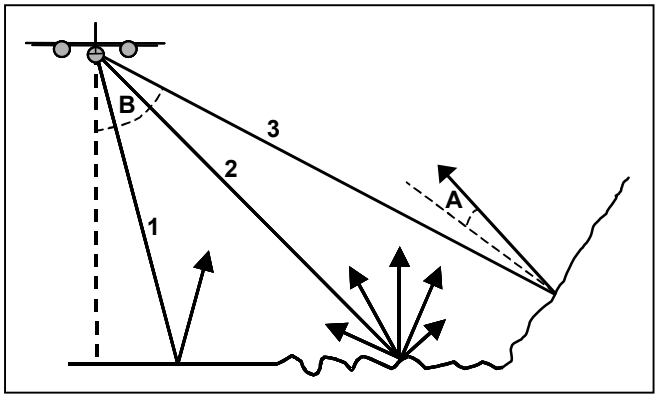

Figure 5: Radar reflection on smooth and rough surfaces

Figure 5 shows the possibilities for a radar signal when reflected by a target: if the surface is smooth, the signal will be reflected away from the sensor, leading to generally low grey values in the image (1). This explains, for example, why roads appear as dark lines (cf. Figure 7, right image). Rougher surfaces usually scatter the received energy into all directions, returning some of the received energy directly back to the sensor, thus leading to higher grey values (2).
Considering the radar viewing and surface geometry relationship, another factor comes into effect. The *local incidence angle*, being the angle between a line perpendicular to the local terrain slope and the incoming radar beam (A), usually differs significantly from the radar's look angle (B) for any terrain with relief (3). Therefore, slopes facing the radar sensor appear brighter than terrain facing away from the system.

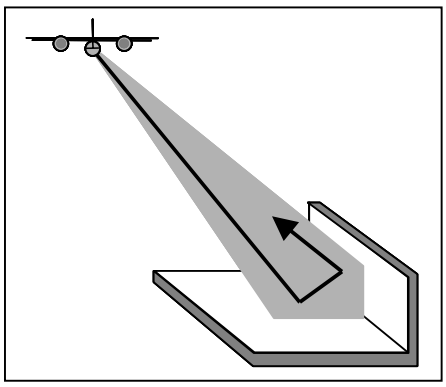

Figure 6: Corner reflector

Furthermore, smooth surfaces at a right angle to each other may cause so-called *corner reflection*, illustrated in Figure 6. The incoming radar beam reaches the first surface, is reflected perpendicularly towards the second surface and is then returned directly to the radar sensor. Thus, corner reflectors appear as very bright areas in the image. While corner reflections may occur in natural areas (e.g. severely folded rock), they are much more likely to be found in urban areas (e.g. buildings, bridges and other man-made structures). In metropolitan areas, image interpretation from radar data can be challenging because of multiple corner reflections. Besides this, artificial corner reflectors are used for surveying purposes, e.g. as reference points in radar images, which enable the orientation and orthorectification of the acquired image.

An important but undesirable effect in radar images is the so-called *speckle*. It occurs mostly in open areas, where small irregular structures (grass, soil etc.) reflect some of the received intensity back to the radar, resulting in a large amount of noise in the grey scale image. This effect can be compared to visible spectrum reflected off a finely structured object, e.g. wind-moved water. Applying different kind of filters to the raw radar image can reduce the speckle effect.

Finally, moisture content in an object can change electrical properties, which leads to changes in its reflectivity, absorption or transmission properties to microwaves. Generally speaking, the reflectivity increases with an increase in moisture. Therefore, radar can penetrate below the surface of an object more easily if it is dry and smooth.

2.4. Differences between radar and optical imagery

Differences between radar and optical data are present in almost all steps from data acquisition to the actual image output.

The *energy source* or *illumination* for optical images is provided naturally by the sun, emitting – besides near and medium infrared waves (0.7 to 0.9 µm) – the whole visible spectrum of electromagnetic radiation with wavelengths from 0.4 to 0.7 µm. Therefore, no active energy generator is needed; the system is working passively.

Radar systems, being active remote sensing systems, generate the energy that is needed to observe the targets themselves, using wavelengths in between 1 mm and 100 cm, the ones used most commonly for imaging being the X-band (2.4 to 3.75 cm), C-band (3.75 to 7.5 cm), L-band (15 to 30 cm) and P-band (30 to 100 cm).
When *interacting with the target*, the reflective properties discussed in chapter 2.3 apply to radar as well as optical radiation. However, because of the much shorter wavelengths in the visible spectrum and the large distance from the illumination source, the radiation returned by the targets is scattered more evenly into all directions. Radar beams, in contrast, are more likely to be reflected altogether, due to their longer wavelengths (cf. Figure 5, chapter 2.3).
More apparent differences between optical and radar imagery arise in *recording* the received energy backscattered by the targets. To store the information received from the surface, optical airborne systems mainly use analogue aerial photographs that are scanned afterwards for computerized image interpretation. Radar data is stored in a digital format directly, as the emitted amount of energy is compared to the received. An image has then to be derived by processing the stored data.

Aerial photograph (1.7 m resolution) Radar image (2.5 m resolution)

Figure 7: Aerial photograph and radar image

Figure 7 shows an aerial photograph with 1.7 m ground resolution and a radar image with 2.5 m ground resolution, covering the same area of 1 km^2 extension. The region mainly consists of urban and open areas. The previously discussed differences concerning radar image properties (cf. subchapter 2.3) are shown. Whereas roads appear generally lighter than their surroundings in the aerial photograph, their appearance in the radar image is darker than the adjacent regions. In the bottom left corner of the radar image it can clearly be seen how houses function as corner reflectors, resulting in extremely bright grey values. A more detailed investigation on appearances of different regions in aerial and radar images follows in chapter 3.

2.5. Areas of application for radar images

The application areas for radar images are generally defined by their advantages in relation to other remote sensing systems. Therefore, the advantages and disadvantages of using radar imagery have to be explained first of all.
As radar sensors do not use the visible spectrum of electromagnetic waves, the radar signal has to be generated by the radar system itself in order to be received again, carrying information about the objects it has interacted with. This fact may seem like a disadvantage. However, two advantages stand against it:
Firstly, as the system only depends upon the signals it generated itself, it does not need natural sources of electromagnetic radiation, like e.g. the radiation provided by the sun. As an active system, it is therefore totally *independent of daylight* and can be operated 24 hours a day.
Secondly, the long wavelengths generated by the radar system enable it to *penetrate* through clouds, haze, fog and dust, as they are not susceptible to be scattered in the atmosphere, which is the case for shorter wavelengths, i.e. the visible spectrum.
Those two properties of microwave radiation allow a *weather-independent* collection of data at virtually any time.
Disadvantages of radar systems are, among others, the image distortions explained in subchapters 2.1 and 2.3: foreshortening, layover, radar shadows and speckle have to be modelled carefully in order to extract useful information from the image. Furthermore, a manual interpretation of radar images is difficult because the appearance of objects differs significantly from what the human eye is used to. Therefore, only experienced operators can interpret radar images correctly, although some ambiguities, leading to misinterpretations, may occur.

Application areas for radar images are numerous. As the mere imaging of the earth's surface can only be achieved up to a certain resolution due to technical reasons, radar technology is a major source for the generation of *digital elevation models* (DEM). To acquire altitude information, the radar signal's phase is observed by two antennas and the phase shift is computed. These systems are known as interferometric synthetic aperture radar (IFSAR). The airborne IFSAR method is used, for example, by Intermap Technologies Corp. in its STAR-3*i* system to generate DEMs with an accuracy of up to 60 cm for certain terrain types and flight specifications (cf. [Li et al., 2002]).
Ortho-rectified radar images (ORRI) can be derived by combining the obtained image data with the DEM acquired simultaneously. ORRIs can be used as base maps for GIS applications or output as hardcopy image maps at scales as large as 1:10,000 (cf. [Tennant and Coyne, 1999]).
Examples for value-added products derived from IFSAR data are *topographic line maps* (TLM). ORRIs and DEMs are used to create a stereo compilation environment within a photogrammetric workstation. [Tighe and Baker, 2000] provide detailed information on the TLM generation process.

Concluding, radar products are used as mere images, for environmental purposes (e.g. flood modelling) and, in a more cartographic context, as information for DEMs, ORRIs and TLMs, enabling the generation of value-added mapping products.

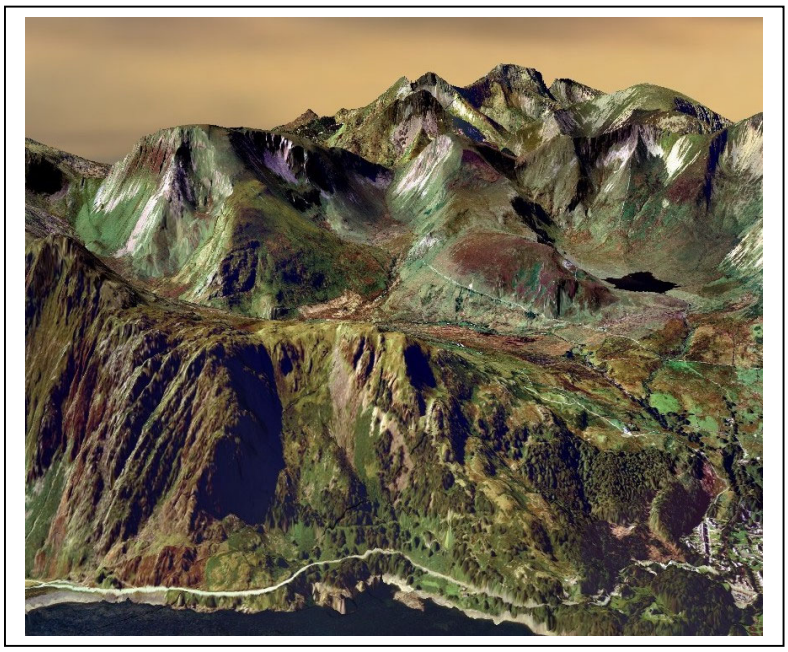

Figure 8: Snowdonia National Park (aerial photograph + radar-derived DEM)

Figure 8 gives an example for a value-added product: a radar-derived DEM was draped over by a coloured aerial photograph of 1 m resolution.

Public interest in radar and the awareness of its possible applications increased significantly when, in February 2000, the National Aeronautics and Space Agency (NASA) launched an 11-day mission to create an almost global data set of land elevation: the *Shuttle Radar Topography Mission* (SRTM). The interferometric radar system was installed on the Space Shuttle Endeavour, one antenna being mounted aboard the shuttle, the other on the end of a 60 meter mast, which was extended from the payload bay once the shuttle was in space.
During the mission, data of 80% of the earth's land surface was gathered in C- and X-band. The released digital elevation models have a ground resolution of 30 meters for the United States and 90 meters for the rest of the world. Further information about this mission is available from the Jet Propulsion Laboratory [JPL, 2003], a subdivision of the California Institute of Technology.

3. Extraction of linear objects from SAR and optical imagery

The extraction of linear features from SAR as well as optical imagery is the main part of this thesis. To adapt an algorithm in order to find the desired results in the type of given imagery, the modelling of roads in the two different sources has to be investigated. Road models for SAR and optical imagery are explained in chapter 3.1. Several algorithms for linear feature extraction have been designed over the last years, employing various approaches. An overview of recent methods is given in chapter 3.2. In chapter 3.3, two of those algorithms are chosen for further analysis and the reasons for the choice are shortly explained.

3.1. Road models for SAR and optical imagery

The first step in automated extraction of roads from any imagery source is the definition of a *road model* for the respective image, as the model defines the appearance of linear structures that will be searched for in the image by the applied algorithm. Therefore, the road model has an immediate influence on whether a real road can be detected as such during the following extraction process: if a linear structure fits the defined road model, it is detected as a road. Furthermore, all other structures that also fit the model, are extracted, although they do not represent real roads. In return, a real road may be rejected if it does not coincide with the defined road model.
As the difference in the appearance of roads in SAR and optical imagery is evident, depending on the sensors' properties and the wavelengths used (cf. Figure 7, chapter 2.4), the two sources will be treated separately from hereon.

3.1.1. Road models for optical imagery

For optical imagery, three major road model approaches have been developed, which are, among others, explained in [Baumgartner et al., 1997] and [Wiedemann, 2002], respectively [Hinz et al., 2000].
It is apparent that one extraction approach cannot serve to deal with all kinds of images. For example, the appearance of roads strongly depends upon the given resolution and is therefore sensor-dependent. While roads appear as narrow lines, composed of only a few pixels in width in low-resolution images (ground pixel size > 2 m), they appear as elongated regions in images bearing higher resolution. Furthermore, it is evident that the road appearance itself varies in different areas. Therefore, *context information* has been introduced in most road models, offering

similar general appearance of roads within the same *context region*. Once the distinction between low and high resolution as well as different contextual appearance has been made, a closer look at different road models can be taken.

The road models proposed by [Baumgartner et al., 1997] and [Wiedemann, 2002] focus on the modelling of context on two levels, a *global* and a *local* one. While global context puts an emphasis on the characteristic parts of the road model in a certain area, taking into account the presence of objects surrounding the road, local context processes explicit knowledge about spatially restricted relations between objects (e.g. buildings, trees, cars, etc.) and the road. Furthermore, [Baumgartner et al., 1997], allow the consideration of high-resolution imagery by employing edge detection algorithms and low-resolution imagery by using a line detection and grouping process. [Wiedemann, 2002] focuses on the model for line extraction only.

In [Baumgartner et al., 1997], the modeling of context is achieved by the use of context regions, which are composed of context sketches:

- The concept of *context sketches* is used for the representation of typical relations between roads and neighbouring objects, e.g. buildings, trees or cars, as well as the effects of occlusion or shadows separating road segments. Context sketches are thus responsible for the local part of the context.
- Because such context sketches do not have to be taken into account in the whole area, *context regions* are introduced, which consist of some – not necessarily all – of the primarily defined context sketches. Context regions are therefore the global counterparts to the local context sketches.

Considering the various sources for local context, it becomes clear that, in fact, the interrelation between both context levels leads to a dependence of local on global context as well. For instance, in a global context consisting of forestry, trees are responsible for shadows, whereas in a more urban global context, buildings and cars may have an influence on the local context.

Explicit knowledge about geometry, radiometry, topology and context is taken into account in the road model used by [Hinz et al., 2000]. In high-resolution images, three levels are observed:

- Firstly, the *real world* level comprises the road network, which is split up into road links and junctions. Lanes are made up of complex junctions and road segments and have to be parallel to each other. A lane segment consists of the pavement itself and the markings, which are subdivided into symbols and long or short line-shaped markings.
- The second level represents the *geometry and material*. The colors of lines and symbols and the structure and type of pavement and junctions represent the 3D shape of the objects as well as their composition.

- The third level, the *image* itself, describes the objects present in the upper two levels. For aerial images, this results in bright lines, symbols and regions.

In low-resolution images, the image level is derived from the real world level directly. Road segments are represented as straight bright lines, while junctions appear as a bright blob.

A composition of both approaches explained above is proposed by [Baumgartner et al., 1999]. However, it is stated that information from local context can only be withdrawn from high-resolution imagery in a satisfactory way, as the objects that make up part of that model cannot be detected in low-resolution imagery.

Nevertheless, in any image, be it of low- or high-resolution origin, the extraction algorithm used has to be chosen considering the context in which the road is situated. Therefore, a *context-driven approach* for road extraction is eminent.

Figure 9: Contextual road appearance in different areas (optical imagery)

Examples for different contextual appearance of roads in aerial photographs are shown in Figure 9. In *open areas*, roads appear as bright thin lines surrounded by generally uniform non-road regions of significantly lower grey values. Road appearance in *urban areas* shows a much more in-uniform distribution of objects surrounding the actual road. The road still appears as a bright line, but here disturbances like driveways, sidewalks etc. are present. The examples given clearly emphasize the need for contextual modelling in road extraction.

3.1.2. Road models for SAR imagery

The investigated road models for optical imagery in chapter 3.1.1 can easily be transferred for use with SAR imagery. Because SAR images generally hold a coarser resolution than optical imagery, roads mostly appear as narrow lines. Roads appearing as elongated regions can therefore only be detected for extremely wide road widths. But, similar to their optical counterpart, SAR images offer different appearances in different surroundings. Therefore, the use of context regions can help in either choosing the appropriate extraction algorithm or in adapting certain parameters for a context-driven extraction.

Considering the local context, disturbing objects like crash barriers, traffic signs and bridges have an immediate influence when applying high-resolution imagery as a data source (cf. [Wessel et al., 2002]), as they act as corner reflectors and therefore disrupt the continuous appearance of the road. Therefore, it is necessary to model the local context for high-resolution SAR imagery.

For low-resolution SAR imagery, in contrast, these local artefacts are not as evident, as a coarser resolution corresponds to a smoother image (cf. [Hinz et al., 2000]). Hence, an explicit local modelling does not seem necessary. Knowing this, the road model has to focus mainly on global context.

Explicit knowledge about geometry, radiometry, topology and context, as in [Hinz et al., 2000] can be taken into account. However, the intermediate level of geometry and material does not come into effect in low-resolution. Here, information about the image level has to be taken from the real world level directly.

Because of the image properties of SAR-derived data explained in chapter 2.3, road segments are represented as straight dark lines, while junctions appear as a dark blob.

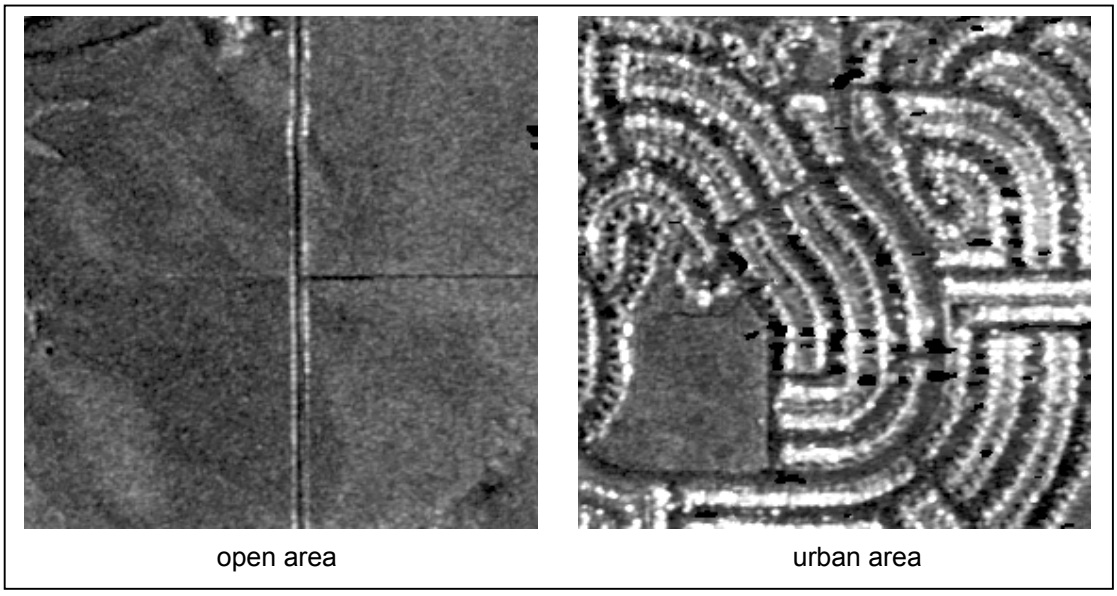

Figure 10: Contextual road appearance in different areas (SAR imagery)

Figure 10 shows examples for the appearance of roads in radar imagery in different context areas. In *open areas*, roads appear as dark lines that may or may not be directly adjoined by a small area of significantly higher grey value. The occurrence of white lines parallel to the road can have various sources: in the example, either hedges or fences are the cause. Furthermore, elevated roads can show high contrast on one side, depending on the flight and look direction. The availability of such disturbing objects actually increases the contrast and therefore leads to better extraction results. However, these effects do not always occur and can therefore not be taken into account for the general open area extraction model. In some cases, roads do not show high contrast against their surroundings. This effect occurs for roads with a structure that does not appear smooth to the radar, e.g. gravel roads. In *urban areas*, roads also appear as dark lines. A high contrast between roads and e.g. houses can be observed. However, the contrast only increases gradually.
The model for SAR imagery depends, however, on the resolution and bandwidth applied, as higher resolution would result in an image less smooth and different bandwidths have a direct influence on the appearance of objects. Summarizing this, it can be concluded that for extraction in SAR imagery, the road model used highly depends on the different global context. Therefore, globally context-driven approaches, employing adapted parameters for different context regions seem appropriate for use in low-resolution imagery of both optical and SAR sources.

3.2. Overview of extraction algorithms for linear features

Automatic extraction of linear features from imagery – be it optical or radar – has been a research topic for several years. First approaches were developed in the early 1980s, e.g. by [Fischler et al., 1981]. In this chapter, however, more recent approaches are dealt with, as road extraction – especially road extraction from SAR – has made increasing progress during the last years.
The following subchapters explain basic principles employed by four different approaches, in a chronological order. Most of these approaches have been designed to be used on different context regions and in images of different origin.

3.2.1. Unsupervised extraction for main road axes

The road extraction approach proposed by [Tupin et al., 1998] implements an almost unsupervised method in order to detect main axes of a road network from low-resolution satellite radar images. The implied road model therefore defines roads as narrow linear structures (cf. chapter 3.1.2).

As a first step, a local detection of linear features is performed, using two line detectors: a *ratio edge detector*, searching for pixels with a higher value than in an a priori chosen threshold and a *cross-correlation detector*, using the correlation between two groups of pixels. The merging of these detectors leads to a unique response and an associated direction for each pixel. Candidate segments are derived from this preliminary detection by further processing.
The second step aims at connecting the road segments found. In addition, certain global criteria are used to refine the generally unsatisfying detection results from step one, as these include only few segments with large gaps, as well as many false positives. The method used to achieve this is based on a *Markov random field* (MRF) model: a priori information about the shape of a road is created by the association of potentials to segment subsets. A *maximum a posteriori probability* (MAP) can be derived from the defined MRF. The MAP criterion then indicates the best graph.
Limitations to this approach occur because of the assumption that all roads can be extracted by connecting the initially detected candidates with segments. Test results have shown that this approach does not seem suitable for hilly areas. However, good results are achieved for flat areas in both an open and agricultural context.

3.2.2. TU Munich road extraction

The extraction approach examined by [Wiedemann, 2002] marks a contrast to the procedure explained in chapter 3.2.1, as it offers a wide variety of controllable parameters, thus representing a more supervised possibility for road extraction. Although the approach was originally designed for optical imagery, this feature enables it to be adapted to images from other sources as well. The applied road model defines roads as narrow linear structures (cf. chapter 3.1.1). Due to the line extraction, this approach is supposed to be applied on low-resolution imagery only.
The extraction procedure is carried out in two steps: in the first step, a preliminary road network is found, using the procedures for extraction of curvilinear structures as described in [Steger, 1998]. Roads are extracted as lines, being brighter or darker than their immediate surroundings. Besides radiometric and geometric properties, topological aspects are considered as well, e.g. global connection criteria. This is achieved by searching for long, connected road segments. This first step can be carried out for more than one image source (e.g. different spectral channels). The results from all of these sources can then be fused to achieve a joined and contingently weighted preliminary road network.
In the second step, an enhancement of the preliminarily extracted road network is performed, using additional network properties. Two main characteristics of road networks are exploited: Firstly, a network is optimized - considering certain restrictions – so that a certain point contained in the network can be reached from any other given point of the network by using the shortest path possible. Path lengths

within a preliminarily extracted network can thus be analyzed to achieve an improvement. Secondly, a given set of roads only becomes a network, if junctions are introduced, which connect these roads. By explicitly reconstructing these junctions, mistakes made by the preliminary extraction can be detected and eliminated, and topologically correct results can be achieved.
Although the algorithm was originally designed for extraction from aerial photographs in open areas, the wide range of adaptable parameters offers a possibility for further use in other context areas as well. However, local context is not modelled at all and is only treated by the closing of gaps during the network generation.

3.2.3. Intermap road extraction

An extraction approach originally designed for SAR imagery is proposed by [Huber and Lang, 2001]. The road model takes into account the linear structures of roads in low-resolution imagery (cf. chapter 3.1.2). The main feature is the application of a so-called *SAR road operator*. The algorithm consists of three steps: Commencing with the extraction of curvilinear structures developed by [Steger, 1998] in order to obtain a provisional road network, it employs the SAR road operator to re-evaluate the results found by the mere line extraction. The road operator comprises two score functions: The first evaluates the presence of road edges, while the second returns a measure for the road center continuity.
The road candidates found by the SAR road operator are further investigated, as an *active contour model* (ACM) is applied to the score image. The model iteratively tries to fit a contour (also known as snake) to the image, in an attempt to find the real road. Because the convergence between real road and active contour model depends upon the contour points initially given, a *genetic algorithm* is used to optimize the contour's starting points.
The algorithm is concluded by a network generation, taking into account collinear and perpendicular reconnection hypotheses as well as a minimum overall length for a road network.

3.2.4. Road extraction from interferometric SAR data

A method for the extraction of linear features from interferometric SAR data is presented in [Hellwich et al., 2002]. The applied road model focuses on narrow linear objects in low-resolution imagery (cf. chapter 3.1.2). As linear objects are often only visible in either the intensity or the coherence image when applying SAR, a fusion of these two sources is carried out by use of a *Bayesian approach*: two vectors – y_1 and y_2 – contain the grey values for pixels of the SAR intensity and coherence images.

The object parameters that have to be estimated for each pixel are either a line state or a no-line state. In the first case, the direction of the line has to be estimated as well. An a priori probability density of these object parameters is then formulated in a *Markov random field* (MRF). The goal is the computation of object parameters, i.e. line / direction / no-line, for which the a posteriori probability is very high. Energy values are then derived for each pixel.

The line extraction is later carried out by use of a template with one line zone and two adjoining side zones. This template is centered at each pixel and the line zone is rotated to handle differing line directions. As a result, line pixels with a line direction and no-line pixels are detected. Additionally, a posteriori probabilities for the most probable line state in relation to a no-line state are computed for each pixel.

Those probabilities are then used for a so-called snake-based linear feature extraction. The position of snakes, also known as *active contour models* (ACM), is determined by an *energy minimization approach*, representing internal smoothness and curvature as well as the grey values' gradient.

As the last step of extraction, the so-called *zip-lock principle* is applied, allowing human interaction not only to define the snake's end points but also at points of high curvature, to achieve a close proximity to the linear feature during the whole optimization.

3.3. Selection of algorithms for further examination

Besides the methods explained in chapter 3.2, several other approaches for automated road extraction have been made during the last years.
For instance, [Cornelis et al., 2000] use a two-step model-based approach. By exploiting local information related to geometric and radiometric properties of the structures to be extracted, a set of line segments is provided. The following segment linking process incorporates contextual knowledge and organizes the line segments as a graph. The graph's nodes are labelled and modelled as an MRF. The linear feature extraction is completed by an MAP estimation.

Generally speaking, the selection of an algorithm for further testing strongly depends on the adaptability and suitability for the images used. As the resolution of any image directly influences the appearance of roads as lines or region-like objects, and as the context is of high importance, extraction algorithms taken into account have to be flexible enough to cope with the given problems.
Two algorithms have therefore been chosen for further testing:

- The road extraction algorithm applying an operator fusion, developed by R. Huber and K. Lang at Aero-Sensing Radarsysteme GmbH, now Intermap Technologies GmbH Wessling. This algorithm was especially designed for urban road extraction from SAR imagery. The possibility of changing certain parameters within the algorithm to adapt it to certain images makes it suitable for a context-driven approach.
- The road extraction algorithm designed by C. Wiedemann at the TU Munich. It offers a wide variety of parameters to supervise the extraction itself as well as its evaluation. The parameters may also be used for adapting the algorithm to cope with different global contexts. Furthermore, the ability to fuse data from different channels makes it eligible for an enhanced form of road extraction.

Because the available images offer resolutions of 2.5 m for radar source and 1.0 m for aerial photographs, a line-shaped extraction approach is possible only. Both algorithms have been designed for this. The orthorectified images were re-scaled to a resolution of 1.7 m to allow an optimal work-flow for both the algorithms themselves as well as the occurring computation time.
A detailed description of both algorithms follows in chapter 4. The practical analysis is explained in chapters 5 and 6.

4. Extraction algorithms

This chapter offers a more detailed explanation of the two extraction algorithms chosen for further investigation in chapter 3. Because the consideration of global context and its acquisition is important for further investigation, the chapter commences with an overview about these subjects. Following, the general approaches for both algorithms are shown, and a presentation on how global context can be considered by them is given. Concluding, the necessary adaptations for optical and SAR imagery, respectively, are discussed.

4.1. Acquisition of global context

In order to carry out extraction procedures that take into account the global differences within a site, context regions have to be acquired. The use of context regions enables the application of separate road models that are especially suited to areas with similar radiometric appearance. Therefore, improvements in the extraction results can be achieved.
Generally, three different possibilities for the acquisition and generation of global context regions exist:

- *Derivation of context regions from an existing GIS:*
  If an existing GIS with region-like objects is already available, these regions can be summarized to several context regions. [Butenuth, 2002] and [Busch and Willrich, 2002] exploit information given by the German ATKIS. [Butenuth, 2002] derives six context regions (urban, agricultural, special crops, pasturage, forestry and small textures) from 109 region-like objects contained in ATKIS.
- *Creation of context regions by extraction of global context knowledge:*
  An alternative to the derivation of context regions from an existing GIS is presented by [Straub et al., 2000]: Here, knowledge about the global context is extracted using an enhanced multispectral classification. As a result, four different classes are determined: settlement, open landscape, forest and water.
  Additionally, commercial products like ERDAS IMAGINE (Leica Geosystems) or eCognition (Definiens Imaging) can also be used to solve the task of detecting regions of similar appearance.
- *Manual digitizing of context regions:*
  In contrast to the two possibilities presented earlier, this is a non-automatic approach. The manual digitizing of context regions requires a trained user who identifies regions of similar contextual appearance and then digitizes them point by point. This procedure can be very time-consuming, especially if

the regions' borders are complex. Therefore, it can only be recommended if the automatic procedures fail or are not available.

4.2. Intermap extraction algorithm

The extraction algorithm developed by K. Lang at Intermap Technologies GmbH Wessling, consists of three steps: Firstly, regions of interest for further investigation are identified. This is followed by a fusion of two basic road feature detectors. In the final step, the higher level road model is generated.
An explanation of the general approach is presented in chapter 4.2.1. The measures taken to consider differing global context are shown in chapter 4.2.2. Concluding, the necessary adaptations for applying the algorithm on optical imagery are given in chapter 4.2.3.

4.2.1. General approach

The Intermap extraction approach offers some alterable parameters in order to adapt the implied road model (cf. chapter 3.2.3) to the given image. The whole process is controlled by so-called "lua"-files, which are part of a higher programming language and hold all parameters (cf. [Tecgraf, 2002]). An overview is given in Table 1.
Following, the alterable parameters are explained in detail:

- To model the *differential geometry*, the line detection algorithm developed by [Steger, 1998] is used. It searches for curves with characteristic two-dimensional profiles. In reality, the changes of grey values in an image occur discontinuously. In order to apply differential geometry, rounded grey value profiles are assumed by the application of Gaussian kernels. While the original approach by Steger employs contrast values (cf. chapter 4.3.1), the use of differential parameters is employed here. A candidate for a line can then be found by defining two conditions:
  a) p'(x,y)=0: The first partial derivatives of pixels belonging to a supposed line must be equal to zero. This represents a non-existent slope of the curve in that point.
  b) p''(x,y)=max/min: The second partial derivatives in the same point should reach a maximum or minimum in order to ensure that the curvature in the respective point is significant.

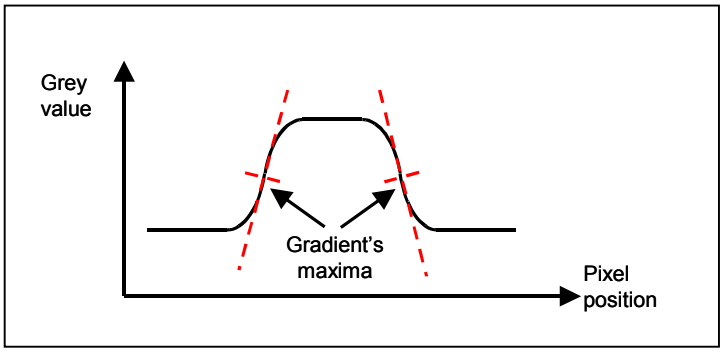

Figure 11: Line width determination

In order to detect the line's width, the gradients' maxima have to be determined (cf. Figure 11). The calculated line width is the distance in between these maxima. An important phenomenon can be derived from the figure: if the line profile's gradient is weak, the maxima are significantly shifted away from the true line width. This has to be taken into account when using this extraction approach on imagery with low contrast, e.g. SAR imagery.

- Six parameters are available to control the *low-level feature extraction*. The maximum value for the first and the minimum value for the second derivative can be defined, as well as the maximum distance in between the two. Parameter four reflects the size of an applied blur filter. Different line widths can be modelled in one single process. The fifth variable defines the number of widths investigated during the line extraction. The last parameter, sigma, represents the line width itself.
  In order to model different contextual appearance as well as different imagery sources, the first and second derivatives are of highest importance, as they define the change rate in grey value that decides whether or not linear structures are detected according to the road model. Together with sigma, which represents the line width that is searched for, these parameters offer possible contextual and image adaptations.

- The following steps carry out image-related processes like erosion and a histogram equalization of the eroded image. However, no changes can be made to these parts in the lua-files.

- The main feature of this extraction algorithm is the application of a so-called *SAR road operator*. The objective is an enhancement of the previous line detection.
  Roads often appear as central homogenous regions, which are neighboured by two homogenous regions to either side. In this approach, masks representing this model are overlaid on the previously detected road pixels.

The mask is then rotated and calculated for each direction: the central and the adjacent regions are divided into three subregions and the mean values are calculated for each subregion. By doing so, an evaluation for the previously extracted lines is carried out. A high score is given to regions that provide a great amount of uniformity in the line's direction and a significant distinction to their surroundings. These procedures are based on the Duda road operator (cf. [Fischler et al., 1981]). Two functions are then calculated:

a) The *road edge scoring function*, which is defined as:

$$F(r) = \begin{cases} \frac{1}{6} & r \geq e_2 \\ M - \frac{M-\frac{1}{6}}{e_2-e_1}(r-e_1) & e_1 < r < e_2 \\ M & r \leq e_1 \end{cases} \quad (1)$$

M is the maximum score that can be achieved, e_1 and e_2 are the lower and upper edge detection thresholds for the ratio. While everything below e_1 is considered to be no edge, values greater than e_2 are considered to be an edge. In between e_1 and e_2, values between 1/6 and M are assigned.

b) The *road uniformity scoring function*, which is defined as:

$$G(r) = \begin{cases} 1 & \frac{1}{u_1} < r \leq u_1 \\ 1 - \frac{1-\epsilon}{u_2-u_1}(r-u_1) & u_1 < r < u_2 \\ \frac{1-\epsilon}{\frac{1}{u_1}-\frac{1}{u_2}}(r-\frac{1}{u_2}) + \varepsilon & \frac{1}{u_2} < r \leq \frac{1}{u_1} \\ \varepsilon & r \geq u_2 \text{ or } r \leq \frac{1}{u_2} \end{cases} \quad (2)$$

In this function, ε is the minimum score; u_1 and u_2 are the lower and upper uniformity detection thresholds for the ratio. Everything below u_1 is considered to be uniform; everything above u_2 is not uniform. In between u_1 and u_2, values between ε and 1 are assigned.

These two functions are then fused to the *score function*, applying the following equation:

$$S = \frac{G(\frac{a_1}{a_2}) \cdot G(\frac{a_2}{a_3})}{\sum_{i=1}^{3} F(\frac{b_i}{a_i}) \cdot F(\frac{c_i}{a_i})} \quad (3)$$

The center region's mean values are a_i, while b_i and c_i reflect the adjacent regions. The indices 1 through 3 represent the different subregions.
The application of these three functions to the road candidates derived from the line extraction reflects the *SAR road operator* (cf. [Huber and Lang, 2001]).
Alterable parameters are M – the maximum value in the road edge scoring function – and ε – the minimum value in the uniformity scoring function.

Furthermore, the upper and lower thresholds within those two functions can be defined. Additionally, the applied mask extension, consisting of the road width, a guard strip and the adjoining regions' width, can be changed.
In order to adapt the algorithm to different imagery sources and context regions, the highest priority is to be seen in the extension of the mask size, which has to be changed to the according line width, defined earlier by the Gaussian sigma. The values for M and ε, as well as their respective thresholds, do not have to be changed, because they are only used for an internal evaluation and have no outcome on the extraction. They can therefore be used universally.

- The generation of the road network is split into three separate steps: *collinear* and *perpendicular reconnection* and *final trimming*. The conditions for collinear reconnections are the adherence of a defined distance as well as minimum values for the angles in between two endpoints. Perpendicular reconnection is permitted if a defined distance is not exceeded and the deviations of the junction's angles do not exceed a certain value.
  To alter the conditions for collinear reconnection in the parameter file, the upper and lower thresholds for the absolute and relative distances in between the endpoints can be set. Furthermore, a trapezoidal fuzzy evaluation for the angle is carried out. For further explanation of fuzzy functions refer to chapter 4.3.1. For the perpendicular reconnection, the same alterable parameters are given respectively. Additionally, conditions for a line's directional deviation towards the supposed connection are permitted.
  By trimming of the network it is assured that only such new networks are generated that exceed a certain overall length.
  The parameters to be changed for different global contexts and imagery sources are mainly the distance in between possible reconnections and the value for network trimming, as these values can differ significantly in the applied road model, depending on the global context.

The stated alterable parameters within the Intermap extraction software do not all have to be considered for adaptation to model contextual variations or different imagery sources. A closer look on the treating of global context is presented in chapter 4.2.2. The possible alterations for a different imagery source are explained in chapter 4.2.3.

4.2.2. Consideration of global context

Automated road extraction leads to better results if the used extraction algorithm is adapted to the global context it is applied to (cf. chapter 3.1). For a closer investigation on the application of global context, refer to chapters 5.1.2 and 6.1.2.
The extraction software developed at Intermap Technologies GmbH Wessling does not consider global contextual modelling within the program itself, as it was primarily developed for use on urban areas only. However, the number of alterable parameters shows that different contexts may be modelled as well.
The context regions to be used have to be generated manually, if no other source is available. In this thesis, this was done by digitizing regions of similar contextual appearance from the available aerial imagery within a MapInfo® environment.
The program has to compute one or more whole images with the same parameters at a time. Therefore, one suggested approach is to process the images for each global context separately and later assign the results to the respective context regions within a MapInfo® environment. The parameters used for the different regions are displayed in the appendix. A more detailed explanation on practical handling of context is given in chapters 5.1 and 6.1.

Parameter	Default value	Unit	Remarks
Differential geometry			
Upper threshold for p'(x,y)	0.1	---	1st partial derivative
Lower threshold for p''(x,y)	0.55	---	2nd partial derivative
Distance thresholds	0.5	Pixels	Max. distance allowed in between derivatives' extremes
Blur filter size	5	Pixels	Size of blur filter
Number of sigmas	1	---	---
Sigma (σ)	3.5	Pixels	Size of Gaussian blur filter ($\sigma = \frac{b}{2\sqrt{3}}$)
SAR road operator			
Maximum edge score	1.5	---	M
Minimum uniformity score	0.1	---	ε
Lower uniformity threshold	1.0	---	u_1
Upper uniformity threshold	2.0	---	u_2
Lower edge detection threshold	100.0	---	ε_1
Upper edge detection threshold	101.0	---	ε_2
Adjacent region	7	Pixels	Total mask size: 25 pixels
Guard strip	2	Pixels	(2·adjacent region + 2·guard strip
Road region	7	Pixels	+ road width)
Collinear reconnection			
Lower absolute distance threshold	20.0	Pixels	---
Upper absolute distance threshold	30.0	Pixels	---
Lower relative distance threshold	1.0	---	---
Upper relative distance threshold	3.0	---	---
Collinearity evaluation	150.0 170.0 190.0 210.0	Degrees	---
Perpendicular reconnection			
Lower absolute distance threshold	5.0	Pixels	---
Upper absolute distance threshold	20.0	Pixels	---
Lower relative distance threshold	1.0	---	---
Upper relative distance threshold	3.0	---	---
Perpendicular evaluation	60.0 80.0 100.0 120.0	Degrees	---
Deviation of direction	150.0 170.0 190.0 210.0	Degrees	---
Network trimming			
Minimum length of network	100	Pixels	---

Table 1: Alterable parameters for Intermap extraction algorithm

4.2.3. Adaptations for use with optical imagery

The extraction software developed by K. Lang was originally designed for use on SAR imagery only. However, with certain adaptations to the parameter files as well as the image, usage on optical imagery can be applied as well.
Because roads in optical imagery generally appear brighter than their surroundings, as explained in chapter 3.1.1, the model applied by the algorithm has to be adapted accordingly. This is, however, not possible by altering the parameter files; it can only be done by changing the source code. To overcome this obstacle, a simple image inversion is applied to aerial photographs, leading again to a dark road model. Generally, no other features of optical images are lost by doing so (e.g. high contrast). The SAR road operator can then be applied on those images without problems.
In some cases, roads may originally appear darker than their surroundings. This phenomenon cannot yet be modelled, as the output vectors from two different road models cannot be fused within the Intermap software. Therefore, two separate extraction processes for each model would have to be computed and assembled manually.
Because of naturally good contrast between road and surroundings, parameters to be investigated are e.g. the second partial derivatives. A closer look on appropriate changes follows in chapter 6.1.
The changes in the parameter files are generally restricted to image-related variables. The generation of the road network, including the collinear and perpendicular reconnection and the trimming, is not affected, as changes to the real world model cannot occur by only changing the type of sensor.
A closer investigation on the extraction of roads from optical imagery using the Intermap approach is carried out in chapter 6.1.

4.3. TU Munich extraction algorithm

The extraction algorithm designed by C. Wiedemann at the Chair of Photogrammetry and Remote Sensing, Technische Universität München (TUM), comprises a low-level feature extraction and a high-level evaluation and generation of the road network by employing a parameter-supervised method.
An explanation of the general approach is presented in chapter 4.3.1. The measures taken to consider differing global context are shown in chapter 4.3.2. Concluding, the necessary adaptations for using the algorithm on SAR imagery are given in chapter 4.3.3.

4.3.1. General approach

The TUM's extraction algorithm offers a wide variety of alterable parameters, enabling a change of the road extraction's model and hence an optimization for the results of the road extraction. An overview of the different parameters is displayed in Table 2.
The parameters that can be altered in order to enable applications in different context regions and in different image sources (cf. chapter 3.1) are of special interest. Following, the distinct parameters are explained in detail:

- The component *"extr_lines"* represents the low-level linear feature extraction, employing the grouping algorithm developed by [Steger, 1998]. This being an approach of differential geometry, it is taking into account local radiometric properties of the road model.
  The first two parameters of Table 2 offer a choice of whether the extraction is run with or without visualization and whether to extract inside or outside a defined mask.
  The remaining parameters reflect the desired road model. When using the optional parameter THRESHOLD, only pixels below or above the defined value are taken into account. This depends on the parameter LINE_BRIGHTNESS, which can either be chosen as "dark" or "light". If "dark" is chosen, only those pixels below the threshold are taken into account; for "light" this applies reversely. Therefore, a decision can be made about whether darker or brighter roads shall be extracted, in relation to their surroundings.
  By choosing a certain LINE_WIDTH, the extraction is restricted to those lines being narrower than the defined value. This is achieved by the computation of the line width and the given resolution to result in σ, used for the applied Gaussian filter.
  Roads are considered to show relatively high contrast to the surrounding objects perpendicular to their direction, while in the collinear direction the grey value distribution is supposed to be homogenous. These two general properties are modelled by the following two parameters: the parameter CONTRAST_HIGH defines the contrast that is necessary to decide whether a pixel can be considered to be a potential line pixel in relation to its neighbouring pixels and therefore part of a road. This parameter is especially important and has to be adapted in accordance to the road model applied. For imagery and global context regions that bear high, sharp contrast, the value can be chosen relatively high, while for imagery or context regions of low and soft contrast the parameter has to be lowered to generally smaller values in order to cope with the properties related to the respective road model. The parameter CONTRAST_LOW defines the change of grey value along the line pixel chain. If this value is exceeded, the continuous line pixel chain is broken up in that point.

Concluding, the component “extr_lines”, being the first step of the whole extraction algorithm, decides upon how many lines are taken into account for the following high-level evaluation. By carefully choosing appropriate parameters, the number of false positive extractions (lines that coincide with the defined road model without actually being roads) can be restricted to reasonable numbers. Therefore, a parameter selection that suits both the contextual behaviour as well as the image’s properties, is of outmost importance, as the high-level evaluation is based on the results found here.

- The component *“smspl_lines”* applies a smoothing and splitting procedure to the candidates found by the preceding line extraction. The reason for splitting lines at a point of high curvature is that the objects’ properties often change in these points, e.g. the road type or road width (cf. [Wiedemann, 2002]). The parameter SMOOTH_LENGTH defines the length of the linear regression line that is used to smooth the line pixel chains. The parameter MAX_CURVATURE reflects the maximum curvature a line pixel chain can attain without being broken up in that point. As the smoothing facilitates further processing and the definition of a maximum curvature is not restricted to a road model, these parameters do not have to be altered for differing contextual appearance or imagery sources.

- The component *“fuzzy_lines”* carries out a fuzzy evaluation for the pixel chains. The evaluation is composed of five sub-evaluations, each of which can assume values between 0 and 1.

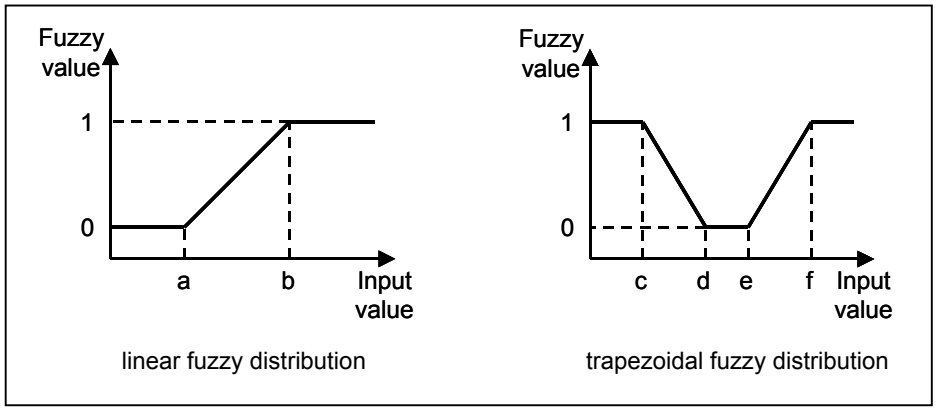

Figure 12: Fuzzy functions

Two possible fuzzy functions are employed. They are shown in Figure 12:
A *linear fuzzy distribution* defines two values a and b. The fuzzy value of an input variable is 0 if it is smaller than a. If it is greater than b, the fuzzy value equals 1. In between a and b, a value between 0 and 1 is assigned linearly to the input variable.

A *trapezoidal fuzzy distribution* defines four values c through f. For input variables smaller than c and greater than f, the fuzzy value is 1. The fuzzy value for input variables between d and e is 0. In between c and d, the fuzzy value decreases linearly, while in between e and f a linear increase is assigned. An inversion of the linear and trapezoidal fuzzy distributions can be applied as well.

The parameter FUZZY_LENGTH is defined by two values, thus applying a linear fuzzy distribution to the input variable. This parameter has to be adapted according to the contextual modelling of roads, as the road segments are, for instance, shorter in urban than in open areas.

The parameter FUZZY_ORIENTATION controls the linearity of the pixel chains. Because roads are generally linear, contextual adaptation does not seem necessary.

The actually extracted line width is evaluated by the parameter FUZZY_WIDTH. A trapezoidal fuzzy distribution is employed to evaluate the possible deviations from a desired optimal line width as defined in the road model. Because of the earlier extracted pixel chains that were determined by the line extraction, this parameter highly depends on the values defined in the component “extr_lines”, as they have already had an effect on the maximum line width.

The parameter FUZZY_WIDTH_DEVIATION allows an evaluation for the deviation of the line width, while FUZZY_GRAY_DEVIATION provides a fuzzy measure as to how much the pixels may deviate from the mean grey value. Both parameters do not have a great influence on context-driven extraction.

The final fuzzy evaluation is a composition of all five single fuzzy values. Assigning meaningful values to the parameters in this component can support a context-driven extraction and lead to satisfying evaluative results that are needed in the succeeding components.

- The possibility of fusing data originating from different spectral channels or different sources is given by the component *“fuse_lines”*. The sources can be weighted distinctly by assigning individual weight values in the parameter WEIGHT_SCALES. For the decision whether two lines are to be fused or not, the parameter BUFFER_WIDTH offers the definition of a buffer size. Additionally, a maximal divergence in the lines’ directions can be assigned. If the buffers of two lines coincide and their direction difference is not greater than the value defined, those lines will be fused to one.

  The possibility of merging lines from different channels is one of the important features of this algorithm and is investigated more closely in chapter 6.5.

- The component *“split_lines”* generates a new junction if a line’s endpoint is close to a neighbouring line. The parameter DISTANCE defines the maximum distance an endpoint can be apart from a line in order to insert a new node

into that line. New nodes are necessary in order to close possible gaps within the road network, which will be carried out by the following component.

- The final step in the algorithm is the creation of the road network, using the component *"calc_paths"*. Potential connection hypotheses are generated in between seed points, taking into account the evaluated lines. Various parameters control the network generation:
  The parameter FUZZY_ABS_DISTANCE checks the absolute minimum and maximum length of a gap in between two extracted end points in order to create a connection. Its relative counterpart, FUZZY_REL_DISTANCE, controls the length of a gap in relation to the shortest extracted line adjacent to the respective gap. The higher the tolerances for closing gaps are chosen, the more false connections may occur. Therefore, this parameter highly depends on the context region used and has to be altered accordingly. Additionally, gaps being smaller than the lower value in FUZZY_ABS_DISTANCE, the parameter for collinearity is not taken into account.
  In order to join two connections in their respective directions, the parameter FUZZY_COLLINEAR requests a minimum and maximum collinearity. The parameter for perpendicular connections is FUZZY_JUNCTION, which defines the minimum and maximum angle allowed in between two lines at junctions in order to be considered for later connection.
  Whether or not a connection from an endpoint to a line is actually created, is defined by the parameter MAX_DIST_JUNCTION. If the distance in between the two exceeds the defined value, the connection is rejected.
  The parameter WEIGHT_SEEDPOINT reflects the minimum fuzzy value for a line segment in order to be considered as a seed point for the connection hypotheses. It therefore highly depends on the evaluation results from the *"fuzzy_lines"* component.
  The minimum length of the newly generated networks is defined by the parameter MIN_DISTANCE. If one of the independent networks does not reach this overall minimum length, it will not be taken into account for the final output.
  Concluding, the parameters of the component *"calc_paths"* are closely related. As the impact of alterations in context-dependent modelling on the final results is not clear yet, no changes are made for most of the contained parameters. However, the distance in between recognized junctions may differ and has to be adapted accordingly. Further investigations on context-dependent controlled extraction are presented by [Butenuth, 2002].

The explained parameters within the different components of the TUM's extraction software are not all to be considered for adaptation to model contextual variations or different imagery sources. A closer look on how global context can be treated is

given in chapter 4.3.2. The possible alterations for a different imagery source are explained in chapter 4.3.3.

4.3.2. Consideration of global context

Because of variations in the contextual appearance, extraction approaches have to be adapted according to the global context in the respective areas.
The TU Munich software offers an easy application of different parameters by the use of masks. The extraction carried out can be restricted to an area either inside or outside the mask (cf. chapter 4.3.1).
A rough distinction of global context can be carried out by defining urban and open regions within the considered area. The context regions can be given by a number of region-like objects within an existing geographic information system (GIS). [Willrich, 2002] uses pre-knowledge given by the German Authoritative Topographic-Cartographic Information System (ATKIS). The numerous objects are summed up to three context classes: rural, urban and forestry.
If there is no GIS present, the context regions can be generated manually. In this thesis, this was done by digitizing regions of similar contextual appearance from the available aerial imagery within a MapInfo® environment. The extraction parameters used for the different regions are listed in the appendix. A closer explanation on practical handling of context is given in chapters 5.2 and 6.3.

Parameter	Default value	Unit	Remarks
Component extr_lines			
WITH_WINDOW	1	---	1=yes 0=no
EXTRACT_INSIDE_MASK	---	---	For extraction inside masks, a file containing the mask regions must be defined at the parameter MASK. For extraction outside a mask, parameter must be changed to EXTRACT_OUTSIDE_MASK.
THRESHOLD	140	Grey scale	Greater values considered if “light”, smaller values if “dark” is applied.
LINE_WIDTH	5.0	Meters	---
CONTRAST_HIGH	40	Grey scale	---
CONTRAST_LOW	20	Grey scale	---
LINE_BRIGHTNESS	Light	---	light / dark
Component smspl_lines			
WITH_WINDOW	1	---	1=yes 0=no
SMOOTH_LENGTH	5.000	Pixels	---
MAX_CURVATURE	0.1	Gradient	---
Component fuzzy_lines			
WITH_WINDOW	1	---	1=yes 0=no
FUZZY_LENGTH	5 50	Meters	---
FUZZY_ORIENTATION	0 20	Degrees	---
FUZZY_WIDTH	2 3 6 10	Meters	If smaller (larger) than 2 m (10 m) then 0, if in between 3 and 6 m then 1
FUZZY_WIDTH_DEVIATION	0 5	Meters	---
FUZZY_GRAY_DEVIATION	0 20	Grey scale	---
Component fuse_lines			
WITH_WINDOW	1	---	1=yes 0=no
WEIGHTS	1.000	---	Assignment of weights to each channel
WEIGHT_SCALES	2 2	---	Assignment of scales to each channel (optional)
BUFFER_WIDTH	20	Meters	Definition of buffer for fusion
DIRECTION_DIFFERENCE	30	Degrees	---
Component split_lines			
WITH_WINDOW	1	---	1=yes 0=no
DISTANCE	5.000	Meters	---
Component calc_paths			
WITH_WINDOW	1	---	1=yes 0=no
FUZZY_ABS_DISTANCE	5 120	Meters	---
FUZZY_REL_DISTANCE	1 8	---	---
FUZZY_COLLINEAR	0 25	Degrees	---
FUZZY_JUNCTION	55 90	Degrees	---
MAX_DIST_JUNCTION	5.000	Meters	---
WEIGHT_SEEDPOINT	0.500	[0 , 1]	Fuzzy value
MIN_DISTANCE	100	Meters	Minimum length for completed road network

Table 2: Alterable parameters for TUM software

4.3.3. Adaptations for use with SAR imagery

The extraction software developed by C. Wiedemann was originally designed for use with aerial imagery. In order to be able to use it with SAR image sources, some adaptations have to be made, which are explained in this chapter.
According to the road model for SAR imagery, described in chapter 3.1.2, roads generally appear darker than their surroundings and – in low-resolution imagery – as narrow lines. Therefore, the parameter LINE_WIDTH in the extraction software's first component has to be switched to "dark". A separate modelling for roads that may appear brighter than their surroundings does not have to be taken into account, because the occurrence of bright roads in radar imagery is highly improbable, as the explanation of radar systems' properties in chapter 2.3 show.
Although the actual road width in SAR imagery does not seem to be significantly different from the road with in aerial photographs, the lack of high contrast surroundings leads to important changes in the line extraction. As stated in chapter 3.1.2, the contrast increases gradually towards the neighbouring buildings. Therefore, the line width to be extracted has to be increased in order to exploit the higher contrast given by adjacent objects.
For rural areas, road widths close to the actual widths can be applied. However, because of the insufficient contrast to the surroundings, the parameter CONTRAST_HIGH has to be adapted accordingly. A decrease of this value leads to more false positive extractions, as the algorithm only models the differences in the grey values. Therefore, the layover effects caused in mountainous terrain may be detected as lines. In open areas, alternatives to this problem cannot be presented, because the surroundings simply do not provide better contrast information.
For urban areas, the same problem arises if the actual road width is taken into account. Because of the low contrast between the actual road and its immediate surroundings, a low CONTRAST_HIGH value would have to be chosen, leading to a high amount of false extractions similar to the effects in open areas. However, a closer look on urban contextual appearance in SAR imagery reveals a possible solution to this problem: the further the distance from the actual road, the higher the grey values become. This effect is believed to be caused by the houses, acting as corner reflectors. The gradual increase from the low grey values representing the road to the extremely high grey values given by the houses provides sufficient contrast. In order to exploit this contrast, the line width has to be increased significantly in relation to the real road width. Therefore, houses can be taken into account as additional information in urban areas, serving as an alternative to the otherwise resulting false positive extractions. However, by doing so, the centerline of the extracted road may differ significantly from the real centerline. Summarizing, less false positives can be extracted at the cost of losing accuracy. This effect has to be considered when changing the parameters for the line extraction.
Because the following evaluation depends upon the preliminary extraction, the parameters for the applied fuzzy functions have to be adapted accordingly. All

following steps, however, do not need to be changed, as they are not imagery-dependent.
A closer investigation on the extraction of roads from SAR imagery using the approach by C. Wiedemann (TU Munich) is carried out in chapter 5.2.

5. Practical analysis of extraction algorithms on SAR imagery

This chapter focuses on the practical analysis of the two extraction algorithms explained in chapters 4.2 and 4.3, using imagery stemming from airborne synthetic aperture radar.
Both approaches are investigated regarding their adaptability to SAR imagery in different context regions. The chapter presents the achieved results and provides an evaluation of the extraction approaches comparing their quality measures and overall handling.

5.1. Intermap extraction algorithm on SAR imagery

The Intermap extraction algorithm was originally designed for automated road extraction on urban areas in SAR imagery. Because an adaptation that takes into account different contextual modelling is supposed to lead to better extraction results within each context region, parameters for open areas are investigated and employed.
Chapter 5.1.1 explains the general test approach for this algorithm, while the results and evaluations are stated in chapter 5.1.2.

5.1.1. Test approach

In order to define general contextual parameters for respective context regions with the goal to enhance the extraction results, the given algorithm has to be tested on a well-defined area with given reference.
The test site used in this thesis is part of the “Highlands Ranch Quadrangle”, an area situated in Douglas County, close to Denver, Colorado (USA). At Intermap Technologies Corp., SAR images are generally derived from the original data using several filters. A final procedure, the root enhancement (or logarithmic transform), is generally applied on any SAR imagery and tends to result in an overall brighter image. Manually digitized road vectors generated from SAR imagery by use of a photogrammetric workstation serve as a reference for the tests. The area covered by the reference data spans approximately 96 km^2. The area coinciding with the available SAR imagery results to less than 80 km^2. In order to enable fast and efficient processing, the SAR imagery is tiled into squares of 2 km x 2 km extension, resulting in 18 tiles, covering 72 km^2.
The contextual consistence of the test site bears urban and open areas only. While open regions cover 58.0 % of the test site’s superficial area, urban regions contain the majority of roads with 78.2 %. The overall length of the road network is

approximately 526 kilometres. 373 kilometres of those, or 70.9 %, are urban roads. More detailed context regions, like forestry or agricultures, do either not cover a significantly large area and are not developed by roads, or do not exist at all and can therefore not be taken under investigation.
The imagery data used was obtained by Intermap Technologies' STAR-3*i* system in a multi-look process and holds a ground resolution of 2.5 m.
In addition to the resulting images provided in this chapter, statistical evaluation criteria are derived. The criteria *completeness*, *correctness* and *quality*, as presented in [Wiedemann et al., 1998], are used to enable a comparison in between the different context regions:

- *Completeness* is defined as the percentage of reference data that is covered by the extracted data. The coinciding amount of reference data and extracted data is the measure of completeness:

$$\text{Completeness} = \frac{\text{Length of matched reference}}{\text{Length of reference}} \tag{4}$$

  Practically, a buffer of a certain extension is created around the *extracted vectors*. The choice for the buffer width generally depends on the geometric uncertainty. For all investigated imagery in this work, however, the buffer width was set to *7.5 meters*. This enables a direct comparison of the imagery's reliability and its usefulness for road extraction. Consequently, this immediately affects the quality measures, as any reference data not situated within the extraction's buffer results in a loss of completeness. Therefore, inaccuracies are expressed *directly* by this quality measure.

- *Correctness* is defined as the percentage of extracted data that lies within a buffer around the reference data. The correctness therefore represents the percentage of correctly extracted road data:

$$\text{Correctness} = \frac{\text{Length of matched extraction}}{\text{Length of extraction}} \tag{5}$$

  Here, a buffer of a certain extension is created around the vectors serving as *reference data*. Again, the geometric uncertainty usually has an influence on the choice for the buffer width. For all investigated imagery in this work, however, the buffer width was set to *7.5 meters*. The effects are the same as above: a direct comparison of the imagery's reliability and its usefulness for road extraction can be derived. Consequently, any extracted vectors not situated within the reference data's buffer results in a loss of correctness. Therefore, inaccuracies have an *immediate* influence on the result of this quality measure.

- *Quality* is defined as a combination of the measures completeness and correctness, representing an overall single measure for the final result:

$$\text{Quality} = \frac{\text{Completeness} \cdot \text{Correctness}}{\text{Completeness} - \text{Completeness} \cdot \text{Correctness} + \text{Correctness}} \quad (6)$$

A visual explanation for completeness and correctness is given in Figure 13. Extracted vectors are displayed in green, reference vectors in red.

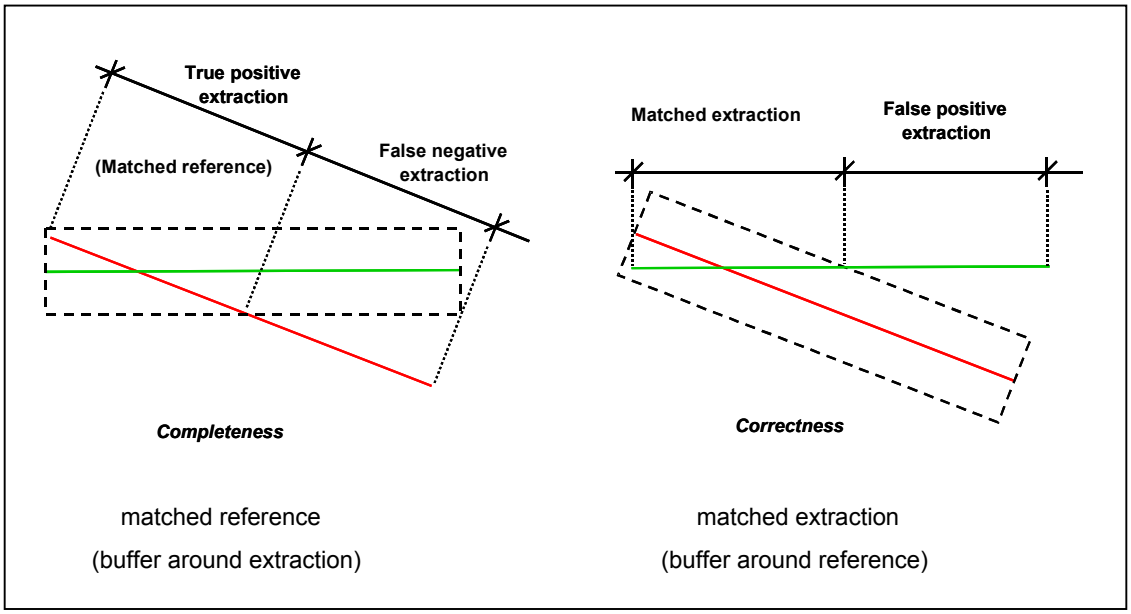

Figure 13: True and false extractions

The case of matched extraction reflects the quality measure *correctness*, while the case of matched reference represents the measure *completeness*.
These quality measures will not only be employed on the extraction approach using SAR imagery, but throughout chapters 5 and 6. Therefore, direct comparisons between all possible combinations of employed extraction algorithms and imagery can be carried out.

5.1.2. Results and evaluation

The extraction approach developed by K. Lang at Intermap Technologies GmbH Wessling does not support extractions restricted to a previously defined context area. Therefore, the suggestions on how to handle global contexts that are explained in chapter 4.2.2 are employed here. In order to obtain a consistent data set for each tile,

the extraction is carried out with urban and open parameters for the whole image. The results are imported into a MapInfo® environment and cut to fit the respective context regions.

5.1.2.1 Results for urban areas

Figure 14 shows a sample radar image with mainly urban context; open areas are masked out in blue.

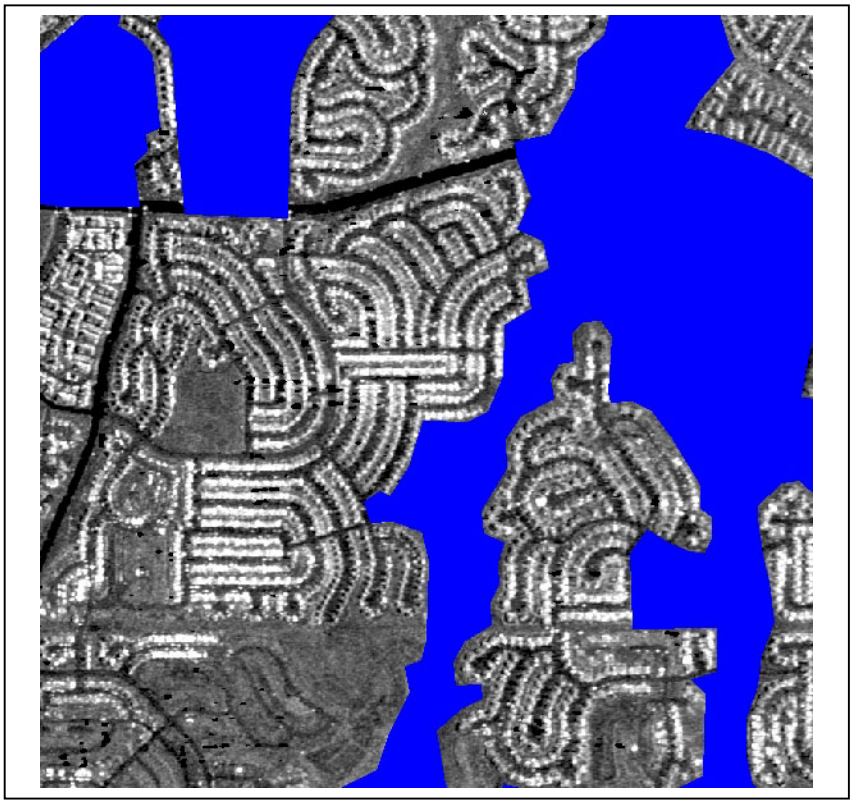

Figure 14: Urban context region (SAR imagery)

The effect of buildings, acting as corner reflectors, can clearly be seen. Roads can be distinguished from other road-like structures (e.g. alleys) that are not part of the reference data.
An example for extracted vectors after the application of the Intermap algorithm and the given reference is shown in Figure 15.

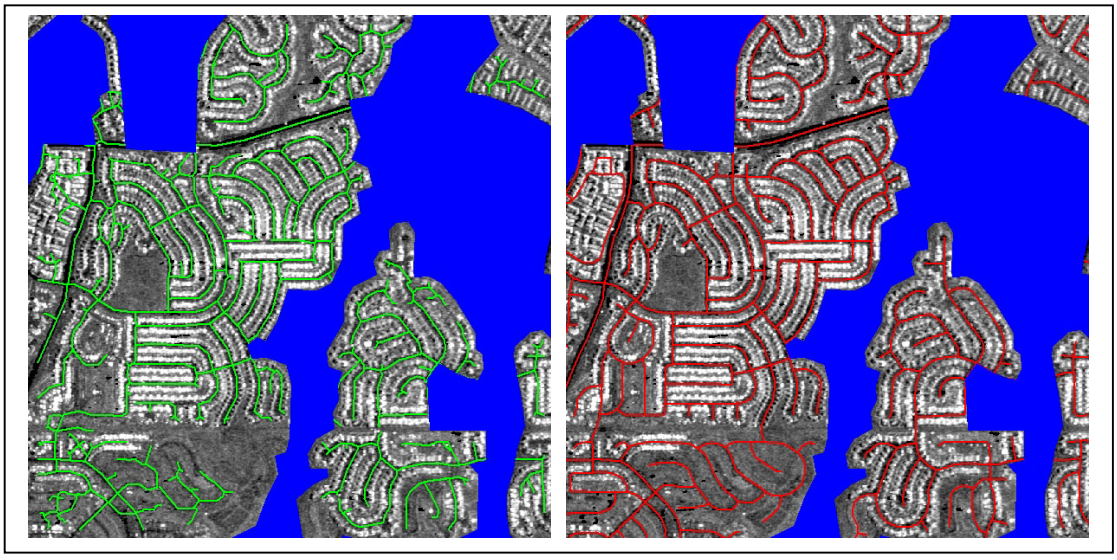

Figure 15: Extraction result (left) and reference (right) in urban areas (SAR imagery + Intermap extraction algorithm)

The images show the extracted roads in green and the manually digitized vector data in red. Regions in blue are not considered as urban areas and therefore not further investigated.
Areas of urban context in SAR imagery are characterized by relatively good contrast, because of the occurrence of buildings that act as corner reflectors, thus resulting in extremely high grey values. As roads bear significantly lower grey values, this contrast can be exploited by the automated extraction. However, it has to be taken into account that the change of contrast from road to buildings does not occur abruptly. In fact, the high grey values are achieved gradually over a wide extension of pixels.

The diagram in Figure 16 shows the smoothed mean grey value distribution for urban roads, perpendicular to their direction. The function is based on 10 randomly picked roads and describes the level of grey value in relation to the distance from the roads' centerlines.

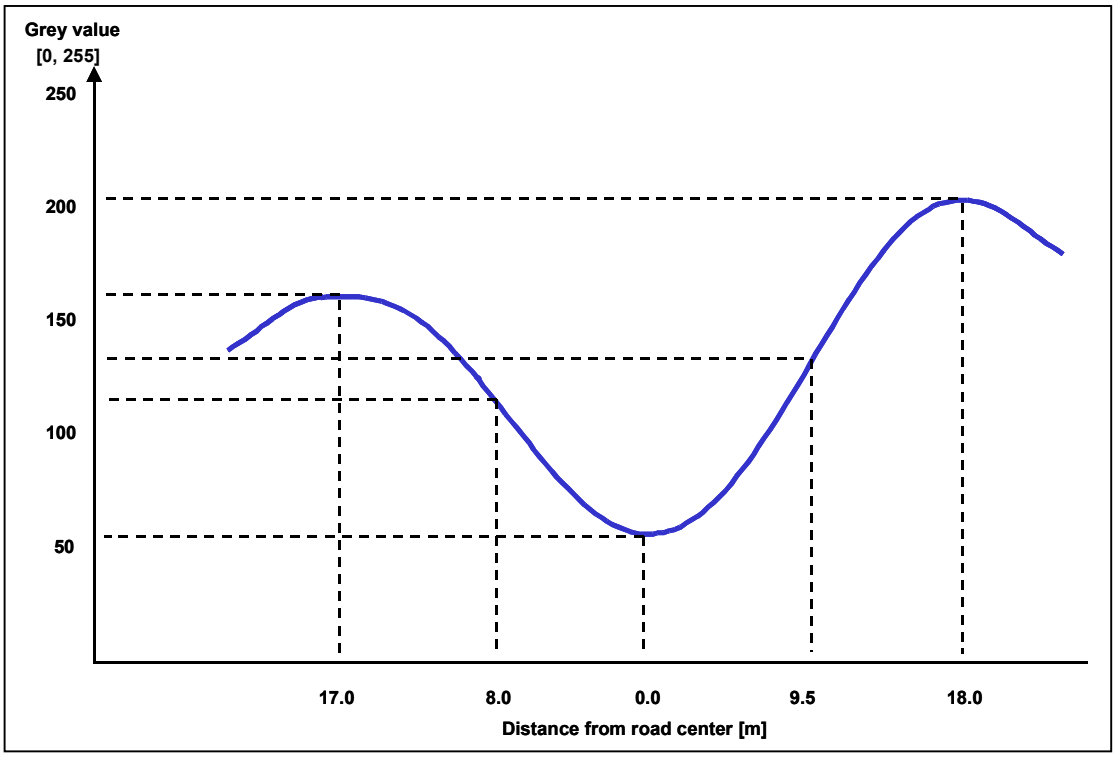

Figure 16: Grey value distribution perpendicular to road direction (urban areas, SAR imagery)

Some important facts can be derived from the diagram:

a) The mean grey value for roads in urban areas varies around 50 to 60, whereas buildings, acting as corner reflectors, may result in grey values in between 160 and more than 200. This leads to an overall average contrast of 100 to 150 in between roads and buildings.
b) The mean distance from road center to buildings, as seen in the radar image, results to 17 to 18 meters to either side, which leads to an average total of 35 meters. It has to be considered that these values are mean values and that in some cases single road widths may differ significantly.
c) The distance in between the function's turning points results to almost 18 meters. This has to be considered for the road extraction parameter that models the line width.
d) The increase in grey value, although offering a high contrast, does not occur suddenly but rather gradually over a wide distance.

These facts show that it is only possible to exploit the given contrast if extremely wide road widths are used. This, however, may result in a loss of accuracy, as the extracted centerline can be significantly shifted away from the true road center. An overview of the parameters altered in order to enable a context-driven extraction is given in the appendix, section A.1.

Figure 15 also shows that the reference data is obviously younger than the radar image: In the lower left corner, already digitized roads are not yet built in the radar image. However, even though those roads are still in the construction process, the extraction algorithm is able to detect some of them. Nevertheless, the accuracy, completeness and correctness cannot be expected to be satisfying in those parts. Such effects influence the statistical results in chapter 5.1.2.3.
A more detailed look on the extracted vectors is provided in the following Figure 17.

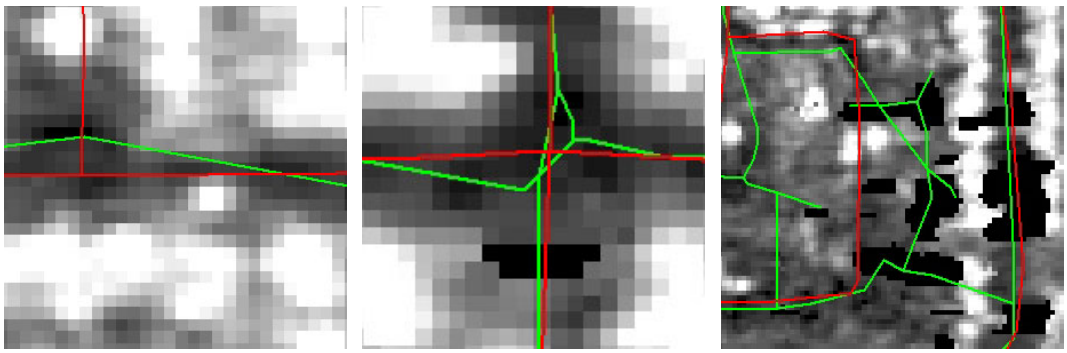

Figure 17: Effects in extracted vectors (urban areas, SAR imagery)

Reference vectors are displayed in red, extracted vectors in green. Three effects can be seen: In the first picture, the previously explained shifting towards pixels of low grey value is shown. Furthermore, the road leading upwards is missed, supposedly because of the bright blob, which could be a vehicle or another structure, acting as a disturbing object. The second picture displays the occurrence of multiple junctions in the extracted data. This effect has not yet been modelled. In the third picture, the results of missing data, e.g. caused by radar shadows, can be seen. The extraction software detects those data gaps as roads, because it does not distinguish between very low grey values that are stemming from actual roads and missing data that simply causes a grey value of zero.
Additionally, Figure 15 shows that no extraction results are achieved in close proximity to an image tile's borders. The area not covered is estimated to stretch 15 pixels inwards from each image border. This general effect is due to the extraction procedure itself and is therefore not context-related. It can only be overcome by creating overlaps in between the tiles. As of now, this overlapping has to be generated manually.
Concluding, it is evident that extraction in urban areas can be, on one hand, supported by the occurrence of buildings acting as corner reflectors, which provide the necessary contrast. On the other hand, radar shadows and disturbing objects may cause a shifting of the vectors and lead to false positive extractions. Furthermore, the modelling of buildings as additional information in order to exploit the contrast bears advantages as well as disadvantages: The application of a high second partial derivative in combination with a high value of sigma leads to the effect

that alleys or backyards are not being detected by the line extraction, because their original contrast is levelled to a lower value. This positive and desirable result has a negative downside: Roads where no adjacent buildings are present can hardly be detected, because the applied model emphasizes on the existence of corner reflectors that supply sufficient contrast as additional information. Using smaller values for sigma, which reflects the road width, in combination with lower values for the second partial derivative, leads to a detection of these roads. However, the number of false positive extractions increases drastically, which worsens the results regarding the correctness. Therefore, it is recommended to exploit the effects given by corner reflections, bearing in mind that urban areas are characterized by the existence of buildings and therefore almost always provide sufficient contrast.

5.1.2.2 Results for open areas

Figure 18 shows a sample radar image with mainly open context; urban areas are masked out in blue.

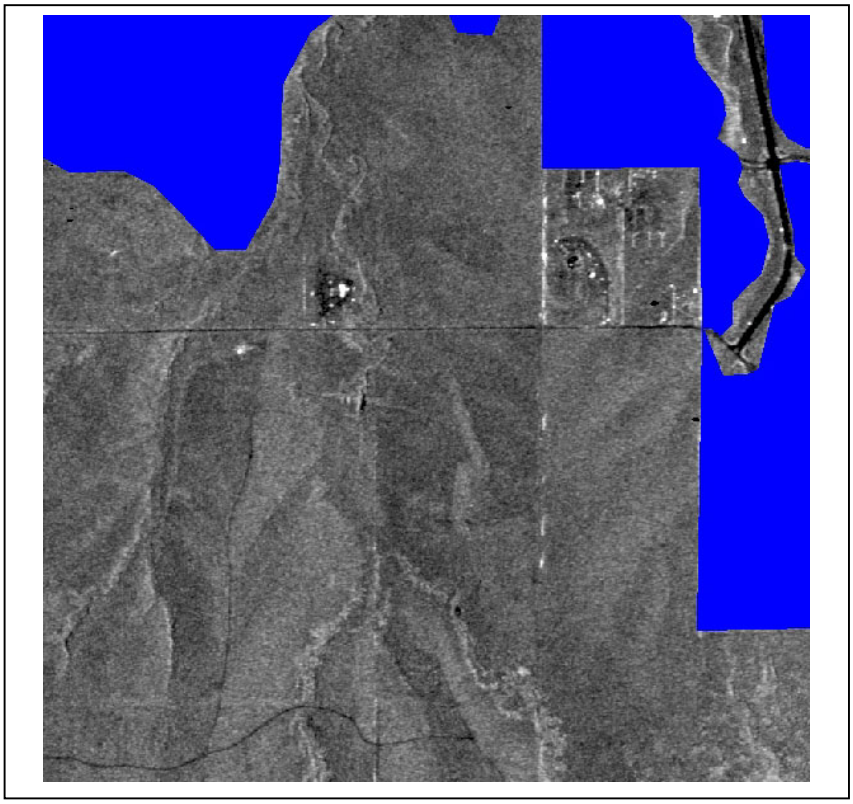

Figure 18: Open context region (SAR imagery)

Generally speaking, open context areas in SAR imagery offer less contrast than the previously explained urban areas, which can clearly be seen in Figure 18. Several causes lead to this effect:

- As explained in chapter 2.3, speckle is caused by the occurrence of small irregular structures like grass, soil etc. This leads to an overall noisier radar image in open areas. Multi-look processing in those areas only results in averaging the grey values, which leads to an overall low contrast. The application of filters to the original image during processing is highly image-dependent and applied manually, according to the amount of speckle present.
- Roads in open areas may not have a plain surface, as they are not always made up of concrete or asphalt, but may consist of gravel or dirt. These reflective properties, which have an influence on the backscattered radar signal then lead to generally higher grey values, similar to those provided by the roads' surroundings themselves.
- Additional information that provides higher contrast does generally not exist in open regions. Buildings serving as corner reflectors can hardly be found,

because they belong to the context region “urban”. Therefore, the procedure used for urban context cannot be applied to open regions.

Figure 19 provides an example for extracted vectors in comparison to their reference in open areas after applying the Intermap algorithm. Extracted roads are displayed in green, reference vectors in red. Regions in blue are urban context areas and are therefore not considered for further investigations in this part.

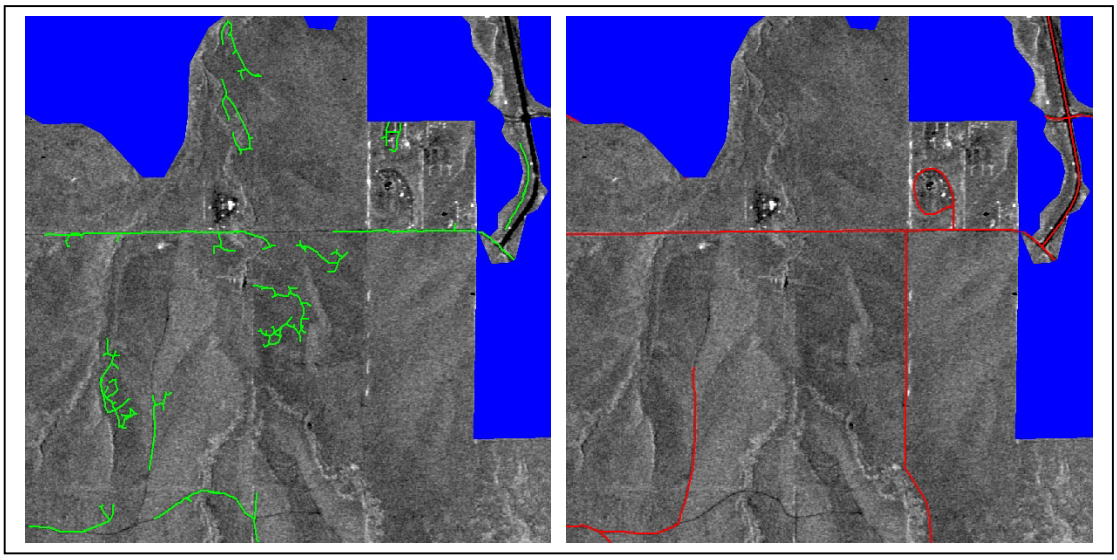

Figure 19: Extraction result (left) and reference (right) in open areas (SAR imagery + Intermap extraction algorithm)

Several effects can be seen in Figure 19. For instance, the extraction algorithm can only detect some of the roads defined in the reference. For instance, the wide road in the upper right corner could not be detected, because the SAR road operator did not consider it for further processing. Additionally, a great amount of false positive extractions can be seen. These occur wherever the partial derivatives set within the extraction parameters are similar to those in the image. Some of the false extractions are eliminated by the application of the SAR road operator and further steps in the higher-level road model. The remaining vectors, however, pass all of these checks and are therefore worsening the overall result.

Figure 20 provides the smoothed mean grey value distribution for open roads, perpendicular to their direction. The function is based on 10 randomly picked roads and describes the level of grey value in relation to the distance from the roads’ centerline.

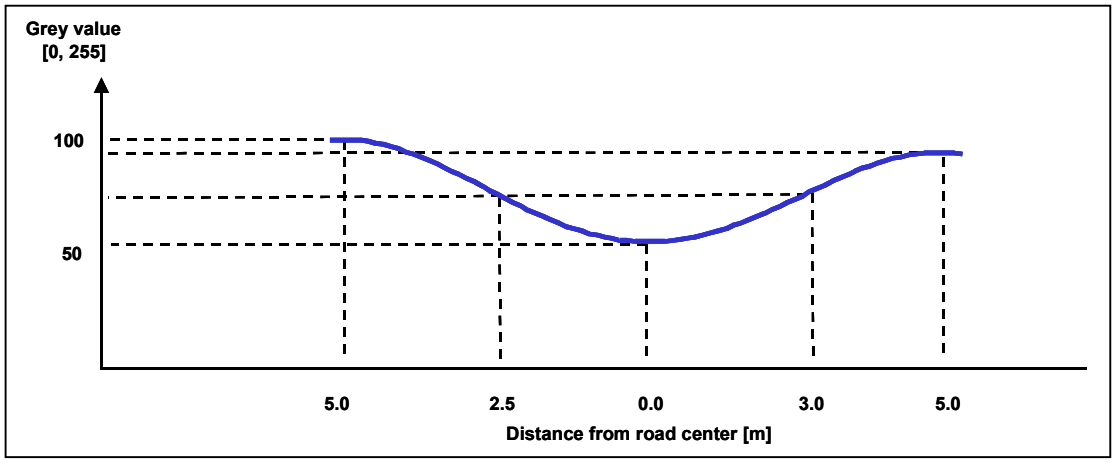

Figure 20: Grey value distribution perpendicular to road direction (open areas, SAR imagery)

The facts that can be seen in the diagram are the following:

a) The mean grey value for roads in open areas varies around 50 to 60, which is within the same range as in urban areas. The overall average contrast, however, varies in between 50 and 60 from road to surroundings.
b) The mean distance from road center to surroundings results to only approximately 5 meters to either side, which leads to an average total of 10 meters. The contrast in urban areas is up to three times higher, but the extension is three times as much, as well. Therefore, the function's gradient – be it in urban or in open areas – does not change.
c) The distance in between the function's turning points results to 5 to 6 meters. This leads to the previously discussed false extractions, as many other structures may offer the same appearance in width and contrast without actually being roads.

These points show that extraction in open areas is especially difficult to model. A compromise has to be found between the amount of correctly extracted roads on one hand and the number of false positives on the other. In addition to this, the previously explained effects of shifted vectors and multiple crossings (cf. Figure 17, chapter 5.1.2.1) appear as well. The effect of missing data in open areas does not occur as often as in urban areas. However, mountainous terrain may cause layover effects that lead to false positive extractions.

In order to adapt the extraction software to open areas, three main parameters are altered: Firstly, the value for the Gaussian blur filter has to be diminished to fit the narrow lines. Secondly, the SAR road operator mask has to be changed accordingly. Furthermore, the network trimming has to be adapted, because the distance in between the networks' junctions in open areas are supposed to be larger than those in urban areas. In the tests carried out here, a sigma of 2.5 and an SAR road operator mask with a configuration of 2 – 1 – 2 (adjacent region – guard strip – road)

have been chosen. The partial derivatives have not been altered, as they do not change significantly in between open and urban areas; in open areas, the lower difference in contrast is achieved over a smaller extension in road width. Furthermore, the value for network trimming was set to 150 pixels, or 375 meters in ground resolution. An overview of the parameters altered in order to enable a context-driven extraction is given in the appendix, section A.2. The results presented in the following chapter 5.1.2.3 were achieved by applying this configuration.

5.1.2.3 Overall results

Table 3 shows the extraction results in open and urban areas in SAR imagery, applying the extraction software developed by K. Lang at Intermap Technologies GmbH Wessling. Values for correctly applied parameters are displayed in italics. The results are based on the 18 images available for the whole test site, covering 72 km^2. The total length of roads contained in the reference is 526 kilometres.

Evaluation					
Context region	Urban		Open		Overall
Applied parameters	Urban	Open	Urban	Open	Urban / Open
Completeness	*67.0 %*	12.3 %	25.4 %	*26.4 %*	*55.2 %*
Correctness	*72.1 %*	59.0 %	25.5 %	*43.5 %*	*63.8 %*
Quality	***53.2 %***	**11.3 %**	**14.6 %**	***19.7 %***	***42.0 %***

Table 3: Evaluation results (Intermap extraction algorithm on SAR imagery)

The results show that contextual modelling for both urban and open areas is important, as the use of wrong parameters leads to a much lower correctness in the extraction results. With correct parameters applied to the respective regions, 67.0 % of the reference data is extracted in urban areas. In open areas, only 26.4 % can be detected. Of all extracted roads, 72.1 % coincide with the reference in urban areas, while 43.5 % correctness is achieved in open context regions.

The relatively good results for urban areas are caused by the effects explained earlier (cf. chapter 5.1.2.1). The achievements for completeness and correctness lead to a quality measure of 53.2 %, which is considered to be satisfying for SAR imagery, according to earlier investigations carried out by Intermap Technologies Corp.

For open areas, only a little more than one third of the results in urban areas can be achieved, revealed by a quality measure of 19.7 %. This is due to the extremely difficult modelling in order to detect roads in open areas. The increase in completeness compared to the extraction with wrong parameters is only marginal. However, the correctness measure leads to much better results when using parameters especially designed for open areas. This means that the number of false

positives can be diminished. The quality value of just under 20 % is not surprising, considering the obstacles in the extraction from SAR imagery in open areas.
The overall results with correctly applied parameters show that not much more than half the vectors given in the reference data were detected from the imagery. Almost two thirds, though, were extracted correctly, resulting in a remaining amount of one third false positives of all extracted vectors. The overall quality of 42.0 % cannot be considered convincing. But taking into account the overall appearance of radar imagery and the fact that some parts of the reference data are younger than the imagery, the achieved quality seems reasonable.

Concerning the general proceedings within the Intermap extraction algorithm, some recommendations can be made:

a) The handling of different context regions is very time-consuming, because the whole image has to be processed once for each context class contained in the image. The more context classes have to be handled, the more computation time has to be considered. Furthermore, the cutting of the extraction results and fitting to the respective context regions in a GIS software takes additional time and may lead to human-related mistakes, as this part of the process is not carried out automatically.
b) In order to view the results and all steps leading to them, the output files have to be imported into a GIS software. A viewer connected to the extraction itself would enable the user to control the process visually and react on any mistakes that may occur during the computation.
c) Due to the extraction procedure, the images' borders are not treated in the output and no extraction result can be derived for those areas. This can be overcome by manually enlarging the images' borders to a certain extent, thus creating an overlap and eliminating gaps. However, the manual handling may cause further mistakes. Therefore, an automatic enlarging of the area covered by the extraction is recommended.

5.2. TU Munich extraction algorithm on SAR imagery

The extraction algorithm developed by C. Wiedemann at the TU Munich was originally designed for automated road extraction on open areas in aerial imagery of low resolution. The existence of control files that steer the whole extraction process allows, however, an easy adaptation to other imagery sources.
Chapter 5.2.1 explains the general test approach for this algorithm, while the results and evaluations are stated in chapter 5.2.2.

5.2.1. Test approach

In order to be able to compare both extraction approaches to each other, the tests on the TU Munich algorithm are carried out on the same area as used for the Intermap algorithm (cf. chapter 5.1.1). Furthermore, the statistical methods defined previously will be employed as well, in order to ensure a qualitative comparison of both methods.

5.2.2. Results and evaluation

The extraction approach developed by C. Wiedemann at the TU Munich allows the application of context regions that have to be defined prior to the extraction itself. In this thesis, the manual possibility for generation of context regions is applied (cf. chapter 4.1): a distinction between open and urban areas within the test site is made and the regions are digitized in a MapInfo® environment.
Because the TU Munich extraction approach is carried out within Halcon – a tool for machine vision distributed by MVTec Software GmbH – the digitized areas have to be transformed into “Halcon regions”. This is carried out under Linux, as is the whole extraction itself. The steps computed by the software are restricted to the respective context regions only, thus speeding up the whole computational process.

5.2.2.1 Results for urban areas

The tests are carried out on exactly the same images as in the previous chapters. A sample radar image with mainly urban context is shown in Figure 14, chapter 5.1.2.1.

An example for extracted vectors after the application of the TU Munich algorithm and the given reference is shown in Figure 21.

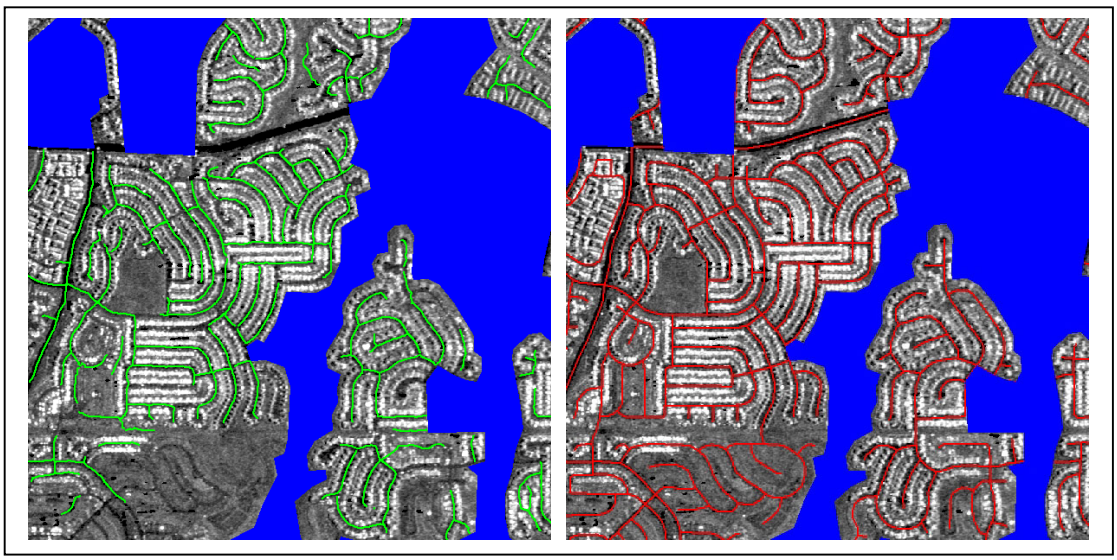

Figure 21: Extraction result (left) and reference (right) in urban areas (SAR imagery + TU Munich extraction algorithm)

The images show the extracted roads in green and the manually digitized vector data in red. Regions in blue are not considered as urban areas and therefore not taken into further account.
In general, the algorithm investigated in this chapter has to exploit the advantages given by the high contrast in between buildings and roads just like its counterpart that is presented in chapter 5.1. However, the adaptation of the responsible parameters has to be modelled differently, as, for instance, only the difference in absolute grey values can be altered, not the second partial derivative of a smoothed function perpendicular to the road.
Referring to the diagram in Figure 16 (chapter 5.1.2.1), which depicts the mean grey value distribution for urban roads in SAR imagery perpendicular to their direction, the key values for extraction from urban areas can be derived.

a) As explained in the respective chapter, the contrast in between roads and buildings results to approximately 100 to 150. The parameter CONTRAST_HIGH should be adapted accordingly. Furthermore, the overall appearance of roads does generally not exceed values higher than 60 on the average. In order not to miss any deviations from this mean value, the parameter THRESHOLD is set to 75. Any pixels with a grey value higher than this are not considered for the line extraction, because only dark lines are extracted.
   The LINE_WIDTH has to be set to especially high values, because of the earlier explained effects (cf. chapter 5.1.2.1). The recommended value for this parameter is 45.0 meters. In tests on the parameter CONTRAST_LOW it was shown that values around 30 lead to satisfying results.

b) Because the parameters which are contained in the module that carries out the fuzzy evaluation highly depend upon the primarily extracted line widths, the values applied here have to be adapted accordingly. In detail, this means that the evaluation of the length of an extracted pixel chain is carried out applying the parameters 5 – 10, considering pixel chains with a length shorter than five meters as poor and those with a length of ten meters or longer as good. The parameter FUZZY_WIDTH is run in a 3 – 5 – 35 – 50 configuration, allowing narrow and wide roads to be considered with a good evaluation. Although no roads wider than 45.0 meters are extracted in the line extraction conducted before, the highest value in this parameter equals 50. This leads to the effect, that e.g. lines with a width of 45 meters are assigned a fuzzy value of 0.67 instead of 0.
c) In order not to miss any smaller networks, especially in areas at the images' borders, the overall network length is set to 100 meters.

The parameter WEIGHT_SEEDPOINT is not changed and remains at a value of 0.5.
It has to be considered, that this extraction algorithm mainly uses absolute values. Although the results achieved for urban areas in this test site seem to be satisfying (cf. chapter 5.2.2.3), the absolute grey values may vary on other sites due to the radar configuration or processing. Therefore, the absolute parameters may not work in the same way, and revising has to be considered. This especially applies to the parameter THRESHOLD, as it masks out certain pixels that will not be considered for the line extraction. However, a general omission of threshold values is not recommended, as the amount of pixels considered for extraction is broadened and more false positives may occur. An overview of the parameters altered in order to enable a context-driven extraction is given in the appendix, section B.1.

Referring to the tests presented here, the same effects as described in chapter 5.1.2.1 apply when comparing extraction and reference due to the time discrepancy that originates from younger reference data. Accuracy, completeness and correctness cannot be expected to be satisfying in parts that show time-dependent deviations. Such effects influence the statistical results in chapter 5.2.2.3, but do not impair the comparisons made in between both extraction algorithms.
A more detailed look on the extracted vectors is provided in the following Figure 22.

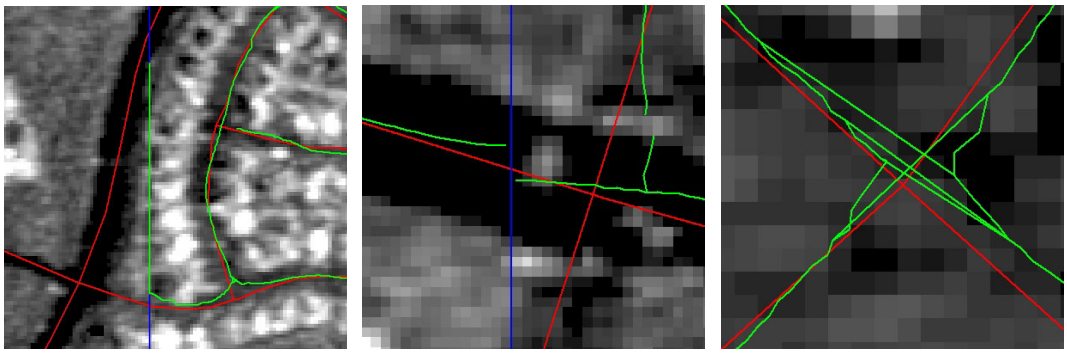

Figure 22: Effects in extracted vectors (urban areas, SAR imagery)

Reference vectors are displayed in red, extracted vectors in green and the image tiles' borders in blue. Three effects can be seen: The first image shows an extraction along the border of the image tile. The origin of this false extraction is not clear. However, it is assumed that the extraction algorithm considers non-existent pixels outside the image's borders as zero values. Thus, a significant contrast is found in between these and the high grey value objects on the right of the extracted line. Another effect caused by tiling is depicted in the second image. The two extracted lines show an offset towards each other, because each tile is processed separately and the algorithm does not model connections in between the tiles. Furthermore, the effect of the parameter CONTRAST_LOW can be seen in the upper right corner, where the extracted pixel chain is split, because of a higher contrast than defined along the line. In the third picture, the effect of multiple crossings, already known from the Intermap algorithm, can be seen. This is due to the non-existent explicit modelling of intersections during the line extraction. An approach to overcome these effects is presented in [Wiedemann, 2002]. Additionally, the known effects of shifting towards pixels of lower grey values and extraction behaviour in areas of missing data occur as well.
Concluding, the extraction in urban areas benefits from the same advantages given by SAR imagery as explained in the respective chapter for the Intermap algorithm (chapter 5.1.2.1). The explained disadvantages apply respectively. Main differences in between both extraction algorithms can be detected in the handling of extraction on the images' borders and the general approach of absolute versus relative handling of parameters.

5.2.2.2 Results for open areas

The tests for open areas refer to the same images as in the respective chapters treating the Intermap extraction algorithm. A sample radar image with mainly open context is given in Figure 18, chapter 5.1.2.2.
Because of the difference in appearance of open areas compared to urban areas, the extraction algorithm has to be adapted accordingly. Characteristics of open areas in SAR imagery are explained in detail in chapter 5.1.2.2.
Figure 23 shows an example for extracted vectors in comparison to their reference in open areas after applying the TU Munich extraction algorithm. Extracted roads are displayed in green, reference vectors in red. Regions in blue are urban context areas and are therefore not considered for further investigations in this part.

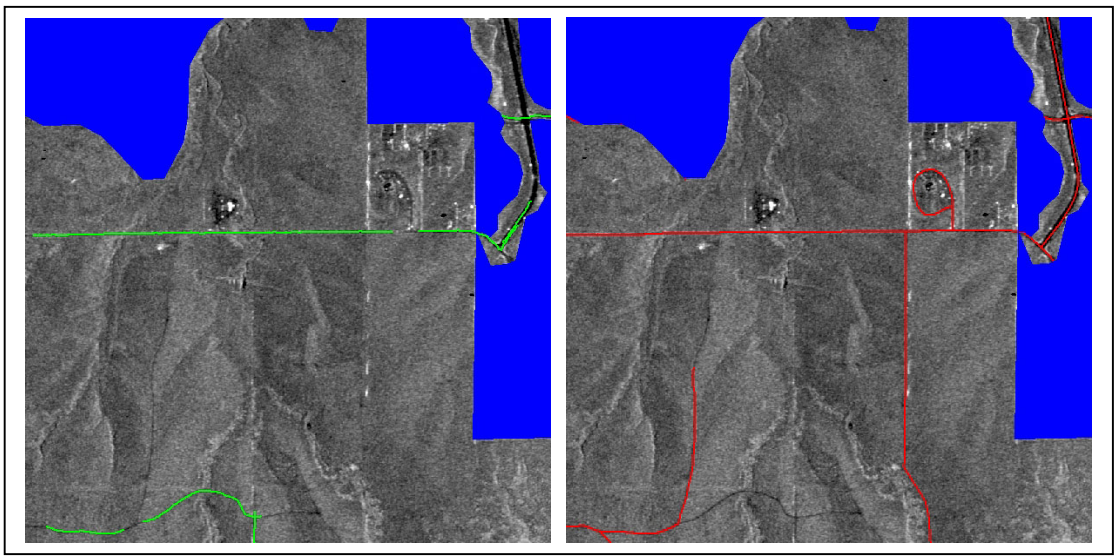

Figure 23: Extraction result (left) and reference (right) in open areas (SAR imagery + TU Munich extraction algorithm)

Several effects can be derived from the figure. Due to the poor contrast behaviour in open areas, only some of the data defined in the reference can be extracted. In order to exploit the low contrast, the parameter CONTRAST_HIGH was decreased to a value of 50. Figure 20 in chapter 5.1.2.2 shows the grey value distribution in open areas perpendicular to the road's direction, which supports this decision. The line width to be extracted has to be lowered to 7.5 meters, because too many false positive extractions occur otherwise.
At this point, it is important to show the interrelation between the number of false positive and true positive extractions: by choosing parameters that detect a greater number of real roads (true positives) it is inevitable that the number of extracted lines that are actually no roads (false positives) increases as well. Changing the applied parameters to detect relatively less false positives leads to a higher number of non-detected real roads (false negatives). Therefore, a compromise between the number

of false positives on one side, and the number of false negatives on the other, has to be found. In the tests carried out, it was decided to attempt a minimization of false positives, being well aware of the potentially lost roads. This decision was made because of the occurrence of a relatively *high* increase of falsely extracted roads when changing the parameters in order to obtain a relatively *small* increase in the number of extracted real roads.
Focusing on the diagram in Figure 20, chapter 5.1.2.2, further conclusions concerning the parameters to be applied can be made:

a) The parameter THRESHOLD has to be increased to values around approximately 90 in open areas, as the appearance of roads is generally brighter, due to their structural consistency.
b) In order to apply an appropriate evaluation, the parameter FUZZY_WIDTH has to be run in a 4 – 6 – 12 – 15 configuration.

Furthermore, considering only line pixel chains with an overall high fuzzy evaluation can minimize the occurrence of false positives. Therefore, the parameter WEIGHT_SEEDPOINT is raised to a value of 0.75. This is necessary because the fuzzy evaluation carried out here, leads to higher overall values than in urban areas. Additionally, the network length that has to be achieved in order for a conjunction of extracted lines to be considered for the final network generation is increased to 150.0 meters. An overview of the parameters altered in order to enable a context-driven extraction is given in the appendix, section B.2.

Modelling the extraction parameters for open areas is especially difficult. The parameters have to be defined very sharply, which leads to more false negative results. Additionally, the effects of offsets, border extractions, shifted vectors and multiple crossings (cf. Figure 22) occur as well.

5.2.2.3 Overall results

Table 4 shows the extraction results in open and urban areas in SAR imagery, applying the TU Munich extraction software developed by C. Wiedemann. Values for correctly applied parameters are displayed in italics. The results are based on the 18 images available for the whole test site, covering 72 km^2. The total length of roads contained in the reference is 526 kilometres.

Evaluation					
Context region	Urban		Open		Overall
Applied parameters	Urban	Open	Urban	Open	Urban / Open
Completeness	*56.2 %*	4.0 %	10.4 %	*22.6 %*	*46.4 %*
Correctness	*81.9 %*	25.4 %	31.4 %	*47.0 %*	*71.8 %*
Quality	***50.0 %***	**3.6 %**	**8.5 %**	***18.0 %***	***39.3 %***

Table 4: Evaluation results (TU Munich extraction algorithm on SAR imagery)

The results for both open and urban areas with the application of wrong parameters need no further explanation but emphasize once more the necessity of contextual modelling. For urban areas, and the application of correct parameters, 56.2 % of the reference vectors are detected, while less than half of that value can be achieved for open areas with 22.6 %. The correctness of the extracted vectors can be considered as very good in urban areas, reaching a value of 81.9 %. In open areas, only 47.0 % of the extracted vectors coincide with the given reference.
As was to be suspected, good results can be achieved for urban areas, which is due to the effects explained earlier. The achievements for completeness and correctness lead to a quality measure of 50.0 %, which is considered to be satisfying for SAR imagery.
The poor results for open areas are not surprising, considering the conditions given in these regions. However, the increase in both completeness and correctness when applying correct parameters reveals that less false positives as well as less false negatives were detected. The quality measure of 18.0 % emphasizes the difficulties the extraction algorithm is faced with in open areas.

The overall results with correctly applied parameters show that less than half the vectors given in the reference data were detected from the imagery. However, more than two thirds were extracted correctly, resulting in a remaining amount of less than one third false positives of all extracted vectors. The overall quality of 39.3 % seems to be poor. But considering the overall appearance of radar imagery and the fact that some parts of the reference data are younger than the imagery, the achieved quality seems reasonable.

5.3. Comparison of TU Munich and Intermap extraction algorithms on SAR imagery

Comparing the outcome presented by both algorithms, no significant differences can be found. Both algorithms can be adapted to the respective context regions and show reasonable results. When focusing on urban areas, where the best extraction results were achieved, it can be seen that results presented by the TU Munich extraction algorithm are less complete. However, a higher percentage of correctness is achieved.

Concluding, both algorithms can compete when processing urban areas in SAR imagery. Within open areas, the results are similar to each other, but not overall satisfactory. The usefulness of road extraction from SAR in these contexts is highly doubtable.

Referring to the user-friendliness and handling of both extraction algorithms throughout the periods of intensive testing, it can be said that the TU Munich extraction algorithm shows some advantages in these respects: The feature of extraction restricted to a predefined mask results in less time consumed in post-processing of the extraction results, i.e. the assignment to the respective context regions. Furthermore, the possibility of immediate visual control after each module is carried out and the use of absolute grey values rather than gradients appear to enable an easier understanding of the procedures, even for untrained users. Considering the computation time needed, the TU Munich extraction software shows a clear advantage, because contextual extractions are restricted to their respective regions and do not have to be processed for the whole image. Especially when handling several context classes the Intermap algorithm is more time-intensive, both on the computer-processing and manual post-processing part.

6. Practical analysis of extraction algorithms on optical imagery

This chapter deals with the practical analysis of the two extraction algorithms explained in chapters 4.2 and 4.3, using imagery originating from aerial photography. Both approaches are investigated regarding their adaptability to optical imagery in different context regions. The chapter presents the achieved results and provides a final evaluation of the extraction approaches comparing their quality measures and overall handling.

6.1. Intermap extraction algorithm on optical imagery

The Intermap extraction algorithm was originally designed for automated road extraction on urban areas in SAR imagery. In order to be able to use the same software on aerial imagery in both urban and open context regions, the alterable parameters explained in chapter 4.2.1 are investigated and employed accordingly.
The general test approach for this algorithm is stated in chapter 6.1.1, while the obtained results and evaluations are shown in chapter 6.1.2. A final comparison to the results obtained by applying this extraction algorithm to SAR imagery is given in chapter 6.2

6.1.1. Test approach

In order to define general contextual parameters for respective context regions with the goal to enhance the extraction results, the given algorithm has to be tested on a well-defined area with given reference. To enable an expressive comparison between the previously stated results for automated extraction on SAR imagery and the respective results for optical imagery, the application of identical tests is desirable.
The test site used in this part of the thesis is covers only a part of the “Highlands Ranch Quadrangle”, used throughout chapter 5. Areas approximately 350 meters wide to the west and 270 meters wide to the east are unavailable for testing. Although the overall test area, compared to the site used for SAR imagery investigations, is diminished by more than 7.4 km^2, it is assumed that the remaining area can still provide representative results. The applied reference data is the same that was used for the evaluation with SAR imagery. This leads to some effects on the final results, which are explained in chapter 6.1.2.1. The overall area coinciding with the available aerial imagery results to 64.6 km^2. The extension of 2 km x 2 km for

each core tile is maintained, leading to an approximate pixel size of 1176 x 1176, due to the finer ground resolution of 1.7 meters.
The overall contextual consistence of the test site with urban and open areas is not significantly changed by the application of a smaller test site. Open regions now cover 60.5 % of the test site's superficial area, a marginal increase by 2.5 percentage points. Urban regions still contain the majority of roads with an amount of 81.5 %. The overall length of the road network is approximately 503 kilometres, a decrease by 23 kilometres. 362 kilometres of those, or 71.8 %, are urban roads. Because of the decrease in area of the test site, no new context regions can be taken under investigation. More detailed context regions, like forestry or agricultures, do either not cover a significantly large area and are not developed by roads, or do not exist at all.
The optical imagery data used throughout this part stems from "digitally orthorectified quarter quadrants" (DOQQ). The original ground resolution of 1 meter has to be reprocessed to 1.7 meters. This is necessary in order to carry out a successful line extraction. In imagery of higher resolution, occlusions and shadows, originating from cars, buildings or vegetation, act as disturbances, which require the use of a different road model (cf. chapter 3.1.1) that, furthermore, takes into account the appearance of roads as elongated regions.

In addition to the resulting images provided in this chapter, statistical evaluation criteria, as previously defined in chapter 5.1.1 are derived. The criteria *completeness*, *correctness* and *quality*, as presented in [Wiedemann et al., 1998], are used to enable a comparison in between the different context regions and, as well, in between the different imagery sources. For the calculation of these quality criteria, refer to chapter 5.1.1.

6.1.2. Results and evaluation

As described in chapter 4.2.2, the extraction approach developed by K. Lang at Intermap Technologies GmbH Wessling does not support extractions restricted to a previously defined context area. Therefore, the handling of global context has to be carried out as explained in the respective chapter. In order to obtain a consistent data set for each tile, the extraction is carried out separately with urban and open parameters for the whole image. The results are imported into a MapInfo® environment and cut to fit the respective context regions.

6.1.2.1 Results for urban areas

Figure 24 shows a sample aerial photograph image with mainly urban context; open areas are masked out in blue.

Figure 24: Urban context region (optical imagery)

The image clearly shows that the distribution of grey values is more inhomogeneous than in the respective radar image (cf. Figure 14, chapter 5.1.2.1). This is due not only to the higher resolution but also to the higher contrast occurring in between neighbouring pixels. The distinction of roads from other road-like structures seems easy, as they appear to be brighter than their general surroundings. A closer look on the appearance of roads in the optical images provided, leads, however, to a more distinctive statement. The following Figure 25 provides a close-up view on part of the urban context region displayed in Figure 24.

Figure 25: Urban context region – close-up view

By taking a closer look on the appearance of roads in urban areas, some effects can be seen: although the grey values contained by the roads are brighter than their overall general surroundings, the immediate neighbouring pixels may contain significantly *higher* grey values. This is caused in part by sidewalks that are generally present on either side of the roads throughout all urban areas within the test site. Adding to the effect of higher grey value than the roads are the occurring driveways. Lower grey values, in contrast, are provided by front yards, lawns and general vegetation. House roofs range within the same grey values as the roads do.
These effects have to be considered for the road extraction, as they may impede a focused extraction process. An example for extracted vectors after the application of the Intermap algorithm on optical imagery and the given reference is displayed in Figure 26.

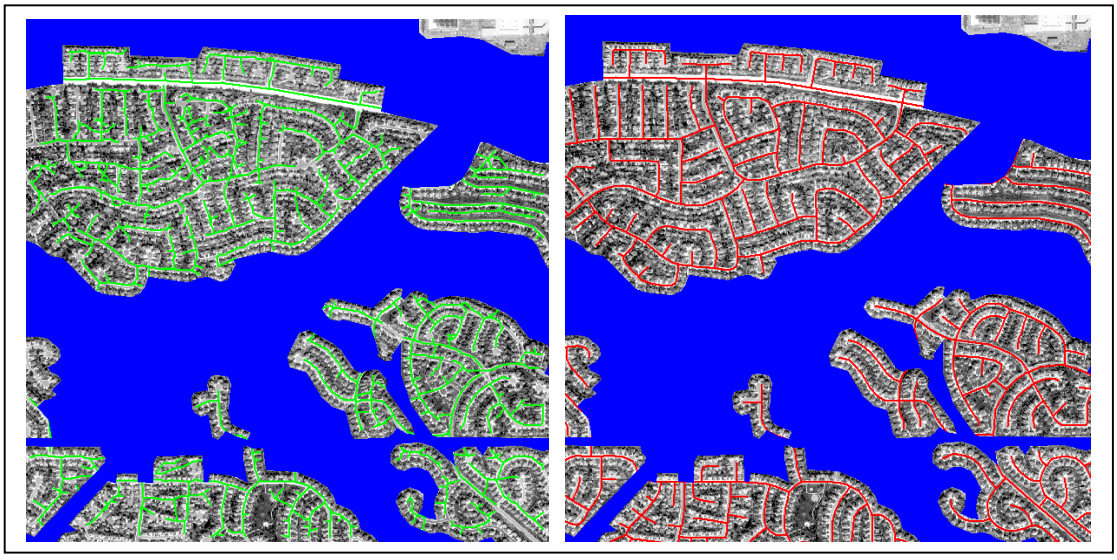

Figure 26: Extraction result (left) and reference (right) in urban areas (optical imagery + Intermap extraction algorithm)

The images show the extracted roads in green and the manually digitized vector data in red. Regions in blue are not considered as urban areas and therefore not further investigated.
Areas of urban context in optical imagery are generally characterized by an inhomogeneous distribution of grey values, as explained earlier. In order to achieve reasonable extraction results, the parameters applied have to be chosen more restrictively, i.e. suited especially for the respective region. This sharp definition of extraction parameters leads, however, to the effect that the extraction may provide good results in some urban areas, whereas in others, the achieved results can be poor, due to effects restricted to that special area, e.g. inclination of roofs towards the sensor, differing road consistency, etc.

The diagram in Figure 27 shows a smoothed grey value distribution for a representative urban road, perpendicular to its direction. In order to show the high contrast effects, only one road has been chosen, as a mean value of several roads would level these effects. The function describes the level of grey value in relation to the distance from the road's centerline.

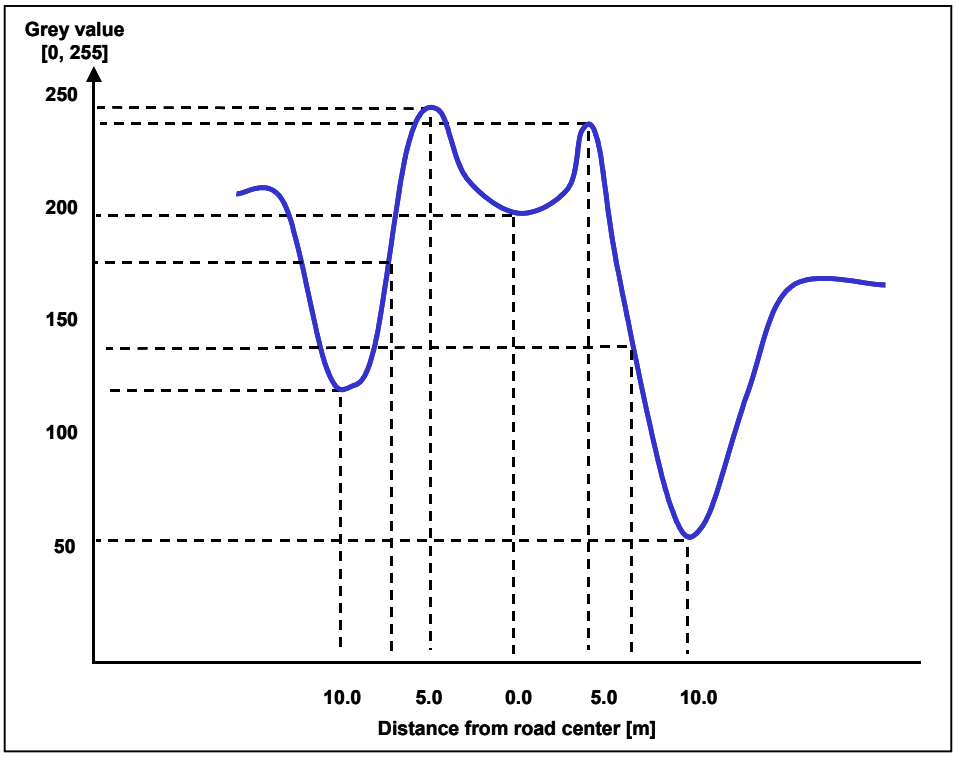

Figure 27: Grey value distribution perpendicular to road direction (urban areas, optical imagery)

The facts that can be derived from this diagram are:

a) The mean brightness for roads in these urban areas reaches grey values around 200 and higher. The effects of disturbing sidewalks lead to a maximum grey value of 255, before the function drops drastically to around 50 to 120. The lowest values are provided by lawns, front yards and other vegetation, as shown in Figure 25. Yet another increase in grey value occurs beyond this point, caused by buildings, driveways or similar structures. The overall contrast between the road and its darkest surroundings reaches values of 100 to 150.

b) The distance from the road's center to darker structures providing good contrast results to approximately 10 meters to either side, which leads to an overall total of 20 meters. It has to be considered that these values are derived from one road only and that in some cases road widths may differ significantly.

c) The distance in between the function's turning points results to almost 15 meters. Although only one road is shown in the diagram, most roads contained in the image are bearing a similar distribution. Therefore, this value has to be considered for the road extraction parameter that models the line width.

d) The decrease in grey value, although offering a high contrast, is disturbed by a sudden increase caused by sidewalks or driveways.

These facts show that, although a significant contrast is given by the general surroundings, the decrease of grey value happens discontinuously. The road's centerline is "caught" in between the maxima provided by the sidewalks and the minima given mainly by vegetation. This leads to problems in the extraction, because generally, only a one-sided approach to detect a road is modelled: the road is either supposed to be generally darker *or* lighter than the structures surrounding it. Roads that are appearing in between these extremes are not considered in the extraction algorithm's road model. In order to solve this problem, two possibilities exist:

a) The road's centerline could be extracted, if the sidewalks were used as additional information. However, various facts oppose against this possibility: The line width that would have to be used in order to apply this method would be extremely small, as the distance in between the turning points would result to six to seven meters. Furthermore, the contrast in between road and sidewalk often results to values of only 45 to 50. In return, the combination of these two parameters – small line width and low contrast – would cause an extremely high number of additionally extracted structures that fit this model, but are in fact no roads; the so-called false positives.
b) The second possibility is to model the road as such and not take into account the sidewalks, as the contrast in between the brighter road and the darker surroundings provides sufficient information. However, the extraction may then mistakenly detect one of the sidewalks as the road's centerline, as it is looking for extremes in the provided image.

Therefore, the decision made is to employ the first of these two possibilities.

In addition to the problems already addressed, a further obstacle comes into effect during the statistical evaluation. The manually digitized vectors that serve as a reference were generated by using stereo imagery stemming from SAR data. In urban areas, this might lead to some mistakes concerning the position of the real centerline of a road. As earlier described, buildings may act as corner reflectors (cf. chapter 2.4). Additionally, radar shadows may occur in urban areas as well, depending on the sensor's flight direction. Corner reflection starts to have an effect on the imagery *before* the actual structure causing this is fully reached. Depending on the structures height and the surface immediately in front of the structure, the appearance in the image might be shifted away from the sensor. In theory, this shift can be as big as the structure's height. Radar shadows lead to the exact same effect, with the only difference that shadows may occur *behind* a structure. These problems have an immediate impact on accuracy, completeness and correctness and influence the statistical results in chapter 5.1.2.3.

A more detailed look on the extracted vectors is provided in the following Figure 28.

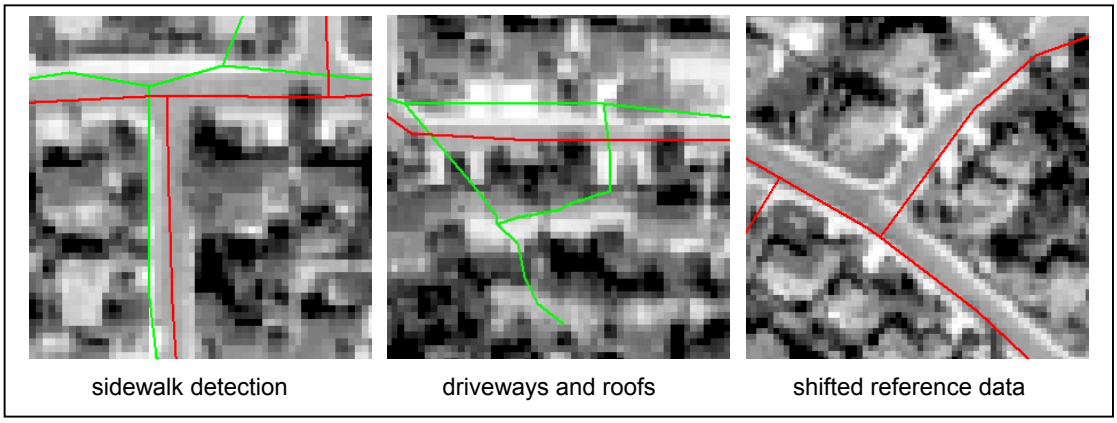

Figure 28: Effects in extracted vectors (urban areas, optical imagery)

Reference vectors are displayed in red, extracted vectors in green. Three effects can be seen: in the first picture, the previously explained extraction of sidewalks, bearing a higher grey value than the actual road, is shown. The second picture displays the effects caused by disturbing objects such as driveways or house roofs. The extraction is shifted towards the high grey value driveway. In extreme cases, the model even allows the creation of extractions far off from the actual road, as shown in the lower part of the image. In the third picture, the shifting of reference data can clearly be seen. This effect is believed to be caused by elevated structures, as it does not occur in open areas.
Additionally, Figure 26 shows that again no extraction results are achieved in close proximity to an image tile's borders. As the area not covered is estimated to stretch 15 pixels inwards from each image border, the actual ground distance results to approximately 25 meters only, whereas in the radar image almost 40 meters were omitted, due to the coarser resolution. As of now, an overlapping in order to overcome this problem would have to be generated manually.
Concluding, it is evident that extraction from optical imagery in urban areas is extremely difficult to model. A decision has to be made as to whether extract more accurate road centerlines at the disadvantage of receiving an extremely high number of false positives, or to model roads in relation to darker surroundings, resulting in a shifted extraction towards brighter sidewalks. Additionally, an obvious problem caused by the applied line extraction model is the lack of sufficient consideration of local disturbances (trees, cars, etc.), which leads to false extractions.

In order to use the extraction software on urban areas in optical imagery, the given image has to be inverted, because the SAR operator only works on roads that are darker than their surroundings. Furthermore, three main parameters are altered: Firstly, the value for the Gaussian blur filter is diminished to fit the narrower lines. Secondly, the SAR road operator mask has to be changed accordingly. In the tests carried out in this part, a sigma of 3.0 and an SAR road operator mask with a configuration of 6 – 3 – 6 (adjacent region – guard strip – road) have been chosen.

Finally, the partial derivatives have to be altered to fit the road model for urban areas in optical imagery. The threshold for the first partial derivative was lowered to 0.07, the threshold for the second partial derivative was increased to a value of 1.0. These values have been determined by conducting several experiments on the images. An overview of the parameters altered in order to enable a context-driven extraction is given in the appendix, section A.3.

6.1.2.2 Results for open areas

Figure 29 shows a sample optical image with mainly open context; urban areas are masked out in blue.

Figure 29: Open context region (optical imagery)

Generally speaking, open context areas in optical imagery often offer a better contrast distribution than the previously explained urban areas, which can clearly be seen in Figure 29. Two main causes lead to this effect:

- Disturbing objects like sidewalks are generally not present in open areas. Additionally, the presence of driveways and roofs, providing appearances similar to those of a road, is much smaller than in urban areas.
- The road's surroundings are more homogenous. Fields, pastures and plains provide sufficient contrast to the road, as they appear generally darker.

Figure 30 provides an example for extracted vectors in comparison to their reference in open areas after applying the Intermap algorithm on optical imagery. Extracted roads are displayed in green, reference vectors in red. Regions in blue are urban context areas and are therefore not considered for further investigations in this part.

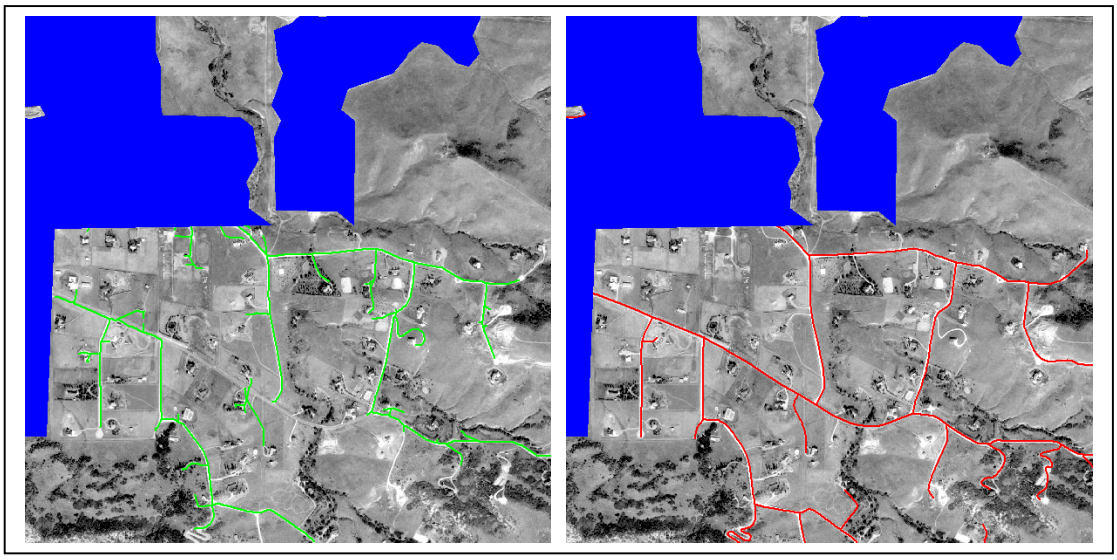

Figure 30: Extraction result (left) and reference (right) in open areas (optical imagery + Intermap extraction algorithm)

The images in Figure 30 show that extraction on optical imagery can achieve good results in open areas. Although some roads are omitted due to low contrast, and a small amount of roads is extracted by the software without being part of the reference (e.g. longer driveways), the overall result can be considered satisfying. The reason for better quality of the extraction in open areas lies in the possibility of a more general adaptation for the extraction's parameters. The greater value of the second partial derivative allows only a few false positive extractions and the succeeding application of the SAR operator eliminates almost all of those. However, some roads may not be found, because the contrast provided in the image is not high enough. This can be seen in the bottom half of both images: the connecting road is simply missed, due to a false negative extraction.

Figure 31 provides a representative grey value distribution for open roads, perpendicular to their direction. The function is based on 10 randomly picked roads and describes the level of grey value in relation to the distance from the roads' centerline.

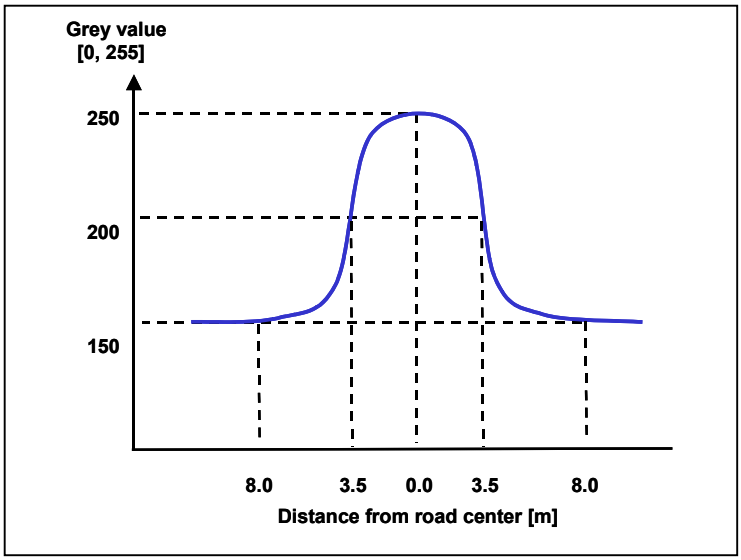

Figure 31: Grey value distribution perpendicular to road direction (open areas, optical imagery)

The facts that can be seen in the diagram are the following:

a) The mean grey value for roads in open areas varies around 250, which is higher than in urban areas. This is due to the structural consistency of the road itself, causing a difference in reflectivity within the visible spectrum. While roads in urban areas often have an asphalt layer, rural roads in open areas consist of concrete, gravel or simply dirt. The overall average contrast results in a grey value difference of about 80. Because of the restrictive conditions that apply to aerial photography flights per se – e.g. a certain inclination of the sun and other general weather conditions – effects changing the appearance of roads (e.g. shortly after rainfalls) do generally not cause any problems.

b) The mean distance from road center to surroundings results to approximately 8 meters to either side, but a significant decrease in the rate change of grey values already occurs after 4 meters. This results to a total of approximately 8 meters. For roads with such a high contrast over a small extension, the gradient is very high.

c) The distance in between the function's turning points results to approximately 7 meters. Although many other structures may bear the same width, it is very rare that they also offer the same contrast towards their surroundings. Therefore, false positive extractions are more unlikely to occur.

Figure 31 shows an almost perfect grey value distribution, which makes it easy to find suitable extraction models in open areas. In order to also find some roads that do not offer such good conditions, the parameters should not be set too tightly. Although the effect of false positive extractions is increased by doing so, the detection of more real roads in return is considered to be a worthwhile advantage.

In order to adapt the extraction software to open areas, four main parameters are altered: Firstly, the value for the Gaussian blur filter has to be diminished to fit the narrower lines. Secondly, the SAR road operator mask has to be changed accordingly. The third parameter to be altered – and the most effective one – is the second partial derivative, responsible for modelling the contrast. Finally, the network trimming has to be adapted, because the distances between the network's junctions in open areas are supposed to be larger than those in urban areas. In the tests carried out here, a sigma of 3.0 and an SAR road operator mask with a configuration of 3 – 1 – 3 (adjacent region – guard strip – road) have been chosen. The partial derivatives were changed to values of 0.07 for the first and 1.0 for the second. The value for network trimming was set to 200 pixels, or 340 meters in ground resolution. An overview of the parameters altered in order to enable a context-driven extraction is given in the appendix, section A.4. The results presented in the following chapter 6.1.2.3 were achieved by applying this configuration.

6.1.2.3 Overall results

Table 5 shows the extraction results in open and urban areas on optical imagery, applying the extraction software developed by K. Lang at Intermap Technologies GmbH Wessling. Values for correctly applied parameters are displayed in italics. The results are based on the 18 images available for the whole test site, covering approximately 65 km^2. The total length of roads contained in the reference is 503 kilometres.

Evaluation					
Context region	Urban		Open		Overall
Applied parameters	Urban	Open	Urban	Open	Urban / Open
Completeness	*24.1 %*	3.7 %	31.8 %	*47.3 %*	*30.8 %*
Correctness	*38.3 %*	23.4 %	41.5 %	*63.2 %*	*45.4 %*
Quality	***17.3 %***	**3.3 %**	**22.0 %**	***37.1 %***	***22.5 %***

Table 5: Evaluation results (Intermap extraction algorithm on optical imagery)

The results show that contextual modelling for both urban and open areas in optical imagery is important, as the use of wrong parameters leads to a much lower correctness and completeness in the extraction results. With correct parameters applied to the respective regions, only 24.1 % of the reference data is extracted in urban areas. In open areas, only 47.3 % can be detected. Of all extracted roads, 38.3 % coincide with the reference in urban areas, while 63.2 % correctness is achieved in open context regions.
The good results for open areas occur because of the positive contrast behaviour explained earlier. The achievements for completeness and correctness lead to a

quality measure of 37.1 %, which is considered to be satisfying for optical imagery in open areas, especially when considering the effects concerning the reference data. For urban areas, less than half of the results in open areas can be achieved, leading to a quality measure of 17.3 %. This is due to the extremely difficult modelling in order to detect roads in urban areas. Although the increase in completeness compared to the extraction with wrong parameters is extremely high and the correctness reaches a higher value as well, the overall result cannot be considered good.

The overall results with correctly applied parameters show that less than one third of the vectors given in the reference data were detected from the imagery. This is mainly caused by the poor results for urban areas, as they make up the most part of the test site. However, almost half of the vectors were extracted correctly, resulting in almost the same amount of false positive extractions. The overall quality of 22.5 % seems disappointing. But taking into account the overall appearance of optical imagery and the fact that some parts of the reference data do not line up with the image, the achieved quality seems reasonable.

Concerning the general proceedings within the Intermap extraction algorithm, the same recommendations as made in chapter 5.1.2.3 apply. Additionally, the following can be stated: a line extraction approach in urban areas fails wherever real roads have intermediate grey values or a generally complex region is present, as local disturbances are not properly modelled. A solution to this might be provided by the detection of low-elevated roads surrounded by high-elevated buildings. For additional research on automatic extraction of urban roads, refer to [Hinz and Baumgartner, 2003].

6.2. Comparison of results from SAR and optical imagery (Intermap extraction algorithm)

Table 6 provides a comparison of both imagery sources in relation to both applied context regions for the Intermap extraction algorithm.

Evaluation				
Imagery source	SAR		Optical	
Context region	Urban	Open	Urban	Open
Completeness	67.0 %	26.4 %	24.1 %	47.3 %
Correctness	72.1 %	43.5 %	38.3 %	63.2 %
Quality	**53.2 %**	**19.7 %**	**17.3 %**	**37.1 %**

Table 6: Comparison of results (Intermap extraction algorithm)

The statistical results for applying correct contextual parameters are displayed. The *quality* measure comprises the measures *completeness* and *correctness*. As such, it gives a summarized final value for the capability of the extraction in relation to the imagery source.
It is obvious that the highest quality value of 53.2 % can be achieved when applying this algorithm to SAR imagery in urban areas. A completeness of more than two thirds and a correctness of almost three quarters show that convincing extraction results can be obtained in this configuration. Not as convincing, but still reasonable, are the results for open areas when using optical imagery. A quality measure of 37.1 % is the effect of almost one half completeness and two thirds correctness. The other two options (SAR in open areas and optical in urban areas) cannot compete with the preceding results.
Therefore, it can be concluded that, when using the extraction algorithm, developed by K. Lang at Intermap Technologies GmbH Wessling, the use of SAR imagery in urban context and the use of optical imagery in open context is highly recommendable.

6.3. TU Munich extraction algorithm on optical imagery

The extraction algorithm developed by C. Wiedemann at the TU Munich was originally designed for automated road extraction on open areas in aerial imagery of low resolution. Parameters for extraction on open and urban areas are investigated and employed.
Chapter 6.3.1 explains the general test approach for this algorithm, while the results and evaluations are stated in chapter 6.3.2. The chapter is concluded by a final comparison of the results obtained by applying this extraction algorithm to either imagery source in chapter 6.4.

6.3.1. Test approach

In order to be able to compare both extraction approaches to each other, the tests on the TU Munich algorithm are carried out on the same area as used for the Intermap algorithm (cf. chapter 6.1.1). Furthermore, the statistical methods defined previously will be employed as well, in order to ensure a qualitative comparison of both methods (cf. chapter 5.1.1).

6.3.2. Results and evaluation

As explained in chapter 4.3.1, the extraction approach developed by C. Wiedemann at the TU Munich allows the application of context regions that have to be defined prior to the extraction itself. The separate regions can either be digitized manually within a GIS software or derived by using an existing GIS, as in [Willrich, 2002]: here, region-like objects from the German ATKIS are used to create regions of similar contextual appearance. In this thesis, a distinction between open and urban areas within the test site is made and the regions are digitized in a MapInfo® environment.
The TU Munich extraction approach is carried out analogously to chapter 5.2. Therefore, the digitized areas have to be transformed into “Halcon regions” (cf. chapter 5.2.2). This is carried out under Linux, as is the whole extraction itself. The steps computed by the software are restricted to the respective context regions only, thus speeding up the whole computational process.

6.3.2.1 Results for urban areas

The tests are carried out on exactly the same images as in chapter 6.1.2.1. A sample image stemming from an aerial photograph with mainly urban context is shown in Figure 24, chapter 6.1.2.1.
An example for extracted vectors after the application of the TU Munich algorithm and the given reference is shown in Figure 32.

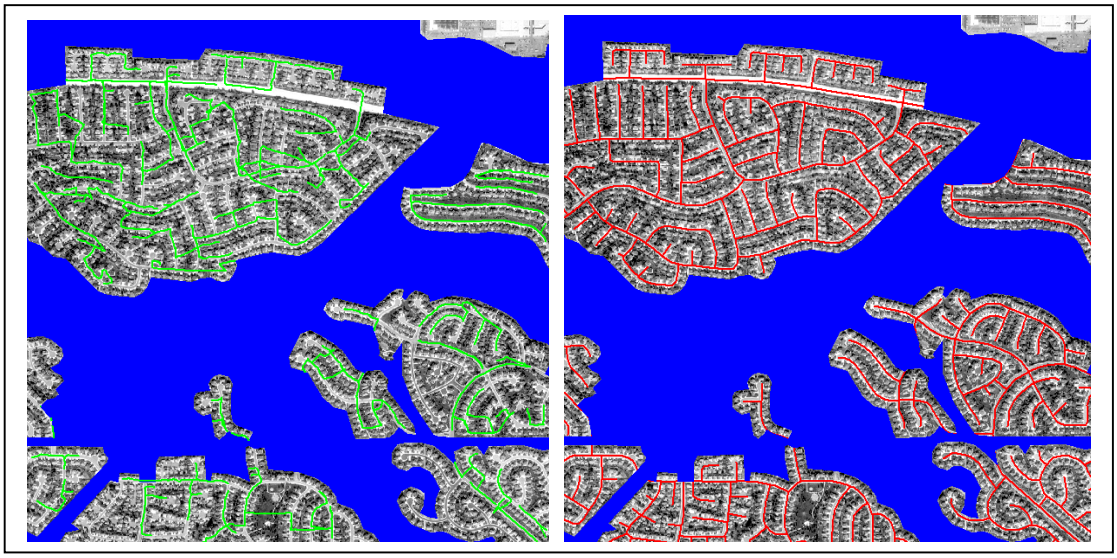

Figure 32: Extraction result (left) and reference (right) in urban areas (optical imagery + TU Munich extraction algorithm)

The images show the extracted roads in green and the manually digitized vector data in red. Regions in blue are not considered as urban areas and therefore not taken into further account.
The algorithm investigated in this chapter generally faces the same problems as explained earlier in chapter 6.1.2.1: the distribution of grey values is more inhomogeneous than in the respective radar image (cf. chapter 6.1.2.1, Figure 24), because of a higher resolution and higher contrast in between neighbouring pixels. Additionally, the frequent occurrence of sidewalks, driveways and roofs bearing similar grey values has a negative effect on the extraction.
The grey value distribution perpendicular to the road, as displayed in chapter 6.1.2.1, Figure 27, applies here as well. Although the problem of brighter sidewalks is *treated* similarly, a different *modelling* comes into effect, as the use of partial derivatives is not available in the parameter files. Instead, thresholds and contrasts have to be applied here. Further problems stated earlier apply to the same extent: discontinuous decrease in grey value from roads to surroundings, and the offset in the reference stemming from SAR imagery are expected to result in overall poor quality measures.

Relating to the diagram in Figure 27 (chapter 6.1.2.1), where a representative grey value distribution for an urban road perpendicular to its direction is given, the values for extraction from urban areas can be derived:

a) The contrast in between the road and its surrounding results to approximately 80, which advises a similar adaptation to the parameter CONTRAST_HIGH. The general appearance of roads themselves does not achieve values lower than 180. In order not to miss any deviations, the parameter THRESHOLD is set to 150. Any pixels with a grey value lower than this are not considered for the line extraction, because only light lines are extracted. The LINE_WIDTH is set to 25.0 meters in order to overcome the local disturbances caused by sidewalks. The parameter CONTRAST_LOW shows the best results when set to 30.
b) The applied fuzzy values have to be adapted in relation to the earlier line extraction. The evaluation for the length of an extracted pixel chain is carried out by applying a 5 – 50 configuration for the parameter FUZZY_LENGTH, considering pixel chains with a length shorter than 5 meters as poor and those with a length greater than 50 meters as good. The parameter FUZZY_WIDTH is run in a 5 – 15 – 25 – 30 setup.
c) The overall minimum network length is set to 100 meters.

Because of the use of absolute values, the recommended parameters may lead to worse results in urban areas other than the test site. This is the case if, for instance, the structural consistency or width of the roads differ. The same applies to the Intermap extraction algorithm. Here, the SAR road operator is modelled absolutely and may cause similar effects. The problems caused by the shift of the provided reference data, as explained in chapter 5.1.2.1, apply here as well and may therefore have negative effects on the results presented in chapter 6.3.2.3. An overview of the

parameters altered in order to enable a context-driven extraction is given in the appendix, section B.3.
A detailed look on the extracted vectors is provided in the following Figure 33.

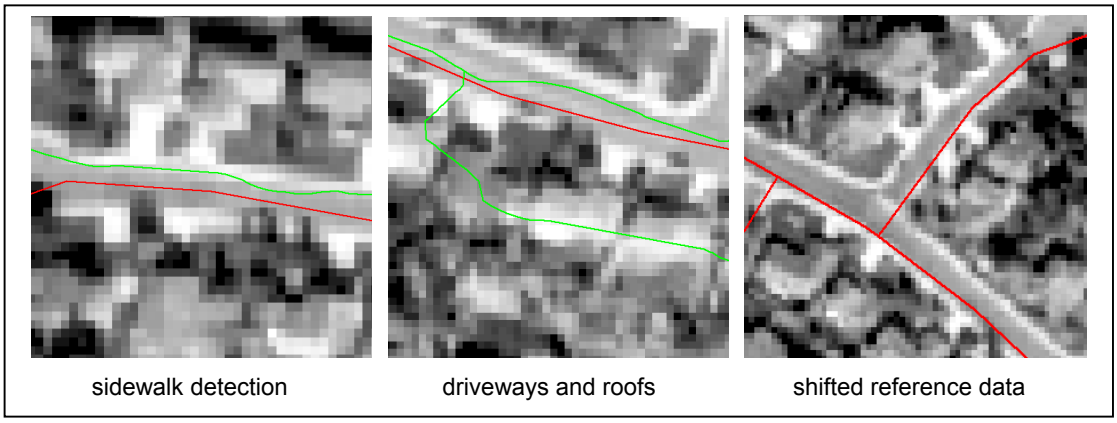

Figure 33: Effects in extracted vectors (urban areas, optical imagery)

Reference vectors are displayed in red, extracted vectors in green. The same effects as in the respective chapter 6.1.2.1 can be seen: in the first picture, the previously explained extraction of sidewalks, bearing a higher grey value than the actual road, is shown. The second picture displays the effects caused by disturbing objects such as driveways or house roofs. The extraction may be shifted towards the high grey value provided by the driveways. In extreme cases, the model even allows the creation of extractions far off from the actual road, as shown in the lower part of the image. In the third picture, the shifting of reference data can clearly be seen. This effect is believed to be caused by elevated structures, as it does not occur in open areas. Additionally, the effects of extraction on images' borders, as in the respective SAR images, occurs as well.
Concluding, it is evident that the extraction approach by C. Wiedemann faces the same problems as its counterpart. A road model for urban areas is extremely difficult to model and a compromise between the detection of road center lines and the number of inevitable false positive extractions has to be found.

6.3.2.2 Results for open areas

The tests for open areas refer to the same images as in the respective chapters treating the Intermap extraction algorithm. A sample optical image with mainly urban context is given in Figure 29, chapter 6.1.2.2.
Because of the difference in appearance of open areas compared to urban areas, the extraction algorithm has to be adapted accordingly. Characteristics of open areas in optical imagery are explained in detail in chapter 6.1.2.2.
Figure 34 shows an example for extracted vectors in comparison to their reference in open areas after applying the TU Munich extraction algorithm. Extracted roads are

displayed in green, reference vectors in red. Regions in blue are urban context areas and are therefore not considered for further investigations in this part.

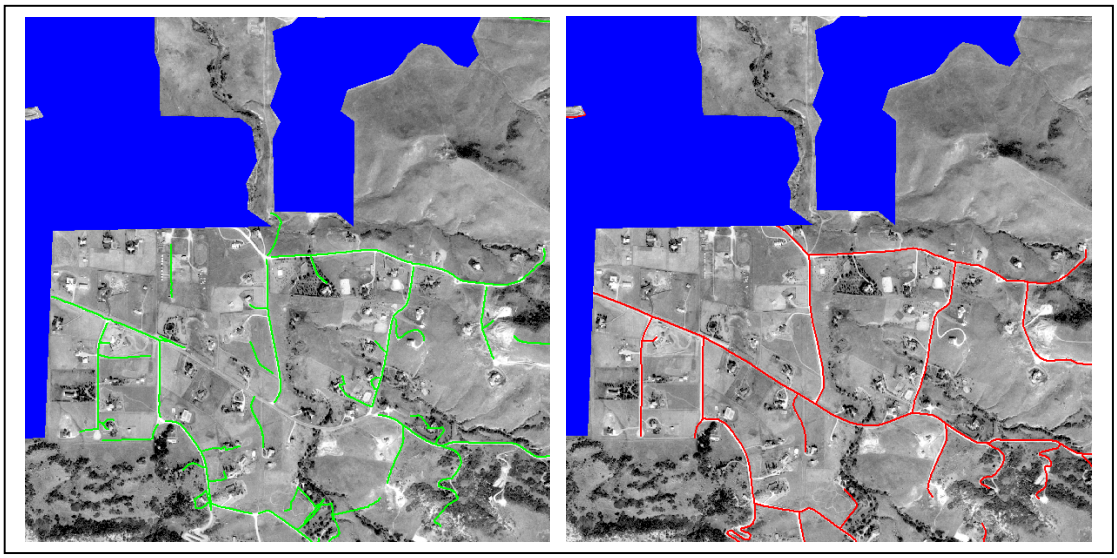

Figure 34: Extraction result (left) and reference (right) in open areas (optical imagery + TU Munich extraction algorithm)

As can be seen in the figure, the algorithm achieves good results in open areas, because of the generally better contrast provided by roads and surroundings. Some roads are omitted due to low contrast and some false positive extractions occur. However, the overall result can be considered satisfying.
Referring to Figure 20 in chapter 5.1.2.2, the key parameters that have to be modelled in order to receive competitive extraction results can be derived:

a) The parameter LINE_WIDTH can be set to 7.5 meters in order to restrict the line extraction to narrow lines only.
b) The parameter THRESHOLD can be raised to 150, allowing only brighter pixels to be taken into account for the line extraction.
c) In order to apply an appropriate evaluation, the parameter FUZZY_WIDTH has to be run in a 2 – 5 – 10 – 13 configuration.

Additionally, the network length that has to be achieved in order for a conjunction of extracted lines to be considered for the final network generation is increased to 150.0 meters. An overview of the parameters altered in order to enable a context-driven extraction is given in the appendix, section B.4.

Modelling the extraction parameters for open areas in aerial imagery is easier than in urban areas, because sufficient contrast is given by the road against its surroundings. However, algorithm-related problems like the effects of border extractions and multiple crossings, as explained in chapter 5.2.2.1 occur nonetheless.

6.3.2.3 Overall results

Table 7 shows the extraction results in open and urban areas from optical imagery, applying the TU Munich extraction software developed by C. Wiedemann. Values for correctly applied parameters are displayed in italics. The results are based on the 18 images available for the whole test site, covering approximately 65 km^2. The total length of roads contained in the reference is 503 kilometres.

Evaluation					
Context region	Urban		Open		Overall
Applied parameters	Urban	Open	Urban	Open	Urban / Open
Completeness	*47.0 %*	26.7 %	20.9 %	*55.8 %*	*49.6 %*
Correctness	*52.4 %*	41.0 %	21.6 %	*67.8 %*	*56.9 %*
Quality	***33.0 %***	**19.3 %**	**11.9 %**	***44.1 %***	***36.0 %***

Table 7: Evaluation results (TU Munich extraction algorithm on optical imagery)

The results for both open and urban areas with the application of wrong parameters support the results found earlier and emphasize the necessity of contextual modelling. For open areas, and the application of correct parameters, 55.8 % of the reference vectors are detected, while 47.0 % can be achieved for open areas. The correctness of the extracted vectors can be considered as good in open areas, reaching a value of 67.8 %. In urban areas, only 52.4 % of the extracted vectors coincide with the given reference.
The statistics show that good results can be achieved for open areas, which is due to the effects explained earlier. The achievements for completeness and correctness lead to a quality measure of 44.1 %, which is considered to be reasonable for open imagery.
The weaker results for urban areas are not surprising, considering the inconsistent conditions given in these regions. However, the increase in both completeness and correctness when applying correct parameters reveals that less false positives as well as less false negatives can be detected. The quality measure of 33.0 % does not get is within the range of the quality provided in open areas.

The overall results with correctly applied parameters show that close to half of the vectors given in the reference data were detected from the imagery. A little more than half of all extracted vectors coincide with the given reference. The overall quality of 36.0 % seems to be poor, but is highly influenced by the greater amount of urban roads.

6.4. Comparison of results from SAR and optical imagery (TU Munich extraction algorithm)

Table 8 provides a comparison of both imagery sources in relation to both applied context regions for the TU Munich extraction algorithm.

Evaluation				
Imagery source	SAR		Optical	
Context region	Urban	Open	Urban	Open
Completeness	56.2 %	22.6 %	47.0 %	55.8 %
Correctness	81.9 %	47.0 %	52.4 %	67.8 %
Quality	**50.0 %**	**18.0 %**	**33.0 %**	**44.1 %**

Table 8: Comparison of results (TU Munich extraction algorithm)

The statistical results for applying correct contextual parameters are displayed. The *quality* measure combines the measures *completeness* and *correctness*. It therefore gives a summarized final value for the capability of the extraction in relation to the imagery source.

The highest quality value of 50.0 % can be achieved when applying this algorithm to SAR imagery in urban areas. A completeness of 56.2 % and a very good correctness of 81.9 % show that convincing extraction results can be obtained in this configuration. The values achieved for optical imagery in open areas are not as good, but still reasonable. 55.8 % completeness and 67.8 % correctness lead to a quality measure of 44.1 %. The remaining two options (SAR in open areas and optical in urban areas) cannot compete with the preceding results, although the quality measure for optical imagery in urban areas achieves 33.0 %.

Concluding, it can be stated that, when using the extraction algorithm, developed by C. Wiedemann at the TU Munich, the restriction of using SAR imagery for urban context and optical imagery for open context is most important.

6.5. Comparison of TU Munich and Intermap extraction algorithms on optical imagery

Comparing the outcome achieved by both algorithms, no significant differences can be found. Both algorithms can be adapted to the respective context regions and show reasonable results. When focusing on open areas, where the best extraction results were achieved, it can be seen that the results presented by the TU Munich extraction algorithm provide higher values in both completeness and correctness. Concluding, both algorithms can compete when processing open areas in optical imagery. Within urban areas, however, the results cannot be considered satisfying. The usefulness of road extraction from optical imagery in these contexts, applying the presented approaches, can be doubted.
The results concerning user-friendliness and general handling for both extraction algorithms, as stated in chapter 5.3, apply here in the same way. Considering the computation time needed, the TU Munich extraction software shows a clear advantage, as it already did in the handling of SAR imagery, because contextual extractions are restricted to their respective regions and do not have to be processed for the whole image. Especially when dealing with an increasing amount of context regions the Intermap algorithm is more time-intensive, both on the computer-processing and manual post-processing part.

6.6. Enhanced extraction by merging of SAR and optical imagery results

Up to now, the presented extraction results were based on separate approaches dealing *either* with the SAR imagery obtained by Intermap's STAR-3*i* system *or* the optical imagery stemming from aerial photography. These approaches reveal the limitations of each imagery source: SAR data leads to relatively good extraction results in urban areas, while only poor results can be achieved for open areas. For optical data, the same applies vice versa.
This leads to the assumption that a combination of extracted vectors from SAR imagery in urban areas and optical imagery in open areas may lead to overall better results for the whole test site. The extraction algorithm developed by C. Wiedemann at the TU Munich contains a module that offers the possibility of merging extracted vectors from various sources.
In theory, a fusion of the results provided by the two investigated extractions algorithms could also be carried out. However, because both of them provide similar results in the same areas, this procedure is not expected to lead to a strong enhancement regarding the overall outcome. Nonetheless, yet another option that can be carried out by a fusion is the joining of separate smaller tiles to a bigger,

continuous image, covering a greater area. By doing so, the earlier explained effects in areas close to the original images' borders can be overcome, because the network generation takes into account available images on either side of previously existing borders.
Chapter 6.6.1 explains the general test approach for the module that carries out the fusion of optical and SAR imagery, as well as the necessary steps to achieve a final combination of the extracted vectors. The results and evaluations are given in chapter 6.6.2, followed by a comparison to the earlier obtained results without a combination of imagery sources.

6.6.1. Test approach

In order to combine extracted vectors originating from two different imagery sources, the area covered by both has to be connected almost seamlessly to eliminate the possibility of gaps occurring in the final result. Because the available optical imagery covers only part of the test site used for the investigations on SAR imagery, all following procedures are restricted to a smaller area. The test site used for the following investigations is identical with the one described in chapter 6.1.1, where detailed information is given about its properties.

The procedures for line extraction, smoothing and splitting of these lines, and the fuzzy evaluation, are carried out separately for the respective imagery sources. This is necessary because fundamentally different road models apply to each of the two. The modules *"extr_lines"*, *"smspl_lines"* and *"fuzzy_lines"* are processed in the configurations given in appendix sections B.1 and B.4, respectively. The fusion of the extracted and evaluated vectors then creates one consistent data set, applying the module *"fuse_lines"*. Pursuing the extraction algorithm, the modules *"split_lines"* and *"calc_paths"* are applied to the merged vector data, which generate the final road network.
A detailed description of the obtained results is given in the following chapter 6.6.2.

6.6.2. Results and evaluation

The extraction approach designed by C. Wiedemann at the TU Munich supports extractions restricted to a previously defined context area. Therefore, the first three modules (*"extr_lines"*, *"smspl_lines"* and *"fuzzy_lines"*) can be applied to the different images within their respective context regions. Figure 35 shows a part of the test site, containing both urban regions (displayed by SAR imagery) and open regions (displayed by optical imagery). The image contains of four tiles, therefore covering an area of 4 km x 4 km.

Figure 35: Urban context region (SAR imagery) + open context region (optical imagery)

The extracted lines after the application of the algorithm's first module, are displayed in Figure 36.

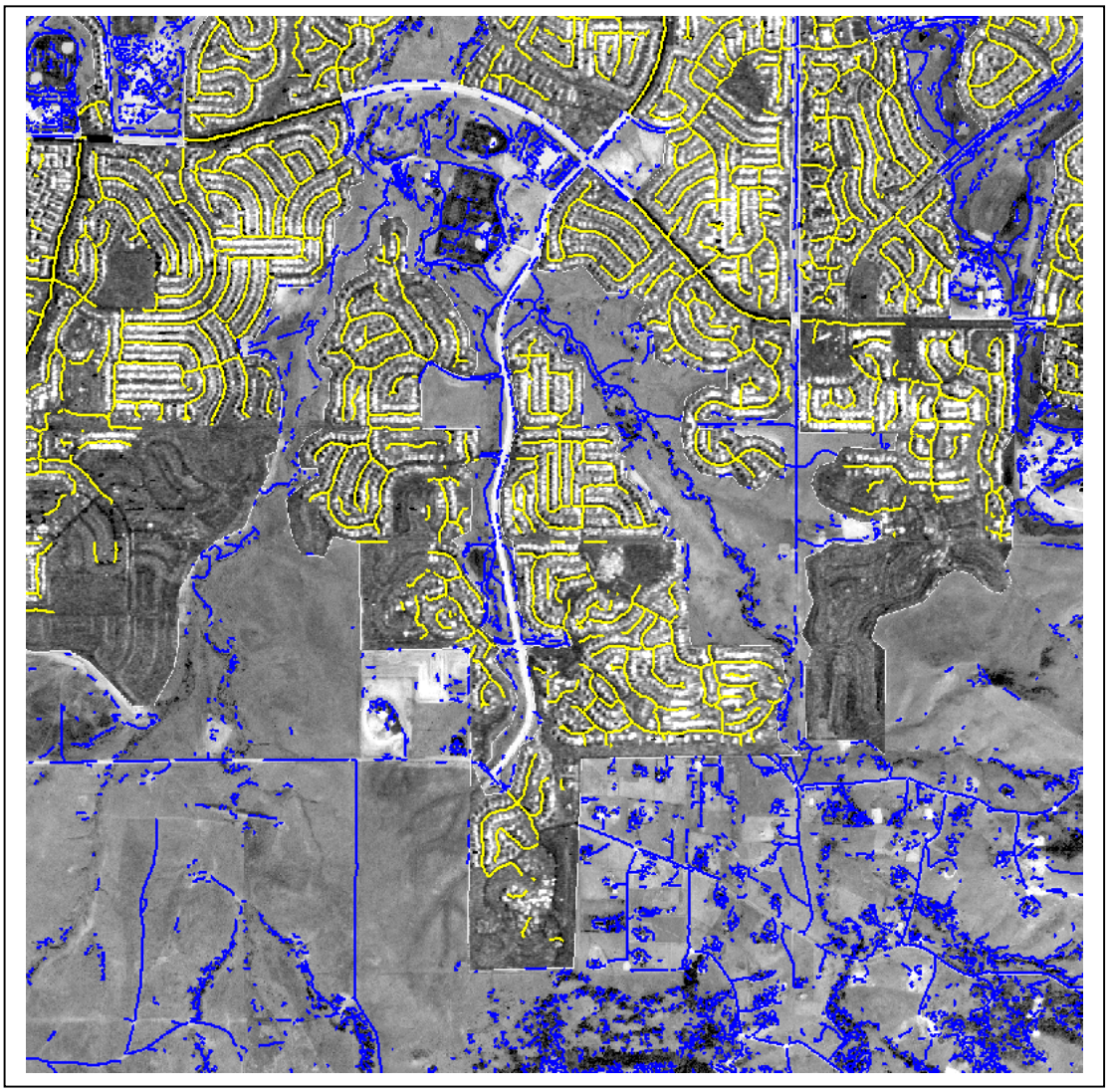

Figure 36: Extracted lines in urban and open context regions

The image shows the lines for urban areas in yellow and for open areas in blue. It is obvious that, at this point, a high amount of false positive extractions is still present. This is especially the case in mountainous regions and in the bottom right corner, where many lines fit the appearance defined in the extraction module. Depending on the last module "calc_paths", which is responsible for the final network generation, most of the small, isolated pixel chains are not taken into account, if they bear an overall fuzzy value that is lower than the one defined in the module. The following Figure 37 shows the fuzzy evaluation for these lines in open and urban areas.

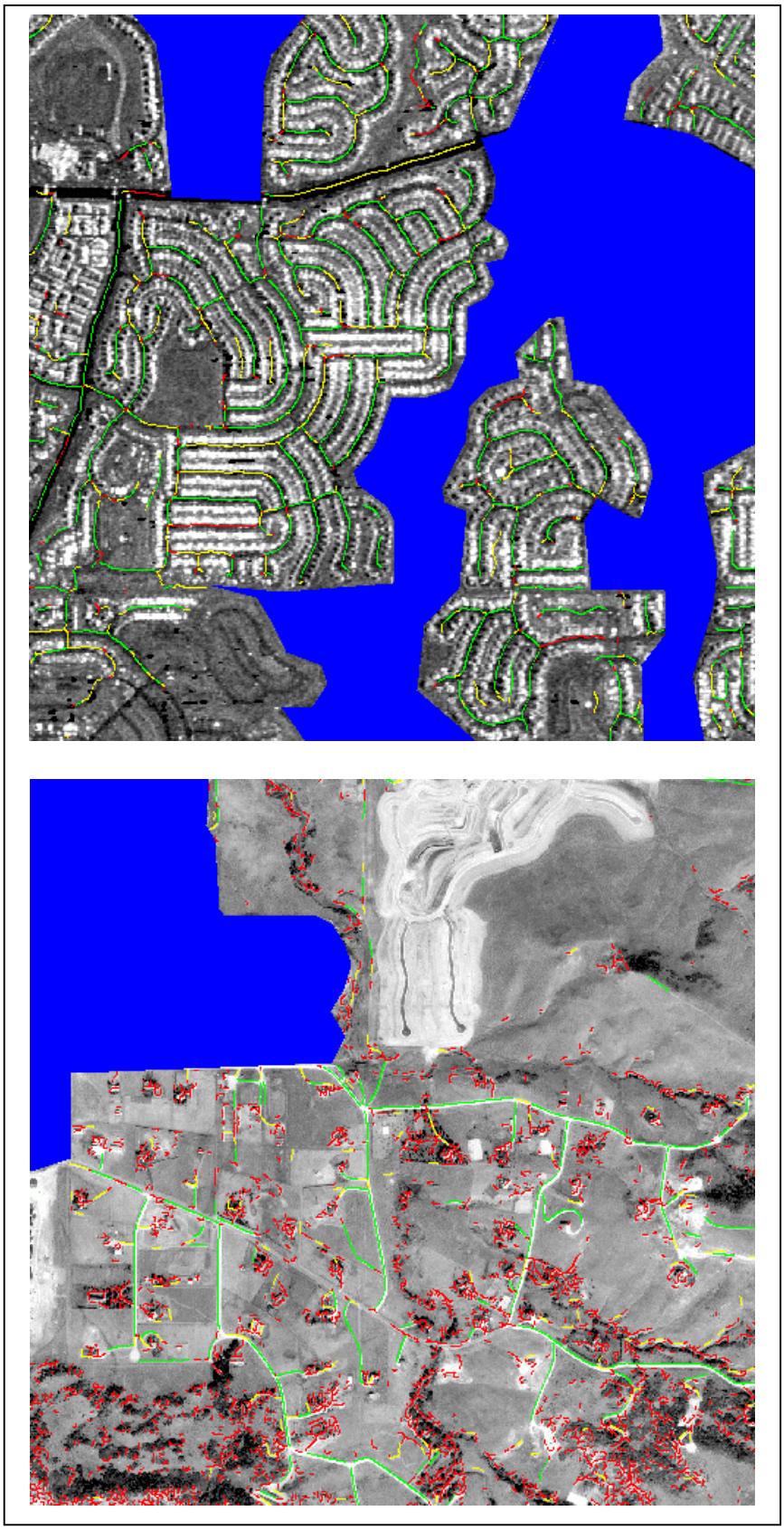

Figure 37: Fuzzy evaluation in urban context from SAR (top) and open context from optical imagery (bottom)

The images show the representation of the overall fuzzy values for urban and open areas in three different colours: green lines achieved a very good overall value, yellow lines a good value and red lines a poor evaluation. Lines that achieved a zero value in one of their evaluation criteria, leading to an overall value of zero, are not depicted.
It can be seen that most of the false positive extractions in open areas have achieved only a poor overall fuzzy value. Most of these pixel chains will not be taken into account for the final network generation, unless they provide a connection in between seedpoints.

The following Figure 38 shows the final extraction result after the fusion of the evaluated vectors from both imagery sources and the reference for the same area. Extracted vectors are displayed in green, reference data in red.

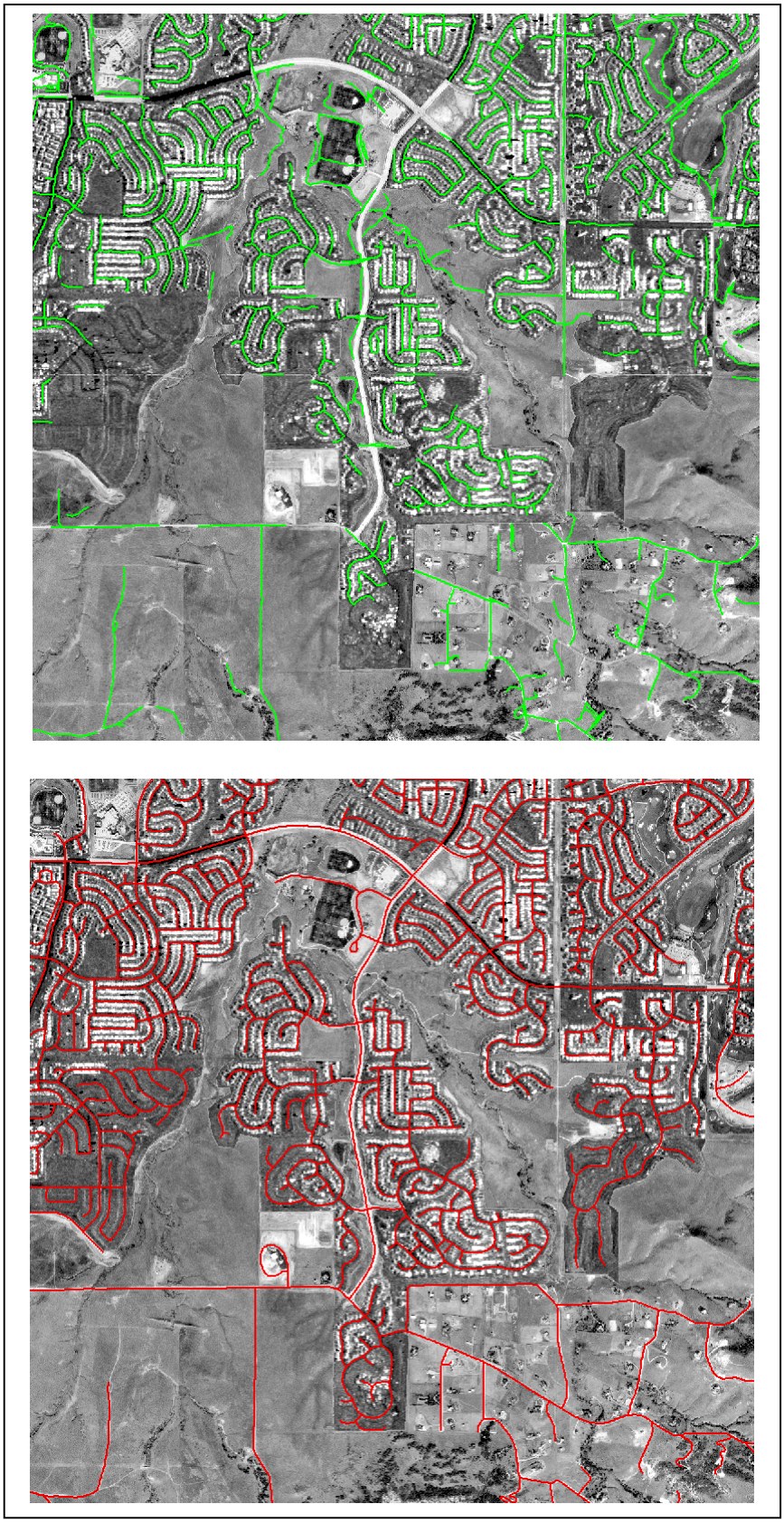

Figure 38: Final extraction result (top) and reference (bottom) after fusion of urban context regions from SAR and open context regions from optical imagery

In comparison to the earlier presented images displaying the extracted lines with their respective fuzzy evaluations, it can be seen that a great amount of false positive extractions in open areas could be eliminated. Furthermore, most preliminary extractions in urban areas are still present in the final result, due to their good overall fuzzy value. Additionally, the image shows that a combination of the extraction from both imagery sources with restrictions to the regions where good results were obtained, can lead to good overall extraction results. The extraction algorithm focuses on one context region for one imagery source only. Therefore, all positive extraction-related effects that are explained in chapters 5.2 and 6.3 can be exploited, while most negative extraction-related effects are eliminated. However, the earlier explained phenomena like offsets and extraction on the image's borders, as well as multiple crossings in intersections still occur, because they are not modelled by the algorithm. Furthermore, the temporal difference between younger reference data and older SAR imagery has an immediate effect on the statistical results. Table 9 shows the overall results achieved by merging SAR and optical imagery sources.

Evaluation	
Context region	Overall
Applied parameters	Urban / Open
Completeness	56.2 %
Correctness	75.7 %
Quality	**47.6 %**

Table 9: Evaluation results (merging of SAR and optical imagery sources)

The results show that the combination of both imagery sources lead to a completeness of 56.2 % for all vectors contained in the test site. More than three quarters of the amount of extracted vectors coincide with the reference and are therefore considered to be correct. This leads to an overall quality measure of 47.6 %.
A comparison of all overall results is displayed in the following Table 10.

Comparison (overall results)					
Extraction algorithm	Intermap		TU Munich		Fusion
Imagery source	SAR	optical	SAR	optical	combined
Completeness	55.2 %	30.8 %	46.4 %	49.6 %	56.2 %
Correctness	63.8 %	45.4 %	71.8 %	56.9 %	75.7 %
Quality	**42.0 %**	**22.5 %**	**39.3 %**	**36.0 %**	**47.6 %**

Table 10: Comparison of overall results

It is evident that the fusion of vectors from both imagery sources leads to an overall better result. In fact, this procedure is the only possible combination that leads to a

value of almost 50 % in quality. Furthermore, it also surpasses the other combinations in completeness and correctness.

The comparison of all overall results clearly shows that automated road extraction can be enhanced by applying special parameters not only to regions of the same contextual appearance, but especially by using different imagery sources for different context regions. By doing so, the advantages provided by each imagery source can be combined and exploited in order to achieve more satisfying extraction results.

Practically, however, SAR and optical imagery for the same site and with a short time difference in between the data acquisition for each of the sources is rarely available.

7. Summary and outlook

This chapter concludes the presented work by summarizing the achieved results. Furthermore, an outlook on possible further investigations is provided.

7.1. Summary

This thesis investigates road extraction algorithms and their adaptability to two different imagery sources, which are radar and optical data. Automated object extraction can provide a time-efficient approach to the tasks of acquisition and updating of vector data within a Geographic Information System (GIS). Radar imagery and aerial photography can serve as sources for the raster images that provide the basis for the extraction procedures, which in turn lead to vector-based results. The thesis offers an insight into the basic principles of radar systems and gives an overview of the specific image properties. The main differences to optical imagery as well as application areas for radar imagery are stated.
The automated extraction of linear objects from any imagery source depends on the given resolution as well as the image properties itself and has to be modelled accordingly. Existing approaches for different road models are presented and an overview of road extraction algorithms is given. Two of these algorithms are chosen for further investigation: the Intermap extraction algorithm, developed by K. Lang at Intermap Technologies GmbH Wessling, which was originally designed for use on radar imagery in urban areas, and the TU Munich extraction algorithm, developed by C. Wiedemann at the Technische Universität München, primarily designed for use on optical imagery in open areas.
In order to improve the extraction results, a restriction to regions of similar contextual appearance is proposed. Possible methods for creating these regions are presented. The two extraction algorithms and their alterable parameters are explained in detail and necessary adaptations for both imagery sources and context regions are examined.
The practical analysis of both algorithms carries out extensive investigations on a test site that is available for both radar and optical imagery and consists of regions with urban and open context. In order to evaluate the results computed by each algorithm, the criteria completeness, correctness and quality are used. Because of the application of identical parameters for the evaluation, the derived results can be compared for each of the two extraction algorithms as well as for each imagery source in open and urban areas.
The stated results show that both algorithms can achieve similar results in identical areas and imagery sources. However, the handling of the extraction process itself shows differences: for instance, the Intermap extraction algorithm employs partial

derivatives in order to model contrast differences and uniformity in the image, whereas the TU Munich extraction algorithm directly uses grey value differences. It is assumed that the latter procedure is easier to understand for untrained users. Additionally, the TU Munich algorithm offers a direct visual control after each extraction step. The results from the Intermap software, in contrast, have to be imported into a GIS environment in order to be displayed.
Both algorithms show that SAR and optical imagery can give relatively good results if restricted to certain areas: While imagery from aerial photography leads to satisfying results in open areas, radar imagery can provide sufficient information for automated extraction in urban areas. Applying the reverse configuration cannot be recommended, as much poorer results are achieved, due to the respective image properties.
The TU Munich extraction algorithm offers a feature for the possibility of fusing extraction processes, for instance extractions from different imagery sources. In order to enhance the overall results, a combination of radar imagery for urban, and optical imagery for open areas is carried out. It is shown that this configuration reaches the highest statistical evaluation. This leads to the recommendation to use radar imagery for extraction in urban and optical imagery for extraction in open areas only. However, when combining these two imagery sources practically, it has to be considered that the acquisition of data for both can hardly be realised within a tolerable time difference. If the two sources are not acquired within a certain period of time, the initial idea of a near-to-date updating of GIS by automated road extraction cannot be achieved anymore.

7.2. Outlook

The investigations concerning the possibilities and limitations of automated road extraction from radar and optical imagery have been carried out to a deep extent in this thesis. However, further research is required, as the achieved results were restricted to the available test site that only consisted of urban and open areas. Other areas, like forests or agricultural regions, have not been considered yet and may need separate modelling.
Additionally, radar imagery with higher resolution could be considered for road extraction as well, although knowing that the extraction of linear features may fail and other road models would have to be taken into account which e.g. model roads as elongated regions.
In general, the application of a two-step approach for road extraction, as proposed by [Fischler et al., 1981], could also lead to improved extraction results. A primary step carries out the road extraction with very restrictive parameters. This leads to a preliminary result that contains few false positive extractions. A secondary, more

tolerable step then generates the road network itself. Recent research in that direction is, for instance, presented in [Gerke et al., 2003].
Furthermore, the implementation of a refined model for the network generation, especially regarding intersection areas, as proposed in [Wiedemann, 2002], could lead to the elimination of multiple junctions and therefore improve the overall operational functionality.

References

BAUMGARTNER, A., ECKSTEIN, W., HEIPKE, C., HINZ, S., MAYER, H., RADIG, B., STEGER, C. AND WIEDEMANN, C. (1999): *T-REX: TUM-Research on Road Extraction.* In: Festschrift für Prof. Dr.-Ing. Heinrich Ebner zum 60. Geburtstag, pp. 43 - 64.

BAUMGARTNER, A., ECKSTEIN, W., MAYER, H., HEIPKE, C. AND EBNER, H. (1997): *Context-Supported Road Extraction.* In: GRUEN, A., BALTSAVIAS, E. AND HENRICSSON, O. (Publishers), Automatic Extraction of Man-Made Objects from Aerial and Space Images (II), Birkhaeuser Verlag, Basel, Switzerland, pp. 299 - 308.

BUSCH, A. AND WILLRICH, F. (2002): *Quality Management of ATKIS Data.* Proceeding CD of the OEEPE/ISPRS Joint Workshop on Spatial Data Quality Management, Istanbul, Turkey, March 21st – 22nd, 2002, pp. 30 - 41.

BUTENUTH, M. (2002): *Steuerung bei der Qualitätskontrolle linienhafter Geo-Daten auf Basis von Orthofotos unter Nutzung eines GIS.* Diploma thesis, Institute for Photogrammetry and GeoInformation, University of Hannover, Germany.

CCRS – CANADA CENTRE FOR REMOTE SENSING (2001): *Introduction to Radar Remote Sensing*. In: http://www.ccrs.nrcan.gc.ca/ccrs/learn/learn_e.html.

CORNELIS, J., NYSSEN, E., KATARTZIS, A., VAN KEMPEN, L., DEKLERCK, R. AND SALOMIE, A. (2000): *Statistical Models for Multidisciplinary Applications of Image Segmentation and Labelling.* In: Proceedings of IEEE World Computer Conference / 5th International Conference on Signal Processing, Beijing, China, 2000, pp. 2103 - 2110.

FHWA (1998): *Our Nation's Highways – Selected Facts and Figures*. In: Federal Highway Administration, U.S. Department of Transportation, http://www.fhwa.dot.gov/ohim/onh/onh98.pdf.

FISCHLER, M., TENENBAUM, J. AND WOLF, H. (1981): *Detection of roads and linear structures in Low-Resolution Aerial Imagery Using a Multisource Knowledge Integration Technique.* In: Computer Graphics and Image Processing 15: pp. 201 - 223.

GERKE, M., BUTENUTH. M., HEIPKE, C. AND WILLRICH, F. (2003): *Graph Supported Automated Verification of Road Databases Using Aerial Imagery.* In: Proceedings of the 2nd International Symposium on Spatial Data Quality, Hong Kong. Shi, W., Goodchild, M. F., Fisher, P.F. (Ed.), pp. 421 - 430.

HELLWICH, O., LAPTEV. I. AND MAYER H. (2002): *Extraction of linear objects from interferomteric SAR data.* In: International Journal of Remote Sensing, 2002, vol. 23, no. 3, pp. 461 - 475.

HINZ, S. AND BAUMGARTNER, A. (2003): *Automatic Extraction of Urban Road Networks from Multi-View Aerial Imagery.* In: ISPRS Journal of Photogrammetry and Remote Sensing, 2003 (Preprint, to appear).

HINZ, S., BAUMGARTNER, A. AND STEGER, C. (2000): *Road Extraction from Digital Aerial Imagery.* Technical report (DFG Final report).

HOFMANN, C., SCHWÄBISCH, OCH, S., WIMMER, C. AND MOREIRA J. (1999): *Multipath P-Band Interferometry – First Results.* In: Proceddings of the 4th International Airborne Remote Sensing Conference and Exhibition / 21st Canadian Symposium on Remote Sensing, Ottawa, Ontario, Canada, 21st – 24th June 1999.

HUBER, R. AND LANG, K. (2001): *Road Extraction from High-Resolution Airborne SAR using Operator Fusion.* Proceedings of the International Geoscience and Remote Sensing Symposium, July 9th-13th, 2001, Sydney, Australia.

JPL (2003): *Shuttle Radar Topography Mission.* In: Jet Propulsion Laboratory, http://www.jpl.nasa.gov/srtm/.

LEBERL, F. (1990): *Radargrammetric Image Processing*. Norwood, Massachusetts, USA.

LI, X., BAKER, A. AND HUTT, T. (2002): *Accuracy of Airborne IFSAR Mapping.* In: FIG, XXII International Congress, April 19th – 26th, 2002.

LONG, M. (2001): *Radar Reflectivity of Land and Sea*. Boston, Massachusetts, USA.

MERCER, B. AND GILL, M. (1998): *Radar-Derived DEMs for Urban Areas.* In: Proceedings of the ISPRS Commission II Symposium, Cambridge, Vol. 32, Part 2, pp. 210 - 216.

SEEBER, G. (1993): *Satellite Geodesy – Foundations, Methods and Applications*. Berlin, Germany.

STEGER, C. (1998): *An Unbiased Detector of Curvilinear Structures.* In: IEEE Transactions on Pattern Analysis and Machine Intelligence, vol. 20 (2), pp. 113 - 125.

STRAUB, B.-M., WIEDEMANN, C. AND HEIPKE, C. (2000): *Towards the Automated Interpretation of Images*. In: Proceedings of ISPRS, Vol. XXXIII, Amsterdam, 2000, pp. 525 - 323.

TECGRAF (2002): *The Programming Language Lua.* In: Pontifical Catholic University of Rio de Janeiro, Brazil, http://www.lua.org.

TENNANT, K. AND COYNE, T. (1999): *STAR-3i interferometric synthetic aperture radar (INSAR): Some lessons learned on the road to commercialization.* In: Proceddings of the 4th International Airborne Remote Sensing Conference and Exhibition / 21st Canadian Symposium on Remote Sensing, Ottawa, Ontario, Canada, 21st – 24th June 1999.

TIGHE, L. AND BAKER, A. (2000): *Topographic line map production using high resolution airborne interferometric SAR*. In: Proceedings of 2001 ASPRS Annual Conference, St.Louis, Missouri, USA, April 23rd – 27th, 2001.

TUPIN, F., MAÎTRE, H., MANGIN, J. F., NICOLAS, J. M. AND PECHERSKY, E. (1998): *Detection of linear features in SAR images: Application to road network extraction.* In: IEEE Transactions on Geoscience and Remote Sensing, 36(2), pp. 434 - 453.

WESSEL, B., WIEDEMANN, C., HELLWICH, O. and ARNDT, W.-C. (2002): *Evaluation of Automatic Road Extraction Results from SAR Imagery.* In: International Archives of the Photogrammetry, Remote Sensing and Spatial Information Sciences, Vol. XXXIV, Part 4, Commission IV, Symposium on Geospatial Theory.

WIEDEMANN, C. (2002): *Extraktion von Straßennetzen aus optischen Satellitenbildern.* Dissertation, Faculty for Photogrammetry and Remote Sensing, TU Munich, Germany.

WIEDEMANN, C., HEIPKE, C. MAYER, H. and JAMET, O. (1998): *Empirical Evaluation of Automatically Extracted Road Axes.* In: BOWYER, K. J. and PHILLIPS, P. J. (eds.), Empirical Evaluation Methodes in Computer Vision, IEEE Computer Society Press, Los Alamitos, California, USA, pp. 172 - 187.

WILLRICH, F. (2002): *Quality Control and Updating of Road Data by GIS-driven Road Extraction from Imagery.* Proceedings of the Joint International Symposium on Geospatial Theory, Processing, and Applications and ISPRS Commission IV, Symposium, July 8th-12th, 2002, Ottawa, Canada.

List of Figures

List of Tables

Appendix

A.1. Alterable parameters for Intermap extraction algorithm (SAR imagery and urban areas)

- *Differential geometry:*

```
-- Initialize the object for the Steger line detection algorithm:
differentialGeometry = DifferentialGeometry:new( 0.1, 0.55, 0.5,
5, 1, 3.5)
```

- *SAR operator:*

```
-- Initialize the SAR Road Operator with the desired parameters:
SRO = SARRoadOperator:new( imgFlat, 1.5, 0.1, 1.0, 2.0, 100.0,
101.0, 7, 2, 7)
```

- *Collinear reconnection:*

```
-- Reconnect the lines based on TUM colinear reconnection scheme
ReconnectLines( imgOriginal, 30.0, 45.0, 1.0, 3.0, 150.0, 170.0,
190.0, 210.0, 0.0, 0.0, 0.0, 0.0, graphWork, RECONNECT_COLINEAR)
```

- *Perpendicular reconnection:*

```
-- Reconnect the lines based on TUM perpendicular reconnection
scheme
ReconnectLines( imgOriginal, 5.0, 20.0, 1.0, 3.0, 60.0, 80.0,
110.0, 130.0, 150.0, 170.0, 190.0, 210.0, graphWork,
RECONNECT_TRIANGULATED)
```

- *Network trimming:*

```
-- Trim the networks to a length of 100 pixels
TrimNetworks( graphWork, graphOut, 100.0)
```

A.2. Alterable parameters for Intermap extraction algorithm (SAR imagery and open areas)

- *Differential geometry:*

```
-- Initialize the object for the Steger line detection algorithm:
differentialGeometry = DifferentialGeometry:new( 0.1, 0.55, 0.5,
5, 1, 2.5)
```

- *SAR operator:*

```
-- Initialize the SAR Road Operator with the desired parameters:
SRO = SARRoadOperator:new( imgFlat, 1.5, 0.1, 1.0, 2.0, 100.0,
101.0, 2, 1, 2)
```

- *Collinear reconnection:*

```
-- Reconnect the lines based on TUM colinear reconnection scheme
ReconnectLines( imgOriginal, 10.0, 50.0, 1.0, 3.0, 150.0, 170.0,
190.0, 210.0, 0.0, 0.0, 0.0, 0.0, graphWork, RECONNECT_COLINEAR)
```

- *Perpendicular reconnection:*

```
-- Reconnect the lines based on TUM perpendicular reconnection
scheme
ReconnectLines( imgOriginal, 5.0, 10.0, 1.0, 3.0, 60.0, 80.0,
110.0, 130.0, 150.0, 170.0, 190.0, 210.0, graphWork,
RECONNECT_TRIANGULATED)
```

- *Network trimming:*

```
-- Trim the networks to a length of 150 pixels
TrimNetworks( graphWork, graphOut, 150.0)
```

A.3. Alterable parameters for Intermap extraction algorithm (optical imagery and urban areas)

- *Differential geometry:*

```
-- Initialize the object for the Steger line detection algorithm:
differentialGeometry = DifferentialGeometry:new( 0.07, 1.0, 0.5,
5, 1, 3.0)
```

- *SAR operator:*

```
-- Initialize the SAR Road Operator with the desired parameters:
SRO = SARRoadOperator:new( imgFlat, 1.5, 0.1, 1.0, 2.0, 100.0,
101.0, 6, 3, 6)
```

- *Collinear reconnection:*

```
-- Reconnect the lines based on TUM colinear reconnection scheme
ReconnectLines( imgOriginal, 30.0, 45.0, 1.0, 3.0, 150.0, 170.0,
190.0, 210.0, 0.0, 0.0, 0.0, 0.0, graphWork, RECONNECT_COLINEAR)
```

- *Perpendicular reconnection:*

```
-- Reconnect the lines based on TUM perpendicular reconnection
scheme
ReconnectLines( imgOriginal, 7.5, 30.0, 1.0, 3.0, 60.0, 80.0,
110.0, 130.0, 150.0, 170.0, 190.0, 210.0, graphWork,
RECONNECT_TRIANGULATED)
```

- *Network trimming:*

```
-- Trim the networks to a length of 150 pixels
TrimNetworks( graphWork, graphOut, 150.0)
```

A.4. Alterable parameters for Intermap extraction algorithm (optical imagery and open areas)

- *Differential geometry:*

```
-- Initialize the object for the Steger line detection algorithm:
differentialGeometry = DifferentialGeometry:new( 0.07, 1.0, 0.5,
5, 1, 3.0)
```

- *SAR operator:*

```
-- Initialize the SAR Road Operator with the desired parameters:
SRO = SARRoadOperator:new( imgFlat, 1.5, 0.1, 1.0, 2.0, 100.0,
101.0, 3, 1, 3)
```

- *Collinear reconnection:*

```
-- Reconnect the lines based on TUM colinear reconnection scheme
ReconnectLines( imgOriginal, 15.0, 60.0, 1.0, 3.0, 150.0, 170.0,
190.0, 210.0, 0.0, 0.0, 0.0, 0.0, graphWork, RECONNECT_COLINEAR)
```

- *Perpendicular reconnection:*

```
-- Reconnect the lines based on TUM perpendicular reconnection
scheme
ReconnectLines( imgOriginal, 7.5, 15.0, 1.0, 3.0, 60.0, 80.0,
110.0, 130.0, 150.0, 170.0, 190.0, 210.0, graphWork,
RECONNECT_TRIANGULATED)
```

- *Network trimming:*

```
-- Trim the networks to a length of 200 pixels
TrimNetworks( graphWork, graphOut, 200.0)
```

B.1. Alterable parameters for TU Munich extraction algorithm (SAR imagery and urban areas)

- *Parameter extr_lines:*

```
WITH_WINDOW                    1
THRESHOLD                      75
LINE_WIDTH                     45.0
CONTRAST_HIGH                  100
CONTRAST_LOW                   30
LINE_BRIGHTNESS                dark
```

- *Parameter smspl_lines:*

```
WITH_WINDOW                    1
SMOOTH_LENGTH                  5
MAX_CURVATURE                  0.100
```

- *Parameter fuzzy_lines:*

```
WITH_WINDOW                    1
FUZZY_LENGTH                   5   10
FUZZY_ORIENTATION              0   20
FUZZY_WIDTH                    3   5   35   50
FUZZY_WIDTH_DEVIATION          0   20
FUZZY_GRAY_DEVIATION           0   20
```

- *Parameter fuse_lines:*

```
WITH_WINDOW                    1
WEIGHTS                        1.00
WEIGHT_SCALES                  1
BUFFER_WIDTH                   20.000
DIRECTION_DIFFERENCE           30.000
```

- *Parameter split_lines:*

```
WITH_WINDOW                    1
DISTANCE                       5.000
```

- *Parameter calc_paths:*

```
WITH_WINDOW                    1
FUZZY_WEIGHT                   0   1
FUZZY_ABS_DISTANCE             5   100
FUZZY_REL_DISTANCE             1   8
FUZZY_COLLINEAR                0   25
FUZZY_JUNCTION                 55   90
MAX_DIST_JUNCTION              5
SCALE_LENGTH                   true
WEIGHT_SEEDPOINT               0.500
MIN_DISTANCE                   100
```

B.2. Alterable parameters for TU Munich extraction algorithm (SAR imagery and open areas)

- *Parameter extr_lines:*

```
WITH_WINDOW                     1
THRESHOLD                       90
LINE_WIDTH                      7.5
CONTRAST_HIGH                   50
CONTRAST_LOW                    20
LINE_BRIGHTNESS                 dark
```

- *Parameter smspl_lines:*

```
WITH_WINDOW                     1
SMOOTH_LENGTH                   5
MAX_CURVATURE                   0.100
```

- *Parameter fuzzy_lines:*

```
WITH_WINDOW                     1
FUZZY_LENGTH                    5   10
FUZZY_ORIENTATION               0   10
FUZZY_WIDTH                     4   6   12   15
FUZZY_WIDTH_DEVIATION           0   5
FUZZY_GRAY_DEVIATION            0   20
```

- *Parameter fuse_lines:*

```
WITH_WINDOW                     1
WEIGHTS                         1.00
WEIGHT_SCALES                   1
BUFFER_WIDTH                    20.000
DIRECTION_DIFFERENCE            30.000
```

- *Parameter split_lines:*

```
WITH_WINDOW                     1
DISTANCE                        5.000
```

- *Parameter calc_paths:*

```
WITH_WINDOW                     1
FUZZY_WEIGHT                    0   1
FUZZY_ABS_DISTANCE              5   50
FUZZY_REL_DISTANCE              1   8
FUZZY_COLLINEAR                 0   25
FUZZY_JUNCTION                  55   90
MAX_DIST_JUNCTION               5
SCALE_LENGTH                    true
WEIGHT_SEEDPOINT                0.750
MIN_DISTANCE                    150
```

B.3. Alterable parameters for TU Munich extraction algorithm (optical imagery and urban areas)

- *Parameter extr_lines:*

```
WITH_WINDOW                     1
THRESHOLD                       150
LINE_WIDTH                      25.0
CONTRAST_HIGH                   60
CONTRAST_LOW                    30
LINE_BRIGHTNESS                 light
```

- *Parameter smspl_lines:*

```
WITH_WINDOW                     1
SMOOTH_LENGTH                   5
MAX_CURVATURE                   0.100
```

- *Parameter fuzzy_lines:*

```
WITH_WINDOW                     1
FUZZY_LENGTH                    5   50
FUZZY_ORIENTATION               0   20
FUZZY_WIDTH                     5   15   25   30
FUZZY_WIDTH_DEVIATION           0   5
FUZZY_GRAY_DEVIATION            0   20
```

- *Parameter fuse_lines:*

```
WITH_WINDOW                     1
WEIGHTS                         1.00
WEIGHT_SCALES                   1
BUFFER_WIDTH                    20.000
DIRECTION_DIFFERENCE            30.000
```

- *Parameter split_lines:*

```
WITH_WINDOW                     1
DISTANCE                        5.000
```

- *Parameter calc_paths:*

```
WITH_WINDOW                     1
FUZZY_WEIGHT                    0   1
FUZZY_ABS_DISTANCE              5   120
FUZZY_REL_DISTANCE              1   8
FUZZY_COLLINEAR                 0   25
FUZZY_JUNCTION                  55   90
MAX_DIST_JUNCTION               5
SCALE_LENGTH                    true
WEIGHT_SEEDPOINT                0.500
MIN_DISTANCE                    100
```

B.4. Alterable parameters for TU Munich extraction algorithm (optical imagery and open areas)

- *Parameter extr_lines:*

```
WITH_WINDOW                     1
THRESHOLD                       150
LINE_WIDTH                      7.5
CONTRAST_HIGH                   50
CONTRAST_LOW                    30
LINE_BRIGHTNESS                 light
```

- *Parameter smspl_lines:*

```
WITH_WINDOW                     1
SMOOTH_LENGTH                   5
MAX_CURVATURE                   0.100
```

- *Parameter fuzzy_lines:*

```
WITH_WINDOW                     1
FUZZY_LENGTH                    5   50
FUZZY_ORIENTATION               0   20
FUZZY_WIDTH                     2   5   10   13
FUZZY_WIDTH_DEVIATION           0   5
FUZZY_GRAY_DEVIATION            0   20
```

- *Parameter fuse_lines:*

```
WITH_WINDOW                     1
WEIGHTS                         1.00
WEIGHT_SCALES                   1
BUFFER_WIDTH                    20.000
DIRECTION_DIFFERENCE            30.000
```

- *Parameter split_lines:*

```
WITH_WINDOW                     1
DISTANCE                        5.000
```

- *Parameter calc_paths:*

```
WITH_WINDOW                     1
FUZZY_WEIGHT                    0   1
FUZZY_ABS_DISTANCE              5   120
FUZZY_REL_DISTANCE              1   8
FUZZY_COLLINEAR                 0   25
FUZZY_JUNCTION                  55   90
MAX_DIST_JUNCTION               5
SCALE_LENGTH                    true
WEIGHT_SEEDPOINT                0.500
MIN_DISTANCE                    150
```